

**Linking
Coordinated Amine Ligands
to Make
Cages**

Sukhpreet Kaur Gill

A thesis submitted for the degree of Master of Science at the
Auckland University of Technology,
Auckland, 2021

The work presented in this thesis was carried out in the Department of Chemistry of
Auckland University of Technology under the supervision of professor Allan Blackman.

TABLE OF CONTENTS

Attestation of Authorship	3
Abstract	4
Acknowledgements	5
Chapter 1	6
1. Introduction	6
1.1 Coordination Chemistry.....	6
1.2 Ligands.....	6
1.3 Stereochemistry.....	8
1.4 Isomers.....	9
1.5 Macrocycles.....	15
1.6 Aim.....	39
Chapter 2	41
2. Experimental	
General Methods	41
2.1 Synthesis of [Co(tren)(en)]Cl ₃	42
2.2 Synthesis of [Co(dien) ₂]Cl ₃	44
2.3 Attempted synthesis of uns-penp.....	46
2.4 Synthesis of [Co(bamp) ₂]Cl ₃	47
2.5 Synthesis of hexaamminecobalt(III) chloride.....	50
Chapter 3	52
3. Result and Discussion	52
3.1 Preface.....	52
3.2 Characterisation of ligands.....	52
3.3 Synthesis and characterisation of the precursor complexes.....	64
3.4 Reaction of the Co(III) complexes with formaldehyde and ammonia	82
Chapter 4	108
4. Conclusion	108
References	109

ATTESTATION OF AUTHORSHIP

"I hereby declare that this submission is my own work and that, to the best of my knowledge and belief, it contains no material previously published or written by another person (except where explicitly defined in the acknowledgements), nor material which to a substantial extent has been submitted for the award of any other degree or diploma of a university or other institution of higher learning."

I -

ABSTRACT

This thesis presents the study of cage complexes that link the coordinated amine ligands containing cobalt(III) ion. New multidentate cage-type amine ligands are synthesised by linking di-, tri-, and tetra-dentate amine ligands coordinated to cobalt(III) through intramolecular condensation with formaldehyde and ammonia. The cobalt(III) complexes used in this study are $[\text{Co}(\text{tren})(\text{en})]^{3+}$, $[\text{Co}(\text{dien})_2]^{3+}$, $[\text{Co}(\text{bamp})_2]^{3+}$, and $[\text{Co}(\text{NH}_3)_6]^{3+}$. All the ligands and starting materials have been synthesised and characterised by NMR spectroscopy and ESI-MS spectrometry. Attempts to synthesise the pure uns-penp ligand was not successful. Attempts to crystallise the products were unsuccessful. All other cobalt(III) complexes were reacted with formaldehyde and ammonia and the cage complex derived from $[\text{Co}(\text{tren})(\text{en})]^{3+}$ is best characterised by NMR and ESI-MS data which suggests the formation of four possible isomers. Structural optimisation using DFT was also performed for this complex which favours the formation of different isomers.

Acknowledgements

I cannot begin to express my sincere thanks to my supervisor Professor Allan Blackman who supported me from the beginning through the experiments and the writing. It would not have completed without your guidance. Not only you have helped me with my project but you have cheered me up at each stage of my research especially when covid-19 pandemic changed the situation.

I would like to thank all staff of the faculty of Science, Auckland University of Technology, lab mates and colleagues for their help and cooperation in various ways. To Tony Chen for running mass specs samples, to Iana Gritcan, Yan Wang, and Saeedah for their unwavering support in locating chemicals and equipment needed. To Professor Lawrie Gahan, University of Queensland, for doing the calculations.

Finally, I gratefully acknowledge the efforts of my parents, my brothers especially Sandeep Singh Gill and the rest of my family for supporting me financially and emotionally. They have always encouraged me and their patience cannot be underestimated. And to all my dear friends, Navneet Kaur Sandhu, Dominique, Fouad, Hoa, Bhanu, Madhu, Chloe Ren and Bronte Carr for creating a great working environment by making me laugh through the bad phase of my research. It could not have done so smoothly without your love and invaluable contribution.

CHAPTER 1

INTRODUCTION

1.1 COORDINATION CHEMISTRY

Coordination chemistry is widely understood to be the study of transition metal complexes, formed from the reaction of transition metal salts with ligands containing one or more donor atoms. The Swiss Chemist Alfred Werner formulated many of the fundamental ideas concerning the structure and the physical and chemical behaviour of transition metal complexes, or as they are often otherwise known, coordination compounds.¹ In such compounds, a central transition metal ion is surrounded by molecular or anionic ligands, which are attached to the central metal atom by a coordinate bond. This bond, while being covalent, formally involves an electron pair donation from a donor atom on the ligand to the transition metal. This therefore means that the metal acts as Lewis acid (an electron pair acceptor) and the ligand acts as a Lewis base (an electron pair donor).



1.2 LIGANDS

Within a ligand, the atom that is directly bonded to the metal atom/ion is called the donor atom. A ligand that attaches to the central metal ion through only one atom is called a monodentate ligand. Simple examples of these include NH_3 , H_2O and CN^- . A monodentate ligand can have more than one lone pair of electrons on the donor atom. For example, the O atom in an H_2O ligand has two lone pair of electrons which can be used for forming a coordinate bond with two metal ions, thus acting as a bridge, as shown in Figure.1.1.

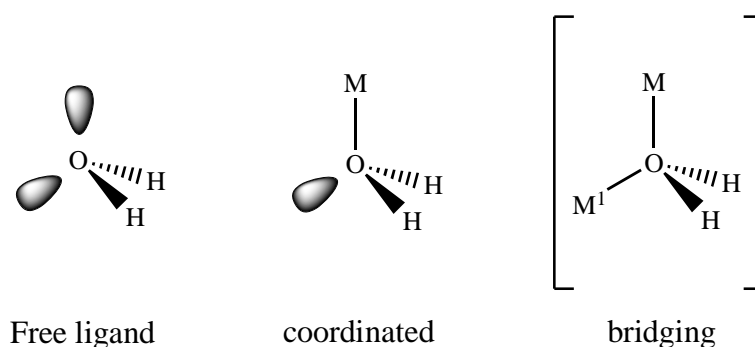


Figure 1.1: The aqua ligand, which can be monodentate or bridging (where M and M^1 are two metal centres).

Ligands that bind to a metal ion using two donor atoms are called bidentate. The classic example of such a ligand is ethylenediamine (variously called 1,2-diaminoethane or the IUPAC-approved ethane-1,2-diamine)¹, which binds through both N atoms, Figure 1.2. Ligands that use more than two donor atoms to bind to a metal ion are generally called polydentate, and the most well-known example of these is probably the hexadentate ligand ethylenediaminetetraacetic acid (EDTA).

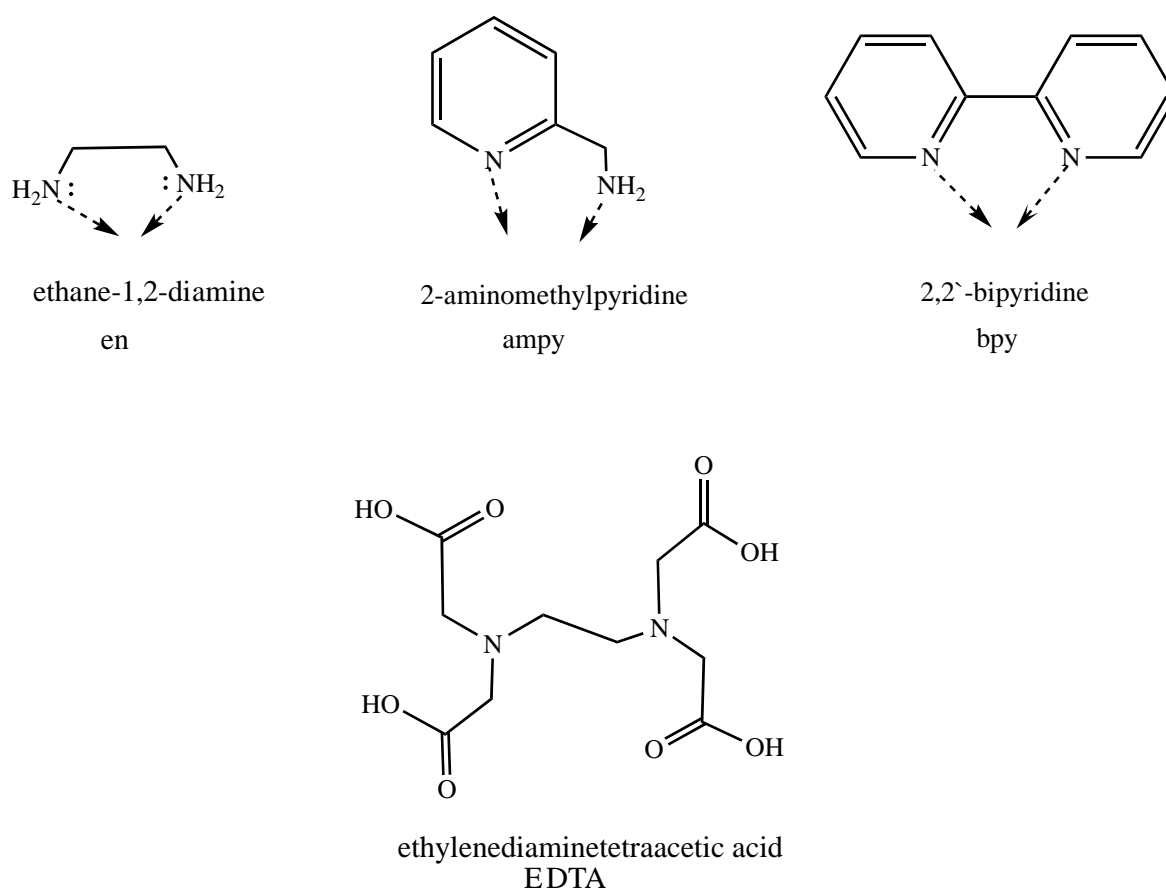


Figure 1.2: Some examples of bidentate and polydentate ligands.

When a ligand uses two or more donor atoms to form bonds to the same metal, one or more chelate rings are formed. Such rings contain the metal ion, two donor atoms from the ligand, and a number of ligand atoms. It has been found that chelate rings of certain sizes lead to enhanced stability of metal complexes when compared to complexes containing only monodentate ligands. Five-membered chelate rings are usually the most stable for light transition metal ions; these are favoured over six-membered rings owing to the necessity to incorporate one bond angle of around 90°.

Some ligands containing more than one donor atom can display a wide variety of binding modes. A good example of this is the acetate ion, pictured below (Figure 1.3, $R = \text{CH}_3$). As can be seen, this ligand can bind in both monodentate and bidentate fashions, with the latter involving either bridging or chelating.

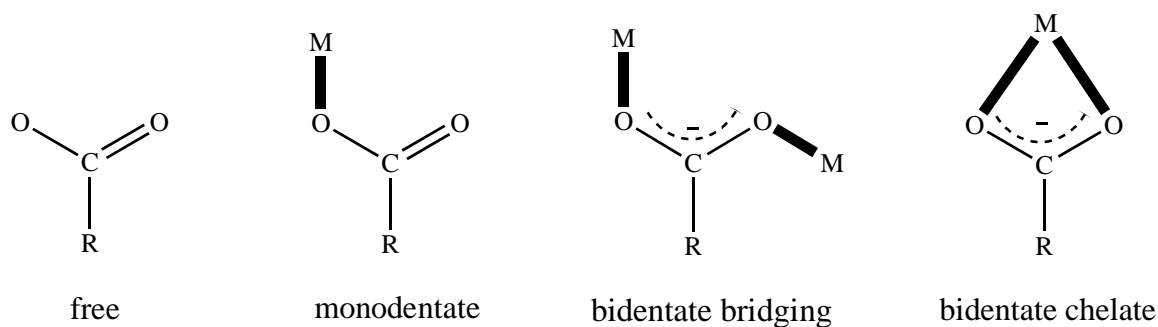


Figure 1.3: Some possible binding modes of the acetate ion ($R = \text{CH}_3$).

1.3 STEREOCHEMISTRY

The ligands attached to a central metal ion can have different possible spatial arrangements and this gives different geometries of the donor atoms about the metal ion. This leads to the important concept of stereochemistry. The stereochemistry of a transition metal complex depends on four key factors:

- Central metal-ligand electronic interactions; this is particularly influenced by the number of d electrons on the metal ion;
- Metal ion size and preferred metal-ligand donor bond lengths;
- Ligand-ligand repulsion forces;
- Inherent ligand geometry and rigidity.

These considerations lead to preferred geometries about metal ions having a particular coordination number. where the coordination number of a metal ion in a complex is defined as the number of ligand donor atoms bonded to the metal ion. For example, the coordination number of the Co^{III} ion in $[\text{Co}(\text{NH}_3)_6]^{3+}$ is 6, as six monodentate ligands each have a single donor atom bonded to the metal ion. These preferred geometries are shown in Figure 1.4.

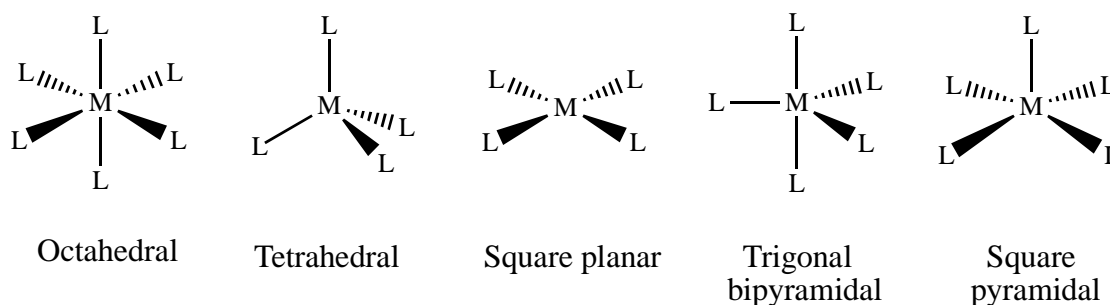


Figure.1.4: Common complex geometries for four- five- and six-coordinate complexes (*M* represents the central atom/ion and *L*, a monodentate ligand).

The majority of coordination complexes are 6-coordinate, and adopt an octahedral, or distorted octahedral geometry. 4-coordinate complexes are the next most abundant, with both tetrahedral and square planar (and their distorted versions) geometries being observed. 5-coordinate complexes can adopt both trigonal bipyramidal and square pyramidal geometries, with the majority lying on a continuum between these extreme geometries.

1.4 ISOMERS

Two or more different compounds comprising the same numbers and types of atoms, and therefore having the same chemical formula, but exhibiting different chemical and/or physical properties are called isomers. Among coordination compounds, two principal types of isomerism, stereoisomerism and structural isomerism, are known. Stereoisomerism can be further subdivided into geometrical and optical isomerism while structural isomerism can be subdivided into coordination, ionisation, hydrate and linkage isomerism.

1.4.1 Constitutional (Structural) Isomerism

These are isomers which have same empirical formula but different physical properties associated with different atom connectivity. Such isomers can be classified into the following groups.

1.4.1.1 Hydrate Isomerism

Hydrate isomerism, also called solvate isomerism, involves hydrated compounds having the same empirical formula, but which differ in colour, charge and number of ions. For example, the following hydrate isomers (Figure 1.5) are possible for the inert compound having the general formula $\text{CrCl}_3 \cdot 6\text{H}_2\text{O}$.

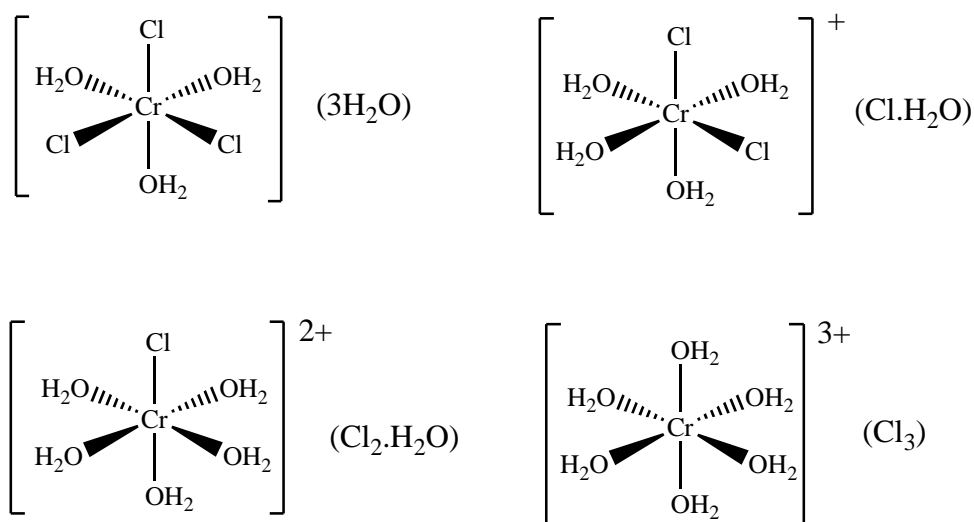


Figure 1.5: Hydrate isomers.

1.4.1.2 Ionisation Isomerism

Ionisation isomers involve complexes which have same molecular formula but form different ions. For example, two ionisation isomers of the cobalt(III) compound having the formula $\text{CoBr}(\text{SO}_4) \cdot 5\text{NH}_3$ are possible, as shown in Figure 1.6. The violet and red compounds differ with respect to which of the anions is coordinated to the Co ion.

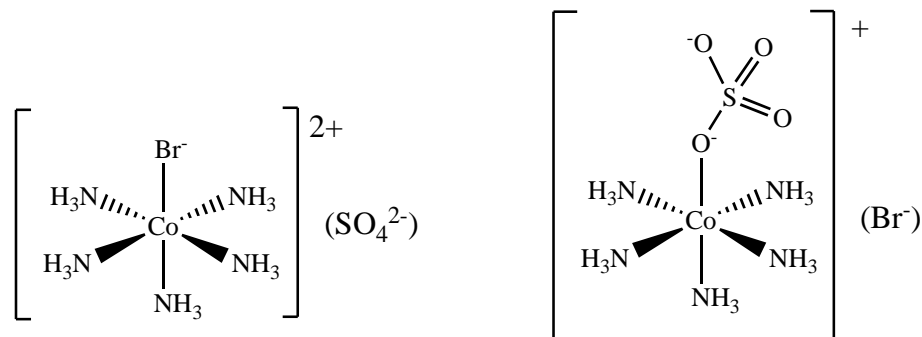


Figure 1.6: Ionisation isomerism.

1.4.1.3 Coordination Isomerism

In coordination isomerism, isomers which contain two (or more) metal ions, the ligands can be bonded to either of the metal ions. For example, the compound having the formula $\text{CoCr}(\text{CN})_6 \cdot 6\text{NH}_3$ can exist as either $[\text{Co}(\text{NH}_3)_6][\text{Cr}(\text{CN})_6]$ or $[\text{Cr}(\text{NH}_3)_6][\text{Co}(\text{CN})_6]$, as shown in Figure 1.7.

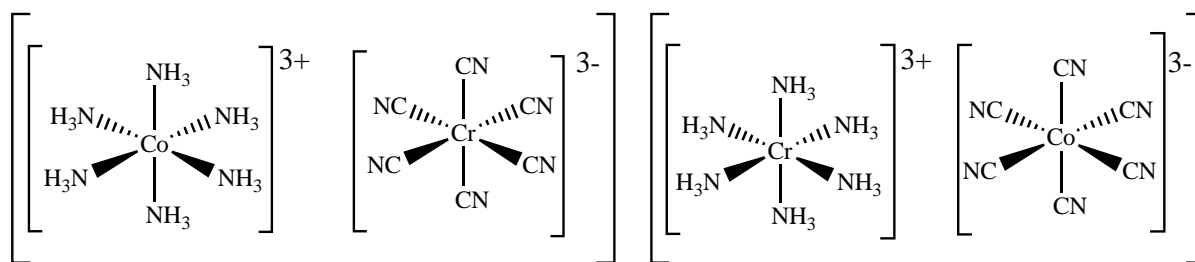


Figure 1.7: Coordination isomerism.

1.4.1.4 Linkage Isomerism

Ligands that contain two different atoms carrying lone pairs, both capable of coordination to a metal ion, are called ambidentate or ambivalent ligands. An example of this is the thiocyanate anion (SCN^-), which can bind to a metal ion through either the N or S atom, depending on the preference of the metal ion. For example, the ‘hard’ Co(III) ion prefers to form Co-NCS complexes with the ‘hard’ N-donor, whereas the ‘soft’ Pd(II) ion prefers the ‘soft’ S-donor and forms Pd-SCN complexes. Ambidentate ligands can display a tendency to ‘bridge’ between two metal ions, with each of the two different donor atoms attached to one of two metal ions.

1.4.2 Stereoisomerism (Positional Isomers – in Place; Optical Isomers – in Space)

General diagram for possible isomers is shown in figure 1.8. Stereoisomers are molecules of the same molecular formula that have the same atom-to-atom bonding sequence throughout, but for which the location of the ligand atoms in space differ. Diastereomers are the general class of stereoisomers and have a subclass of geometric isomers (cis and trans isomeric forms). Enantiomers are stereoisomers that are non-superimposable mirror images of each other. Diastereomers are different from enantiomers. For complexes to have enantiomers, they must be either dissymmetric or asymmetric. A molecule that is asymmetric or dissymmetric (lacks any improper rotation axes) will have a non-superimposable mirror image and is called a chiral compound. Thus, all enantiomers are chiral and will display optical activity, the ability to rotate the plane of plane-polarised light. The rotation of the plane of polarised light is measured using a polarimeter. Compounds that rotate the plane of polarised light clockwise are called (+)-isomers, or dextrorotatory (d) and those that rotate the plane anticlockwise are called (-)-isomers, or laevorotatory (l).

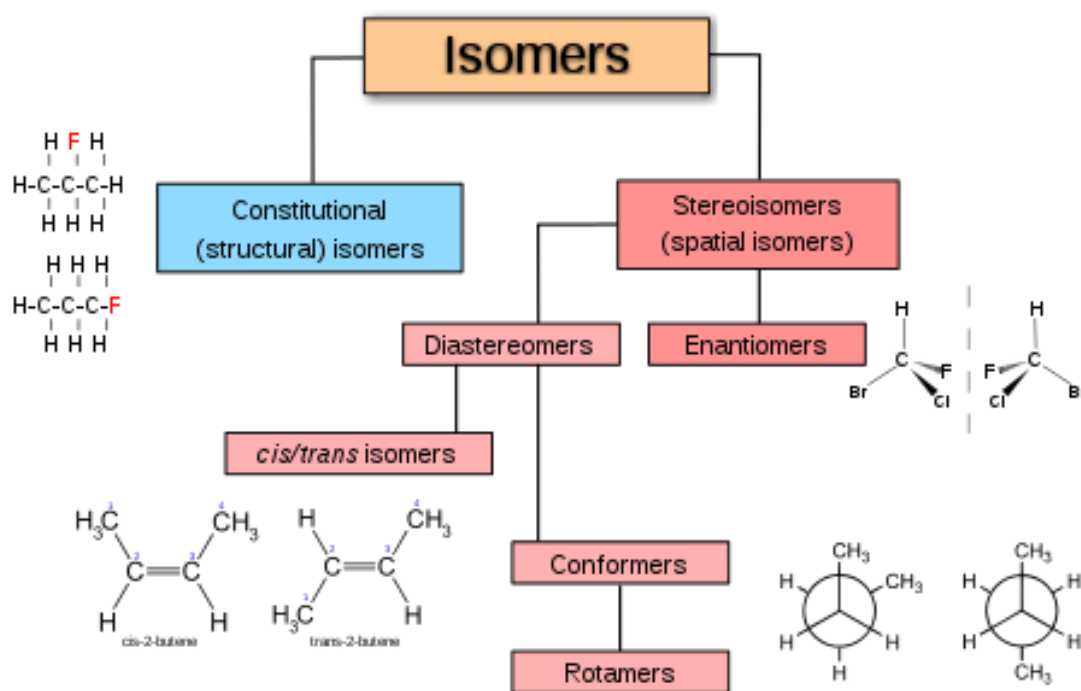


Figure 1.8: General diagram representing the types of possible chemical isomers².

Most simple synthetic reactions lead to equal amounts of enantiomers, called a racemic mixture. The separation of enantiomers is called resolution and is often difficult because the enantiomers have identical chemical properties. Diastereomers usually differ appreciably in their chemical and physical properties, whereas enantiomers differ only in their ability to rotate polarized light and related optical properties.

1.4.2.1 Stereoisomerism in Four-Coordinate Complexes

Four-coordinate complexes can exhibit square planar and tetrahedral geometries. In complexes with simple monodentate ligands such as Br⁻ and Cl⁻, the square planar geometry involves at least one plane of symmetry and as a result these complexes cannot form enantiomers; however, geometric isomers (cis and trans) may be possible (Figure 1.9).

Complexes having a tetrahedral geometry cannot exhibit geometric isomerism because of the symmetrical disposition of bonds but may display optical isomerism.

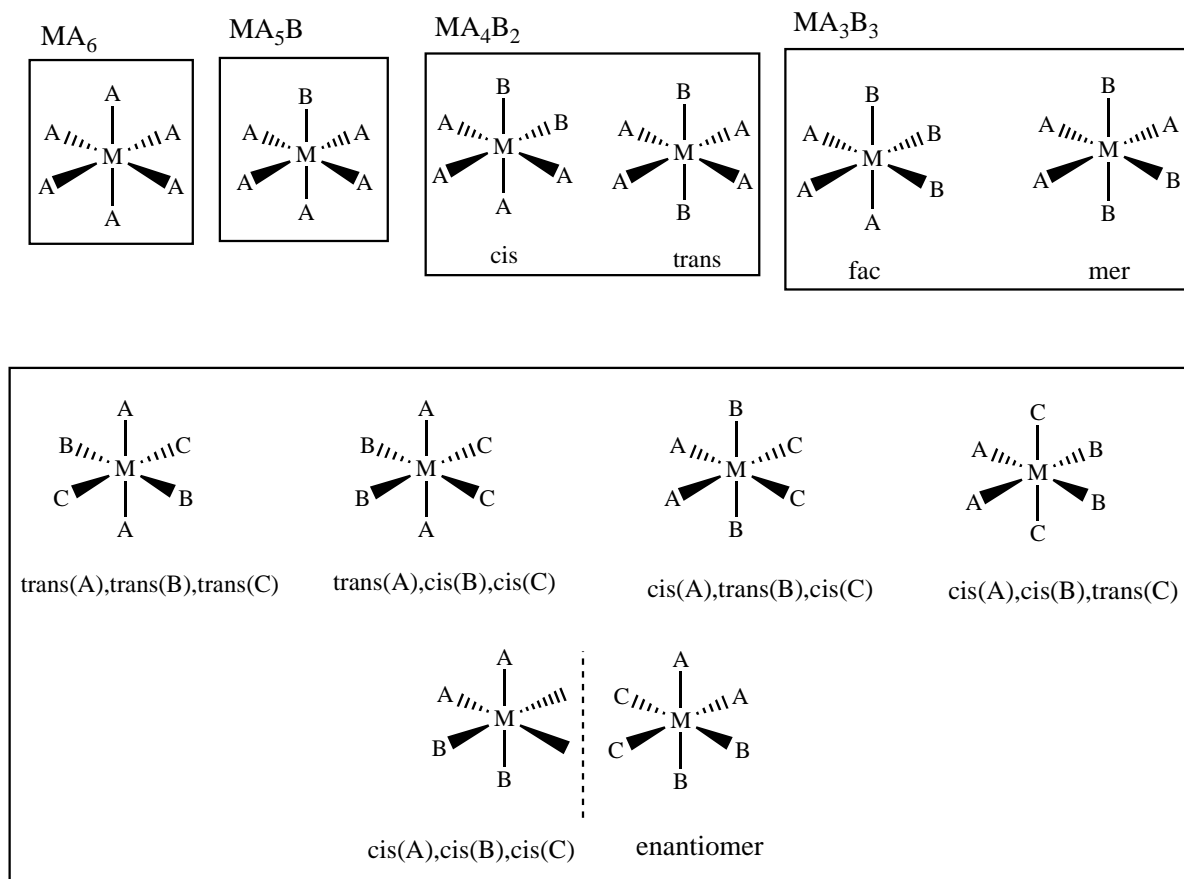


Figure 1.10: Diastereomers and enantiomers possible for octahedral complexes with various sets of monodentate ligands.

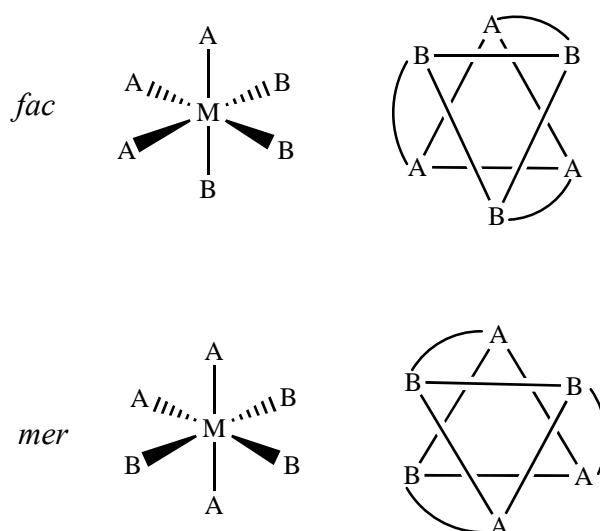


Figure 1.11: Representation of fac and mer isomers.

example, if the metal ion is bound in the cavity, the loss of flexibility reduces the possible pathways for ligand dissociation and this tends to increase the kinetic stability of the system. One of the first examples of synthetic macrocycles are crown ethers, initially developed by Charles Pedersen (Nobel Prize, 1987). These macrocycles consist of the ethereal oxygen atoms, separated (generally) by two methylene groups, with all oxygen atoms essentially coplanar and the methylene groups giving a crown arrangement, hence the name “crown ether”. For example, the crown ether 1,2-crown 4 is shown in Figure 1.13.

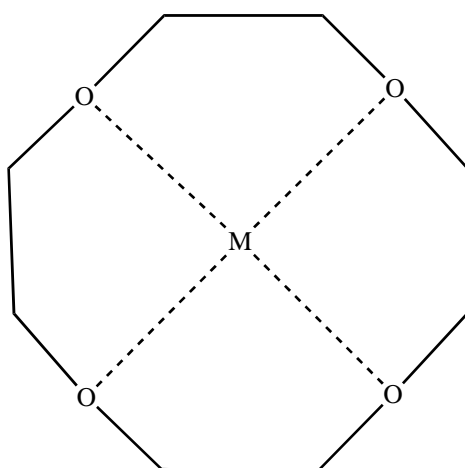


Figure 1.13: Crown ether 1,2-crown 4

In complexes of crown ethers, all the oxygen atoms point inward toward the metal atom. Crown ethers are well known to form stable complexes with alkali metals which can be attributed to the close fitting of the alkali metal ion into the cavity/hole in the centre of ligand. Crown ethers also have the unusual ability to promote solubility of alkali salts in organic solvents due to the large hydrophobic organic ring.

In 1961, the structure of the first macrocyclic ligand was proposed by Curtis and House³, two New Zealand chemists. This discovery was made by chance, when a recrystallisation of $[\text{Ni}(\text{en})_3](\text{ClO}_4)_2$ from acetone gave an unexpected yellow solid, which was later shown to contain the ligand 5,7,7,12,14,14-hexamethyl-1,4,8,11-tetraazacyclotetradeca-4,11-diene. This was the first of many such “Curtis” macrocycles, organic frameworks which bind a transition metal atom via nitrogen atoms with varying substituents on the carbon atoms. The Curtis macrocycles⁴ are formed from the reaction of transition metal di- and triamine complexes with acetone in a 2 + 2 condensation reaction. Two acetone molecules are used to form the head-units, the carbonyl groups of which then condense with the primary amine N atoms of metal ethylenediamine complexes to form the unsaturated macrocyclic ligand (Figure 1.14).

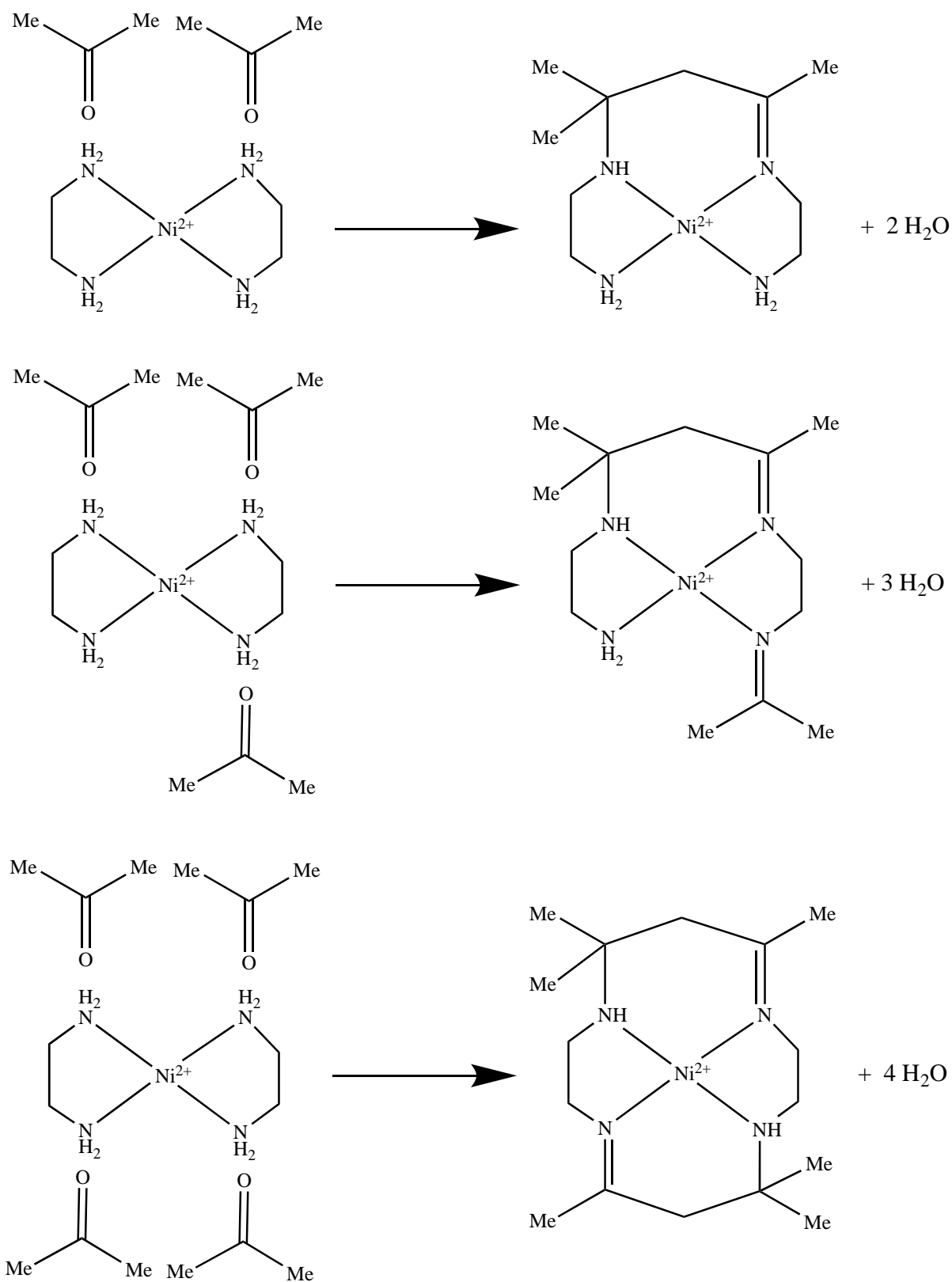


Figure 1.14: Compounds formed by the reaction of nickel(II) 1,2-ethanediamine compounds with acetone. Structure of the first macrocyclic ligand; 5,7,7,12,14,14-hexamethyl-1,4,8,11-tetraazacyclotetradeca-4,11-diene.

Since this time, literally thousands of macrocyclic ligands have been prepared, using a variety of synthetic methods, and macrocyclic chemistry is now a major branch of coordination chemistry.

1.5.1 CRYPTANDS

Cryptands are a family of synthetic bicyclic or polycyclic polydentate ligands which can coordinate both cations and anions. These molecules, which generally contain O and/or/N donor atoms, can be thought of as three-dimensional analogues of crown ethers and macrocyclic ligands, but are often more selective and form strong complexes. The first cryptands were reported in 1969, in papers by the future Nobel laureates Jean-Marie Lehn⁵ and Jean-Pierre Sauvage. The^{5,6,7} most common and important cryptand is [2.2.2] cryptand with the chemical formula $N[CH_2CH_2OCH_2CH_2OCH_2CH_2]_3N$. [2.2.2] indicates the number of ethereal oxygen atoms in each chain and hence the binding sites, as shown in Figure 1.15. Cryptands contain two atoms which are called capping atoms; an example is given by the apical nitrogen atoms shown in Figure 1.15.

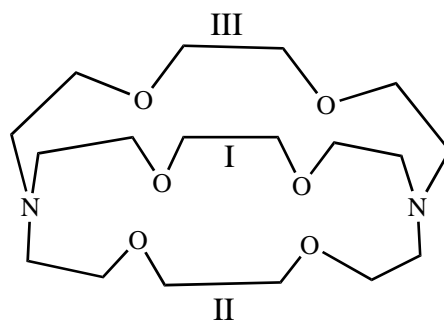


Figure 1.15: The [2.2.2]cryptand ligand, which has N atoms at the apical positions.

Cryptands are a subset of ligands termed clathrochelates, which are defined as ligands that encapsulate metal ions. In addition to the geometric parameters, the thermodynamic and kinetic stability of clathrochelate complexes is determined by the electronic structure of the encapsulated metal ion and the nature of the ligand.

Macropolycyclic clathrochelate ligands⁸ are cyclic ligands containing two or more rings, and are classified on the basis of nature and type of the donor atoms.

1. Polyazamacropolycycles. Nitrogen atoms act as donor atoms.
2. Polyazathiomacropolycycles. Nitrogen and sulfur atoms act as donor atoms.
3. Polyazaselenomacropolycycles. Nitrogen and selenium atoms act as donor atoms.
4. Polythiomacropolycycles. Sulfur atoms act as donor atoms.

5. Polyoxothiomacropolycycles. Sulfur and oxygen atoms act as donor atoms.
6. Polyazaoxothiomacropolycycles. Nitrogen, sulphur and oxygen atoms act as donor atoms.
7. Polyazaoxomacropolycycles. Nitrogen and oxygen atoms act as donor atoms.
8. Polyoxomacropolycycles. Oxygen atoms act as donor atoms.

Polyazamacropolycycles and polyazathiomacropolycycles form stable complexes mainly with transition metal ions.

The synthesis of cryptand and clathrochelate ligands is often demanding, and generally requires extensive protection/deprotection procedures, with reactions often having to be carried out under conditions of high dilution in order to prevent self-condensation processes. Not surprisingly, yields are often poor.

1.5.2 CAGE LIGANDS

In a 1977 communication⁹, Sargeson and coworkers described the structure and chemistry of a cobalt complex of an unprecedented octaazacryptate ligand that they called sepulchrate. Quite remarkably, this was prepared by a simple condensation of the $[\text{Co}(\text{en})_3]^{3+}$ ion with formaldehyde and ammonia in over 95% yield, on a 156 gram scale. The structures of $[\text{Co}(\text{en})_3]^{3+}$ and $[\text{Co}(\text{sep})]^{3+}$ are shown in figure 1.16.

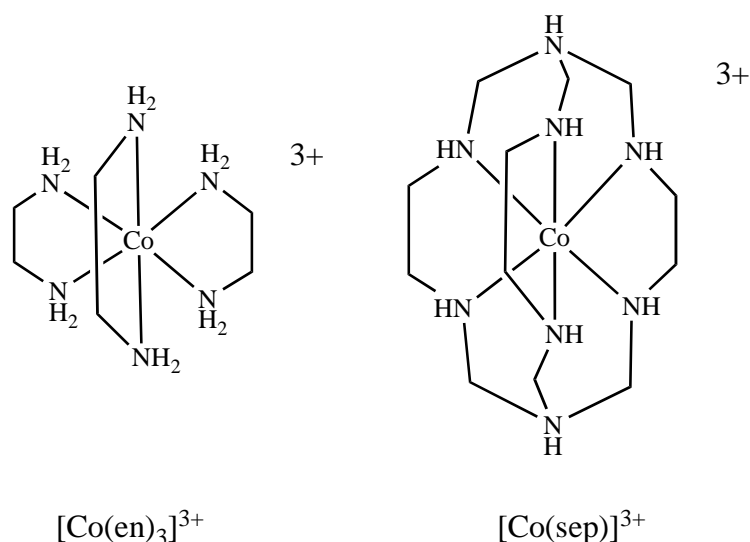


Figure 1.16: The Structures of $[\text{Co}(\text{en})_3]^{3+}$ and $[\text{Co}(\text{sep})]^{3+}$.

The reaction resulted in the addition of tris(methylene)amino caps at both the ends of the parent ion to give the six-coordinate $[\text{Co}(\text{sep})]^{3+}$ complex. When chiral $[\text{Co}(\text{en})_3]^{3+}$ was used as the starting material, retention of chirality in the product was confirmed by the crystal structure. Quantitative conformational analysis calculations indicated that the conformer in the crystal was not the most energetically preferred, but was stabilized through hydrogen bonding with lattice Cl^- ions.

The ^1H and ^{13}C NMR spectra were consistent with an overall D_3 symmetry of the $[\text{Co}(\text{sep})]^{3+}$ ion. The ^1H NMR spectrum showed two signals: one at $\delta = 4.00$ ppm (12 protons) due to the methylene carbons of the cap and the other at $\delta = 3.20$ ppm (12 protons) due to the methylene carbons of the ethylenediamine ligands. The ^{13}C NMR spectrum displayed two signals at $\delta = -0.389$ ppm and $\delta = +13.245$ ppm relative to 1,4-dioxane (66.66 ppm).

Cyclic voltammetry studies showed that the $[\text{Co}(\text{sep})]^{3+/2+}$ reduction potential (-0.54 V) was lower than that for $[\text{Co}(\text{en})_3]^{3+/2+}$ (-0.45 V, irreversible) under the same conditions.

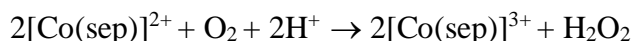
$[\text{Co}(\text{sep})]^{3+}$ was rapidly reduced to $[\text{Co}(\text{sep})]^{2+}$ using Zn dust and this ion was isolated as the ZnCl_4^{2-} salt. $[\text{Co}(\text{sep})]^{2+}$ was reoxidised to $[\text{Co}(\text{sep})]^{3+}$ and H_2O_2 using O_2 , and this occurred with retention of configuration.

In 1982, a full paper¹⁰ describing the syntheses and characterisation of the cage complexes $[\text{Co}(\text{sep})]^{3+}$ (sep = sepulchrane = 1,3,6,8,10,13,16,19-octaazabicyclo[6.6.6]eicosane), $[\text{Co}(\text{sen})]^{3+}$ (sen = 5-methyl-5-(4-amino-2-azabutyl)-3,7-diazanonane-1,9-diamine) and $[\text{Co}(\text{azamesar})]^{3+}$ (azamesar = 8-methyl-1,3,6,10,13,16,19-heptaazabicyclo[6.6.6]icosane) was published. These complexes were synthesised from $[\text{Co}(\text{en})_3]^{3+}$ and their oxidation-reduction potentials, visible spectra, circular dichroism, and acid-base properties were determined. As described in the 1977 paper, $[\text{Co}(\text{sep})]^{3+}$ was synthesised by condensing the $[\text{Co}(\text{en})_3]^{3+}$ ion with formaldehyde and ammonia. Both the $\Lambda(\text{S})$ and $\Delta(\text{R})$ forms of the complex were isolated from Λ - and Δ - $[\text{Co}(\text{en})_3]^{3+}$ respectively. Resolution of the racemic complex as the (+)-tartrate chloride salt was partly successful. $[\text{Co}(\text{sep})]^{3+}$ could be reduced to $[\text{Co}(\text{sep})]^{2+}$ using Zn powder or amalgamated Zn, with retention of chirality.

$[\text{Co}(\text{azamesar})]^{3+}$ was synthesised from partially caged $[\text{Co}(\text{sen})]^{3+}$ ion in the same way as $[\text{Co}(\text{sep})]^{3+}$ and its properties and reactions were similar to those of $[\text{Co}(\text{sep})]^{3+}$.

The ^1H NMR spectrum of $[\text{Co}(\text{azamesar})]^{3+}$ in D_2O showed one singlet at $\delta = 1.0$ ppm and other signals at $\delta = 2.3 - 3.5$ ppm and $\delta = 3.7 - 4.4$ ppm. The integration ratio was 3:18:6 which corresponded to 3 methyl protons, 18 methylene protons of the $\text{N}-\text{CH}_2-\text{CH}_2-\text{N}$ and

N-CH₂-C groups, and 6 methylene protons of the nitrogen cap N-CH₂-N. Cyclic voltammetry studies showed a reduction potential, $E_{1/2}$, of -0.45 V for [Co(en)₃]^{3+/2+}, -0.54 V for [Co(sep)]^{3+/2+} and -0.60 V for [Co(azamesar)]^{3+/2+}. [Co(sep)]²⁺ could be oxidised to [Co(sep)]³⁺ and H₂O₂ using O₂ in aqueous solution, with >99 % retention of the absolute configuration. The stoichiometry of the reaction is given by



The amount of [Co(sep)]³⁺ formed was determined by its visible spectrum and the amount of H₂O₂ by its reaction with iodide ion to give iodine. The self-exchange electron transfer reactions were studied and the rate constant for [Co(sep)]^{3+/2+} was found to be $k_{et} = 5.1 \pm 0.3 \text{ M}^{-1} \text{ s}^{-1}$. The analogous rate constant for [Co(azamesar)]^{3+/2+} was found to be $2.9 \text{ M}^{-1} \text{ s}^{-1}$ while that for [Co(en)₃]^{2+/3+} was $5.2 \times 10^{-5} \text{ M}^{-1} \text{ s}^{-1}$. For [Co(NH₃)₆]^{2+/3+}, the self-exchange rate was estimated to be $k \geq 10^{-7} \text{ M}^{-1} \text{ s}^{-1}$.

On reduction of [Co(sep)]³⁺ with Zn in acid solution or on acidification of [Co(sep)]²⁺ solutions, cage decomposition occurred to give Co_{aq}²⁺, NH₃(CH₂)₂NH₃²⁺, and NH₄⁺. In strongly basic solution, the colour of the cage complexes changed from yellow to dark purple to yellow brown due to deprotonation of one or more secondary amino groups. [Co(sep)]Cl₃ was isolated unchanged from 12 mol L⁻¹ HCl.

The proposed mechanism of the encapsulation of the cobalt ion during the reaction between [Co(en)₃]³⁺, CH₂O and NH₃ to give the macrobicyclic complex [Co(sep)]³⁺, is shown in figure 1.17.

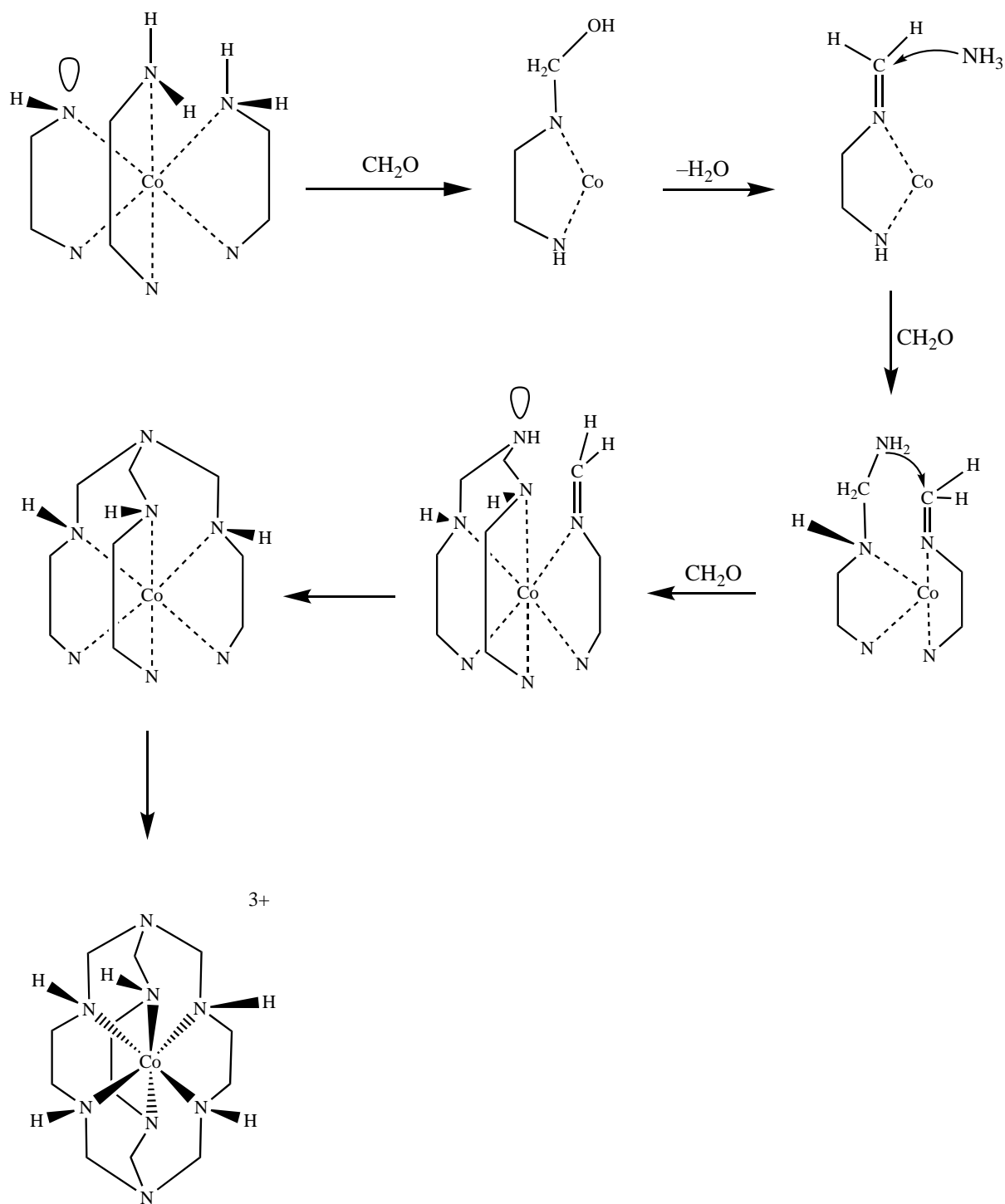


Figure 1.17: Mechanism of the encapsulation of the cobalt ion.

The crystal structure confirmed the hexadentate nature of the capsule with the tris(methyleneamine) cap added at both ends of the parent ion. The ethylene-1,2-diamine rings have the *lel* conformation and the overall symmetry is close to D_3 .

These were the first of many so-called 'cage' complexes. These complexes are named according to the atoms within the cage framework. The framework with diamine chelate

fragments and carbon atoms in the apical positions is called sarcophagine (sar) and those with nitrogen atoms in the apical positions are called sepulchrates (sep) or diazasar, as shown in Figure 1.18. The compounds containing sarcophagine and sepulchrates ligands are capped by the carbon or nitrogen atom via methylene units. Cage complexes of numerous metal (Co, Cu, Mn, Ag, Fe, Cr and many others) ions with various apical substituents on the ligand have been synthesised. The majority of complexes were formed with an encapsulated cobalt ion.

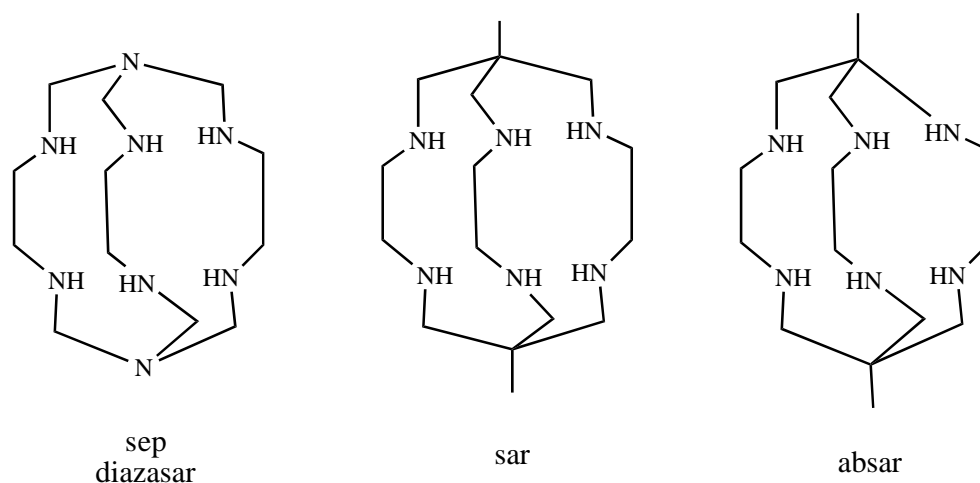


Figure 1.18: Some examples of encapsulating ligands.

These ligands have specific flexibility that allows the synthesis of complexes with metal ions having differing geometric requirements and in various oxidation states. The free ligands can generally be obtained by demetallation of preformed clathrochelate complexes, although this can be difficult. A considerable number of stereoisomers can be obtained that readily interconvert. Reactive sites on the ligands, generally at the apical atoms, provide a wide range of modification reactions allowing preparation of many different substituted sepulchrates and sarcophagines. These complexes can also be obtained by metal ion substitution.

Sepulchrates and sarcophagines have primarily been synthesised via template macrocyclization of the preformed metal tris-diaminates with capping agents, and this is regarded as being the most widely used approach to the synthesis of these compounds. Sargeson and coworkers first prepared the cobalt(III), platinum(IV) and rhodium(III) sepulchrates and sarcophagines, as well as the corresponding cobalt(II) complexes. These synthetic reactions were extended to form other cage-type ligands by using different metal complexes as the templates for the condensation reactions. In 1982, a highly

constrained macrotricyclic caged ion¹¹ [(3,11-dimethyl-7-nitro-1,5,9,13,16,19-hexa-azatricyclo-[9.3.3.3]icosane) cobalt (III)]³⁺ (**1**), shown in figure 1.19(a), was synthesised by the condensation of the [Co(tame)₂]³⁺ [tame = 1,1,1-tris(aminomethyl)ethane] ion with formaldehyde and nitromethane at pH 10.5. A reaction time of 5 h gave a yield of 50%, and the proposed mechanism of the reaction is shown in Figure 1.19(a) and 1.19(b). The single crystal X-ray analysis of the (ZnCl₄)Cl salt showed that a trigonal cap is formed on one side of the complex by the condensation of one nitromethane and three formaldehyde molecules, and on the other side, two four-membered chelate rings (formed through two formaldehyde molecules) fused at the tertiary nitrogen donor.

A minor product was also characterised. The X-ray structure of [(3,11-dimethyl-7,15-dinitro-1,5,9,13,16,19-hexa-azatricyclo-[9.5.3.3]docosane) cobalt (III)]Cl₃ (**2**), shown in figure 1.19(b), showed a similar chelate ring arrangement as (**1**) except with the six-membered ring replacing one of the fused four-membered rings. This ring, resulting from the condensation of one nitromethane and two formaldehyde molecules, is fused at a tertiary nitrogen donor. Due to the trigonal nitromethane-formaldehyde cap on one side and the fused four-membered ring on the other side of the [Co(tame)₂]³⁺ ion, one side of the Co^{III}N₆ chromophore is severely distorted from octahedral geometry.

The generation of the larger Co²⁺ ion is inhibited by the strained macrotricyclic cage, lowering the reduction potential of (**1**) (E = -0.62 V vs. standard hydrogen electrode in 0.1 M NaClO₄) relative to that of [Co(sep)]³⁺ (-0.54 V).

When (**1**) was reduced with Zn in acidic conditions, the four-membered ring was cleaved, the nitro group was converted into the corresponding amine, and the Co^{II} ion was removed from the tripodal sexidentate amine ligand.

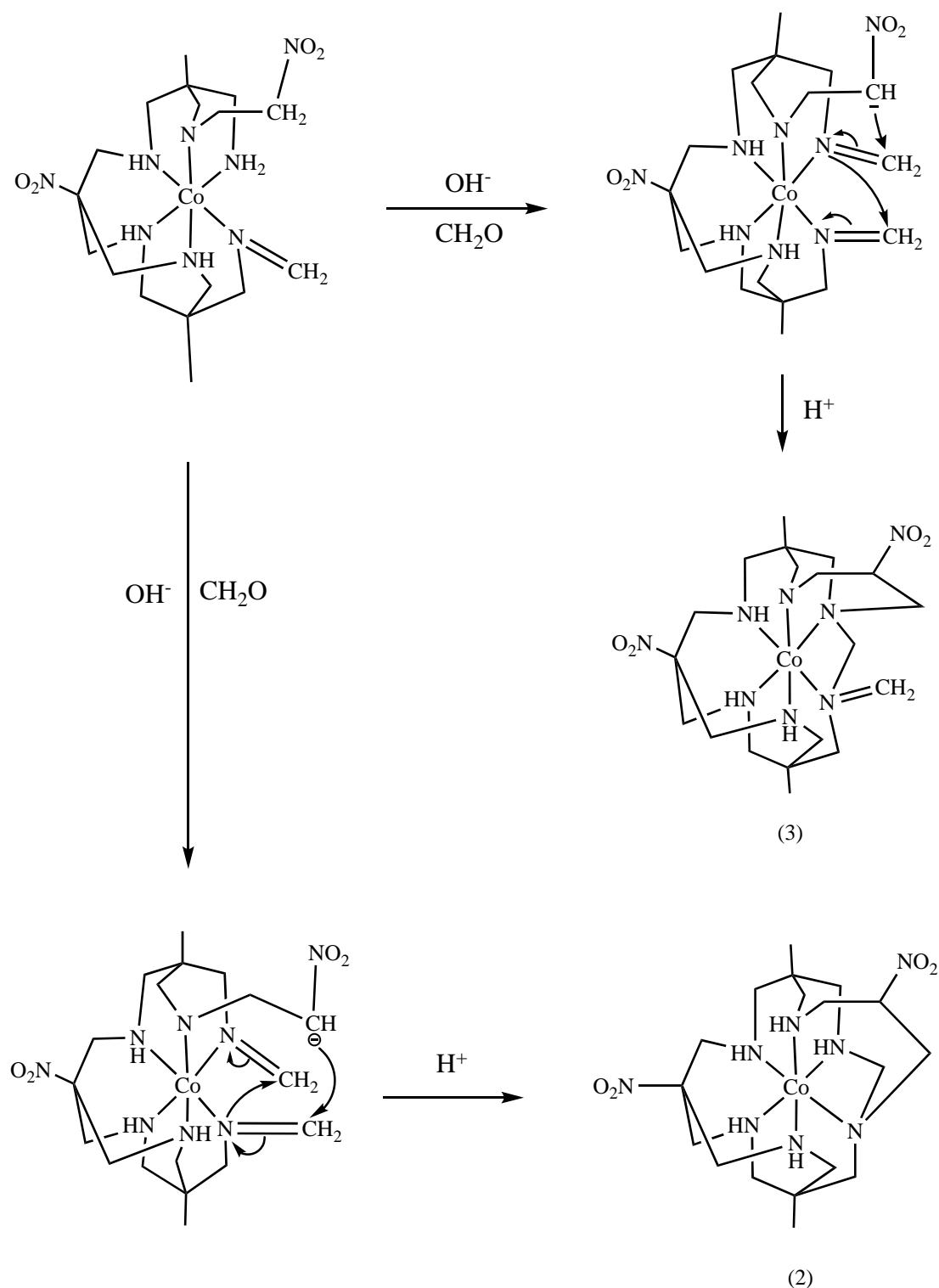


Figure 1.19(b): Shows the mechanism for the formation of (2) and (3).

Using a similar strategy as for (1), the [(3,11-dimethyl-1,5,9,13,16,19-hepta-azatricyclo[9.3.3.3]icosane) cobalt (III)] (6) ion was also synthesised in 30% yield, by replacing the nitromethane nucleophile with ammonia. No decomposition or dissociation of 1 or 6 was

observed in 6 M HCl over several hours at 50-60 °C which implies extraordinary kinetic stability. Treatment of **6** with aqueous $\text{CF}_3\text{SO}_3\text{H}$ over several days at room temperature yielded a tri-imine complex (80%) which has the methene groups, an intact four-membered ring and a ruptured aza cap, shown in figure 1.20.

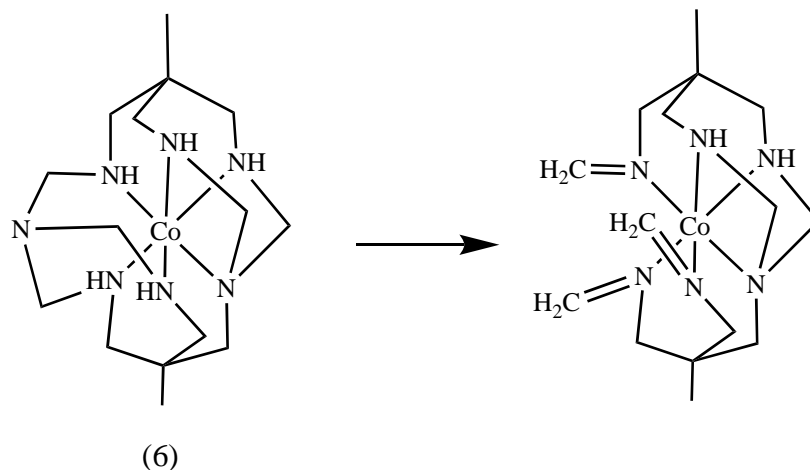


Figure 1.20: Ruptured aza cap, methene groups retained and the four-membered rings are intact when (**6**) was treated with aqueous $\text{CF}_3\text{SO}_3\text{H}$.

In 1983, Hammershoi described the synthesis¹² of the sexidentate ligand 1,4,7-tris(2-aminoethyl)-1,4,7-triazacyclononane (taetacn) and chiral $[\text{Co}(\text{taetacn})]^{3+}$ along with the chiral cage derivatives $[\text{Co}(\text{nosartacn})]^{3+}$ (nosartacn = 9-nitro-1,4,7,11,14,19-hexaazatricyclo[7.7.4.2]docosane), $[\text{Co}(\text{amsartacn})]^{3+}$ (amsartacn = 9-amino-1,4,7,11,14,19-hexaazatricyclo[7.7.4.2]docosane) (the protonated form is $[\text{Co}(\text{amsartacnH})]^{3+}$) and $[\text{Co}(\text{azasartacn})]^{3+}$ (azasartacn = 9-amino-1,4,7,11,14,19-heptaazatricyclo[7.7.4.2]docosane), figure 1.21.

The taetacn ligand was synthesised by reductive alkylation of 1,4,7-triazacyclononane (tacn) with phthalimidoacetaldehyde in the presence of NaBH_3CN followed by acid hydrolysis, shown in figure 1.22.

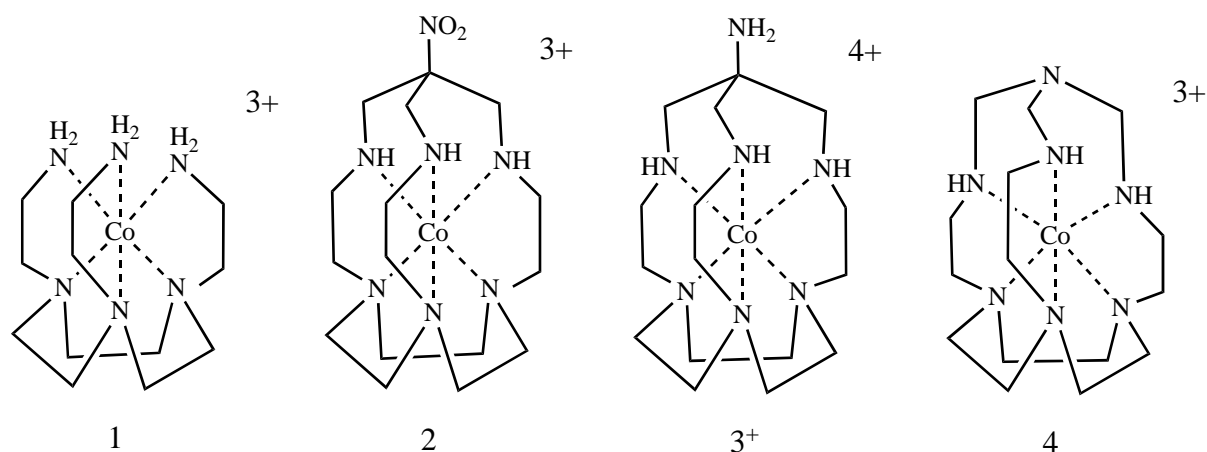


Figure 1.21: Structures of **(1)** $[\text{Co}(\text{taetacn})]^{3+}$ (*taetacn* = 1,4,7-tris(2-aminoethyl)-1,4,7-triazacyclononane); **(2)** $[\text{Co}(\text{nosartacn})]^{3+}$ (*nosartacn* = 9-nitro-1,4,7,11,14,19-hexaazatricyclo[7.7.4.2]docosane); **(3⁺)** $[\text{Co}(\text{amsartacnH})]^{3+}$ (*amsartacn* = 9-amino-1,4,7,11,14,19-hexaazatricyclo[7.7.4.2]docosane); and **(4)** $[\text{Co}(\text{azasartacn})]^{3+}$ (*azasartacn* = 9-amino-1,4,7,11,14,19-heptaazatricyclo[7.7.4.2]docosane).

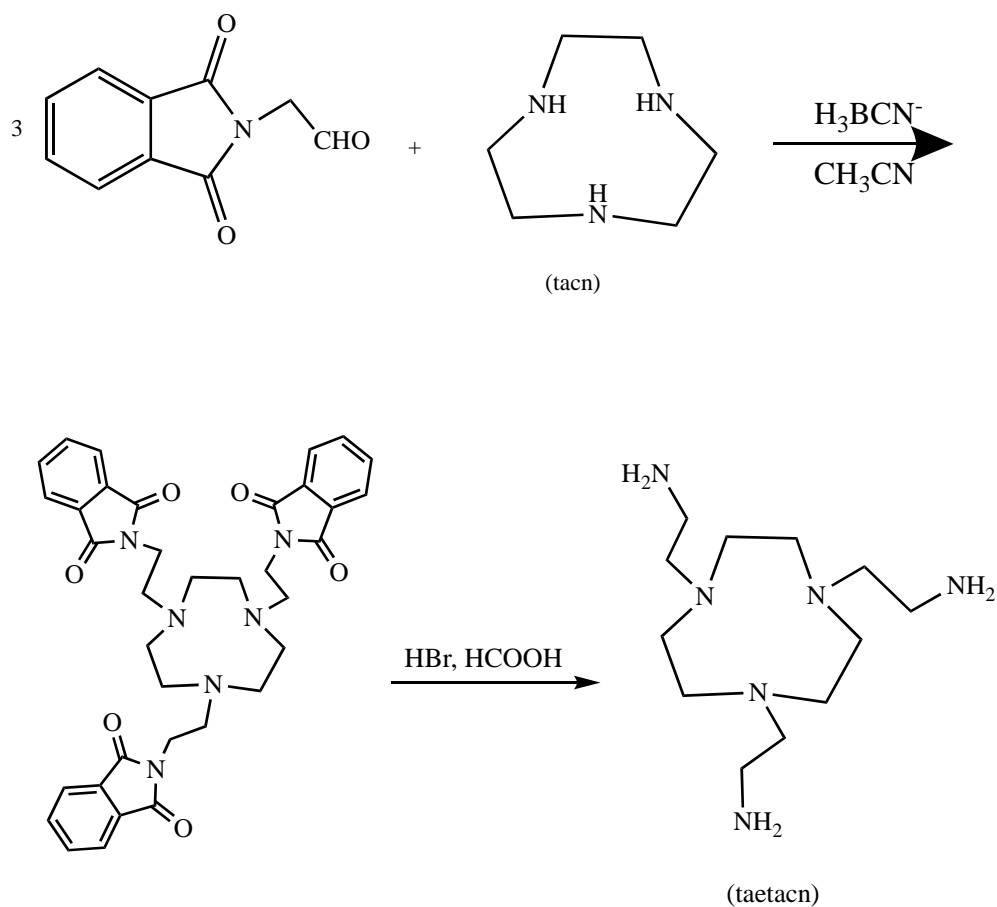


Figure 1.22: Synthesis of the *taetacn* ligand.

The $[\text{Co}(\text{taetacn})]^{3+}$ complex was synthesised by aerial oxidation of Co^{2+} in the presence of activated charcoal and stoichiometric amounts of both H^+ and crude taetacn in water. The complex was collected as a yellow-orange fraction from ion exchange chromatography. The condensation reaction between $[\text{Co}(\text{taetacn})]^{3+}$, formaldehyde and nitromethane led to the synthesis of $[\text{Co}(\text{nosartacn})]^{3+}$, while the condensation reaction carried out between $[\text{Co}(\text{taetacn})]^{3+}$, formaldehyde and ammonia gave $[\text{Co}(\text{azasartacn})]^{3+}$. The capping occurred via intermolecular condensations and cyclizations, shown in figure 1.23. $[\text{Co}(\text{amsartacn})]^{3+}$ was synthesised from $[\text{Co}(\text{nosartacn})]^{3+}$ by reduction of the nitro group to an amine using Zn in HCl followed by reoxidation of the metal ion with H_2O_2 .

Resolution of all the hexamine complexes, except $[\text{Co}(\text{azasartacn})]^{3+}$, into their chiral forms through ion exchange chromatography on SP-Sephadex C-25 resin with the use of chiral eluants was achieved. Chiral precursors were also used for the synthesis of chiral cage complexes.

The ^{13}C NMR spectra of the complexes were consistent with C_3 symmetry in solution. The three close signals in the region δ -2.0 to -3.9 indicated three sets of inequivalent but chemically similar carbon atoms bonded to the coordinated tertiary amine nitrogen atoms. The set of carbon atoms bonded to coordinated primary amino groups in the $[\text{Co}(\text{taetacn})]^{3+}$ ion displayed one signal at δ = -21.3 ppm and in $[\text{Co}(\text{azasartacn})]^{3+}$ at δ = -15.0 ppm (chemical shifts are relative to 1,4-dioxane (= 0 ppm)). The same set of carbons and the equivalent methylene carbon atoms of the cap in the spectra of $[\text{Co}(\text{nosartacn})]^{3+}$ and $[\text{Co}(\text{amsartacnH})]^{4+}$ displayed signals in the region between δ = -12.4 and -13.6 ppm. The single tertiary carbon atom of the cap in the spectrum of $[\text{Co}(\text{nosartacn})]^{3+}$ displayed a signal at δ = +17.8 ppm and that in $[\text{Co}(\text{amsartacnH})]^{4+}$ at δ = -13.7 ppm. The three equivalent methylene carbons of the $[\text{Co}(\text{azasartacn})]^{3+}$ cap displayed a signal at δ = +0.4 ppm which is identical with the chemical shift of the corresponding atoms in $[\text{Co}(\text{sep})]^{3+}$.

position allowed the substitution of a new group on the amine, or replacement of the amine. This led to a new class of detergents which had head group charges $\geq 3+$ and large sizes.

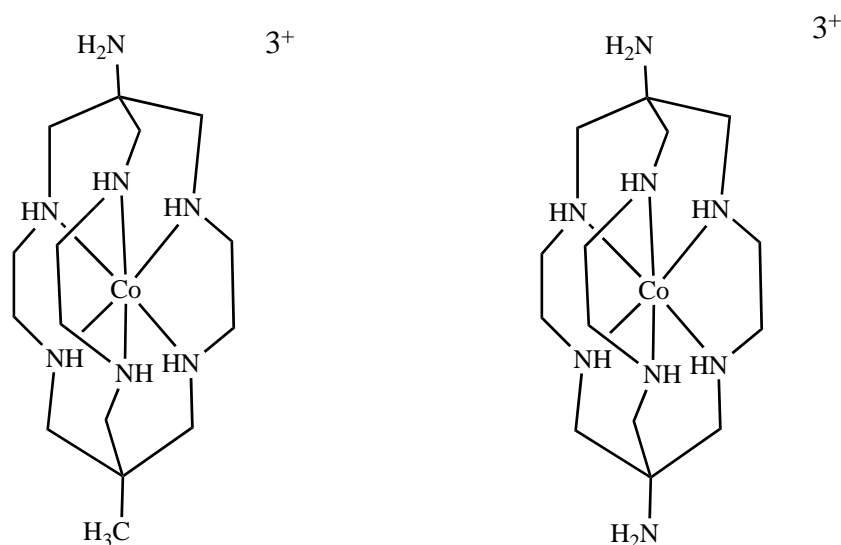


Figure 1.24: 1,8-Disubstituted $[Co(sar)]^{3+}$ complexes, *sar* = sarcophagine (or 3,6,10,13,16,19-hexaazabicyclo[6.6.6]icosane).

A mixture of 1,8 Cl, OH and NO_2 substituted $[Co(CH_3-sar)]^{3+}$ cages and some rearranged products $[Co((XCH_2, CH_3)-absar)]^{3+}$ were synthesised in water through nitrosation of the $[Co((NH_3, CH_3)-sar)]^{4+}$ ion. A CH_2 group in the absar molecules was extruded from the cage causing contraction in the cage size. The same reaction carried out in alcohol solutions, in the absence of the nucleophiles, formed the alkoxy-substituted products $[Co((RO, CH_3)-sar)]^{3+}$ along with hydrogen-, NO_2 -, OH-substituted products and rearranged $[Co((ROCH_2, CH_3)-absar)]^{3+}$ complexes, shown in figure 1.25. The substitution reaction at the appended molecules led to reductive alkylation of ethanediamine-substituted cages with aldehydes and $NaBH_3CN$ to form octyl and dioctyl derivatives.

The 1H NMR spectra of N-deuterated $[Co((RO, CH_3)-sar)]^{3+}$ derivatives displayed two multiplets at 2.65 ppm and 3.35 ppm due to the ethanediamine protons. The methylene protons of the cap appeared as two AB spin systems at c. 2.4, 3.0 and 2.5, 3.1 ppm. A singlet at c. 0.9 ppm was due to the 'cap' methyl protons. The ^{13}C NMR spectrum displayed four signals at $\delta = 51.9-56.4$ ppm indicating methylene carbons of the cage, and two signals at $\delta = 43$ ppm and at $\delta = 78$ ppm indicating inequivalent quaternary carbon atoms of the cap. A signal at $\delta = 20$ ppm indicated a methyl group and signals characteristic of alkoxy substituents were present.

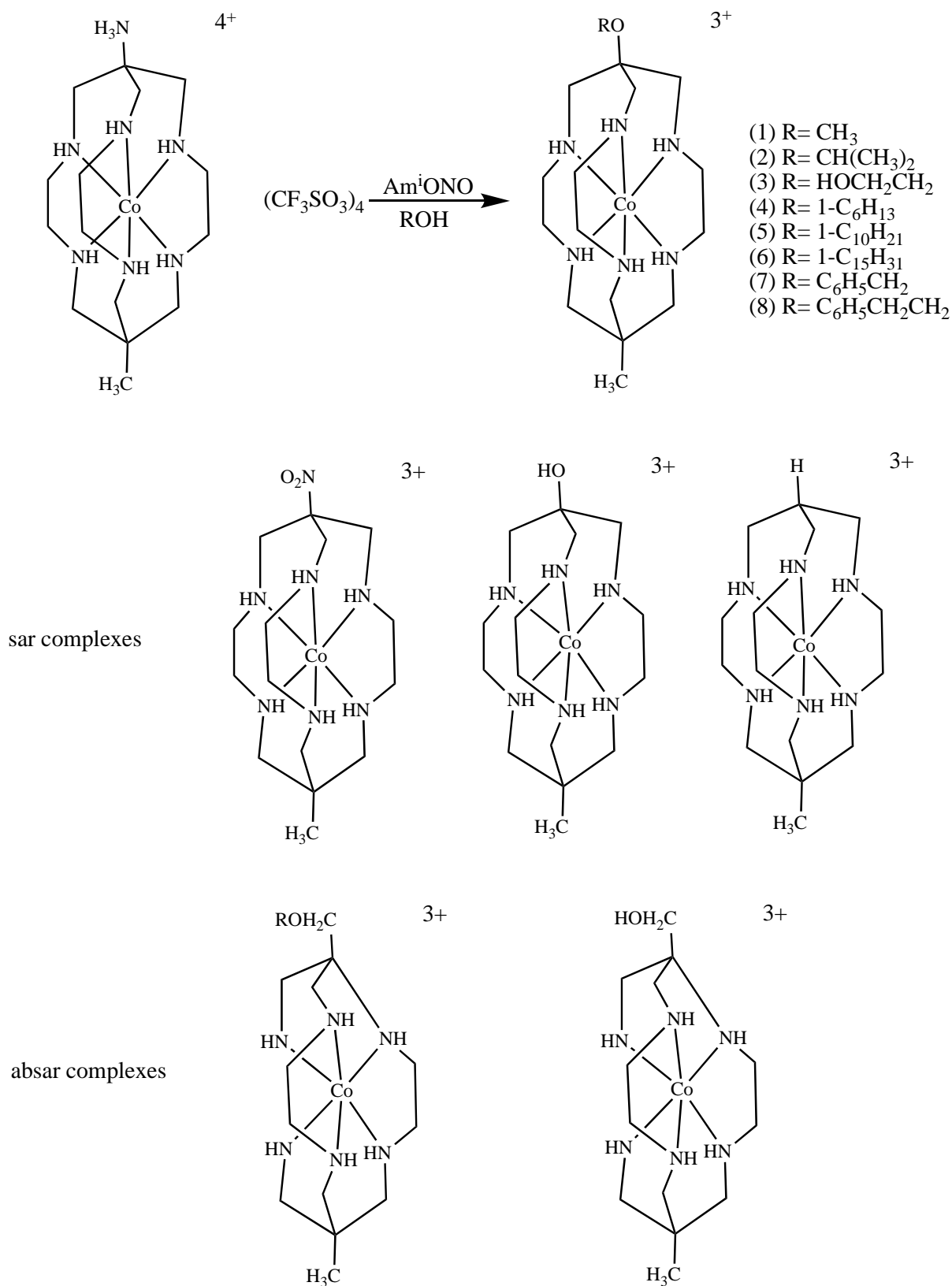


Figure 1.25: Showing the alkoxy-substituted products $[\text{Co}((\text{RO}, \text{CH}_3)\text{-sar})]^{3+}$ along with hydrogen-, NO_2 -, OH -substituted products and rearranged $[\text{Co}((\text{ROCH}_2, \text{CH}_3)\text{-absar})]^{3+}$ complexes.

The labelled $[^{57}\text{Co}((\text{NH}_3)_2\text{-sar})]\text{Cl}_5\cdot\text{H}_2\text{O}$ complex was synthesised by treating the free ligand diamsar with a mixture of tracer $^{57}\text{CoSO}_4$ and bulk carrier $\text{CoCl}_2\cdot 6\text{H}_2\text{O}$ in methanol. Some of the isolated complex was used for animal biodistribution studies and the rest was converted into the acetate complex by an ion exchange method; the acetate complex was then treated with decanal and NaBH_3CN to give the paraffin-trail complexes.

The tritiated $[^3\text{H}]\text{-}[\text{Co}((\text{NH}_3)_2\text{-sar})]\text{Cl}_5\cdot\text{H}_2\text{O}$ complex was synthesised by reacting $[\text{Co}(\text{en})_3]\text{Cl}_3$, CH_2O , $(^3\text{H})_2\text{C}=\text{O}$, CH_3NO_2 and base followed by reduction with Zn/H^+ .

A 2000 article¹⁴ reported the synthesis, chemical reactions, spectroscopic and electrochemical properties of three functionalised cobalt (III) cage complexes. The hexaaza cage complexes were synthesised by reacting $[\text{Co}(\text{sen})]^{3+}$ ($\text{sen} = 4,4',4''\text{-ethylidynetris(3-azabutan-1-amine)}$) with methanal and ethyl cyanoacetate. Ethyl cyanoacetate has nitrile and ester groups that both react with coordinated amines to give the amide, $[\text{Co}(\text{CN},\text{Me-2-oxosar-H})]^{2+}$, and amidine, $[\text{Co}(\text{Me},\text{CO}_2\text{H},2\text{-aminosar-2-ene})]^{3+}$, cage complexes and one with both functional groups, $[\text{Co}(\text{Me-2-aminosar-2-ene})]^{3+}$. These three complexes were isolated through ion exchange chromatography. The ^{13}C NMR spectrum of the amide complex displayed 16 signals which were consistent with an asymmetric cage complex. The nitrile and amide groups displayed signals at $\delta = 116.8$ and 171.3 ppm respectively. The proposed mechanism for its formation is shown in figure 1.26.

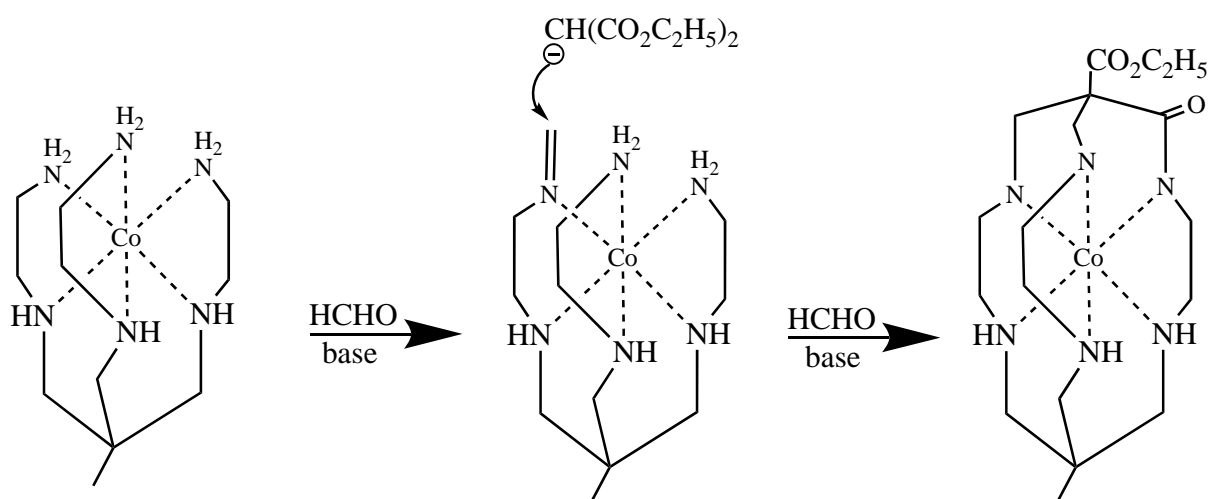


Figure 1.26: Proposed mechanism for the formation of three hexaaza cage complexes by reacting $[\text{Co}(\text{sen})]^{3+}$ ($\text{sen} = 4,4',4''\text{-ethylidynetris(3-azabutan-1-amine)}$) with methanal and ethyl cyanoacetate.

The ^{13}C NMR spectrum of the amidine complex also displayed 16 signals, consistent with an asymmetric functionalised cage, and the carboxylic acid and amidine functional groups at the apical positions displayed signals at $\delta = 173.6$ and 169.4 ppm, respectively. A single broad peak for the amidine exo NH_2 group at $\delta = 8.5$ was displayed in the ^1H NMR spectrum in $\text{Me}_2\text{SO}-d_6$. The IR spectrum displayed a $\text{C}=\text{N}$ stretch at 1671 cm^{-1} and $\text{C}=\text{O}$ stretch at 1723 cm^{-1} . The proposed mechanism for the formation of the amidine complex is shown in figure 1.27.

The final cage complex was similar to the amidine functionalised cage complex except for the carboxylic acid substituent. The ^{13}C NMR spectrum displayed 16 peaks with the peak at $\delta = 169.4$ ppm due to the amidine group. Two peaks for the amidine exo NH_2 group at $\delta = 8.35$ and 8.58 ppm were present in the ^1H NMR spectrum in $\text{Me}_2\text{SO}-d_6$. The IR spectrum displayed a $\text{C}=\text{N}$ stretch at 1654 cm^{-1} .

The amidine cage complexes were inert and stable in aqueous acid and base at room temperature. They were resistant towards nitrosation, methylation with iodomethane, tetrahydroborate reduction, and heating in nitric acid. A small amount of the complex was decomposed on prolonged hydrogenation in the presence of palladium on charcoal. X-ray analysis confirmed the structure of $[\text{Co}(\text{CN},\text{Me}-2\text{-oxosar} - \text{H})]^{2+}$ as the chloride perchlorate salt. The cyclic voltammograms showed quasi-reversible $\text{Co}^{\text{III}}-\text{Co}^{\text{II}}$ couples for the three cage complexes in aqueous solution, the potentials of which varied according to the pH of the medium. The $\text{Co}(\text{II})$ forms of the amidine cage complexes were stable at ambient temperature.

Cobalt(III) ion stabilises amidine in basic solution by inhibiting hydroxide ion attack and in acidic solution it inhibits protonation of both nitrogen positions which hinders nucleophilic additions.

The enhanced charge density at Co^{III} was proposed as the reason for the more negative potentials for all the amide and amidine cage complexes than observed for analogous hexamine cobalt(III) cage complexes.

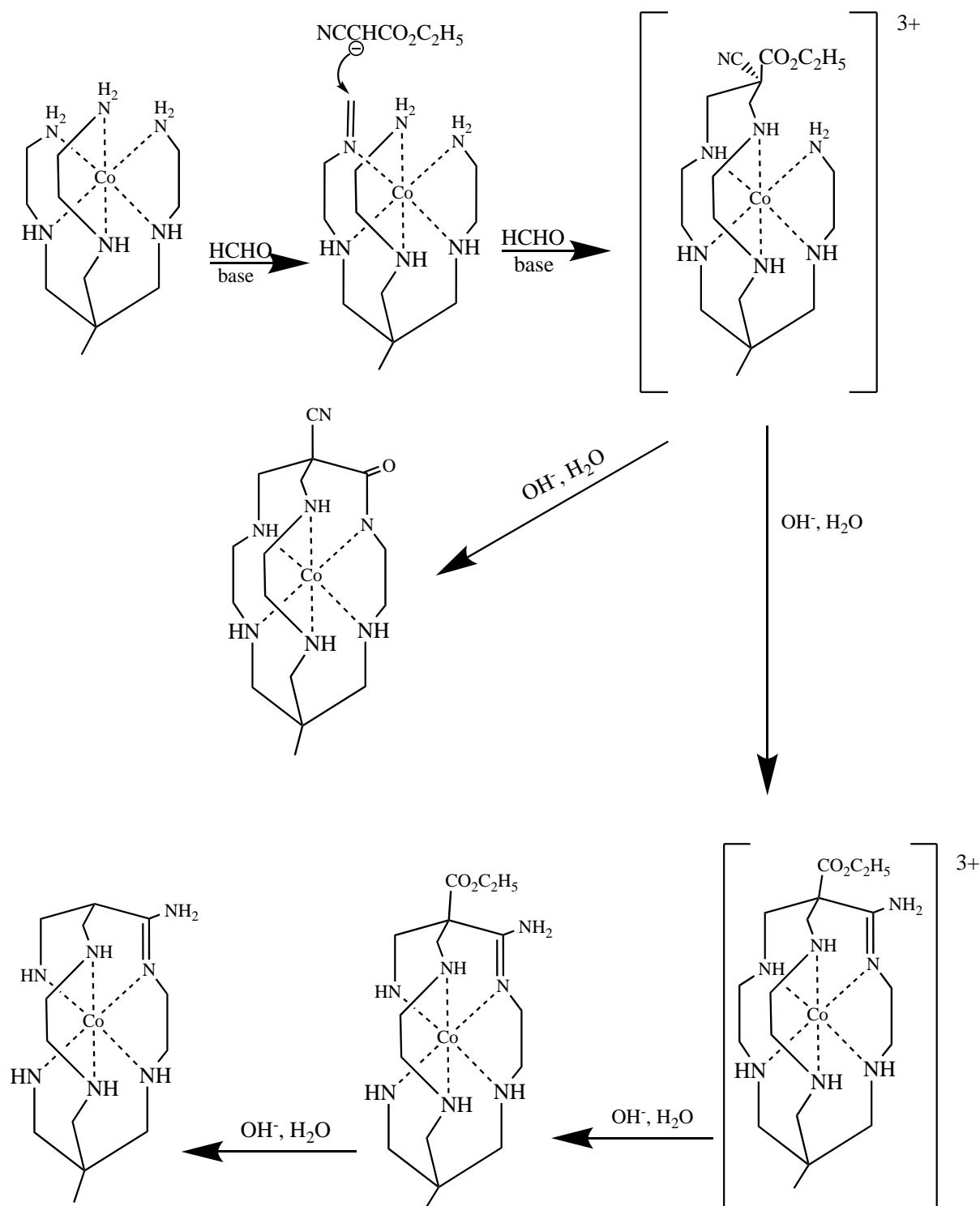


Figure 1.27: Proposed mechanism for the formation of the amidine complex.

The idea of linking coordinated ligands together has rarely been explored. In a 2013 paper¹⁵, new oxidimethaneamine-bridged Co^{III} complexes with 1,4-diazepan-6-amine (daza = L) and 6-methyl-1,4-diazepan-6-amine (Medaza = MeL) were prepared, figure 1.28, and reacted

with paraformaldehyde in an alkaline, non-aqueous medium. The condensation process was studied under variable conditions. A kinetic study of the base-catalyzed degradation of the oxidimethanaeamine bridge in aqueous solution was also performed.

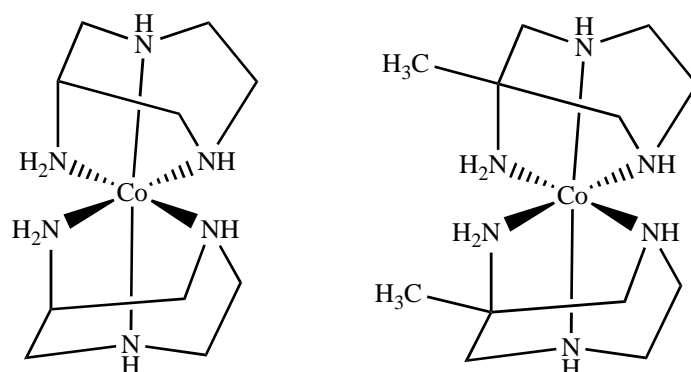


Figure 1.28: Structures of $[\text{Co}(\text{daza})_2]^{3+}$ and $[\text{Co}(\text{Medaza})_2]^{3+}$.

The reaction of the Co^{III} hexaamine complexes, which have primary and secondary amino groups, with paraformaldehyde results in the formation of $\text{NH}-\text{CH}_2-\text{O}-\text{CH}_2-\text{N}$ bridges. These bridged products have a *cis* configuration even when both the *cis*- and *trans*-isomers of $[\text{Co}(\text{daza})_2]^{3+}$ and $[\text{Co}(\text{Medaza})_2]^{3+}$ were used as a starting material. This was due to increased steric strain within the molecular framework of the *trans* isomer according to molecular mechanics calculations. The *trans* isomer rapidly converts to a *cis* arrangement during the bridging reaction because low-spin $\text{Co}(\text{III})$ is substitutionally inert. The chromatographic procedure revealed some traces of Co^{2+} which suggests that the *trans* to *cis* isomerization occurs through an intermediary $\text{Co}(\text{II})$ complex, with formaldehyde acting as a reducing agent in the presence of a base. The $\text{Co}(\text{II})$ was reoxidised by aerial oxygen. Formaldehyde attack on the coordinated amino group results in the formation of a corresponding carbinolamine. In the case of a primary amino group, methylideneimine was formed along with H_2O elimination. The mechanism behind this bridge formation is shown in figure 1.29.

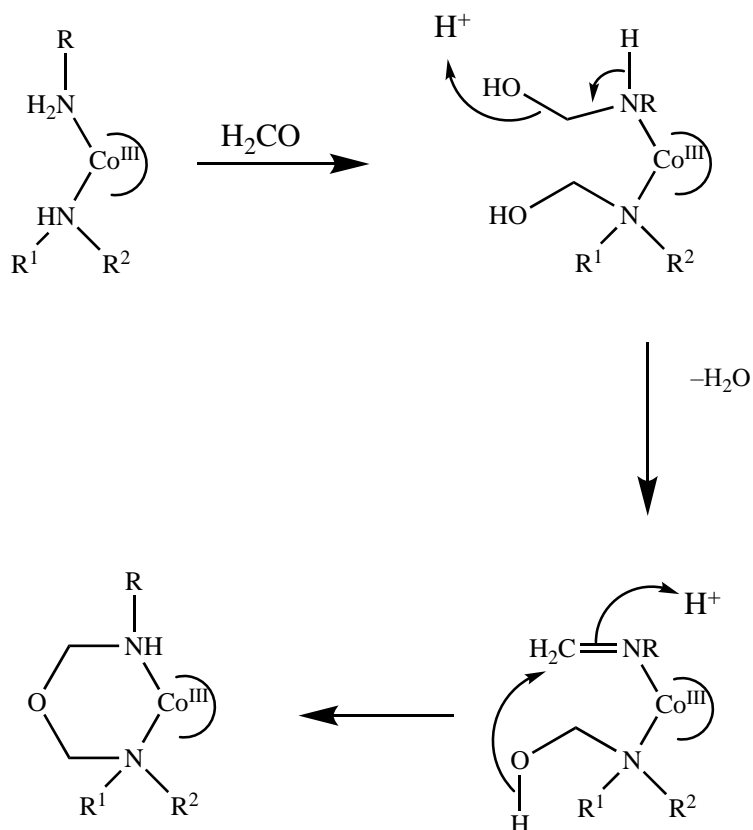


Figure 1.29: Schematic representation of the reactivity of primary and secondary amines coordinated to Co(III) with formaldehyde in an alkaline, nonaqueous medium.

According to this mechanism, the NH–CH₂–O–CH₂–N bridge is formed through the formation of an imine and an aminol. This bridge is formed easily between a primary and secondary amino group, figure 1.30(a) and (b), by conversion of their corresponding amine function to imine and hemiaminal respectively, which marks the end of the condensation reaction.

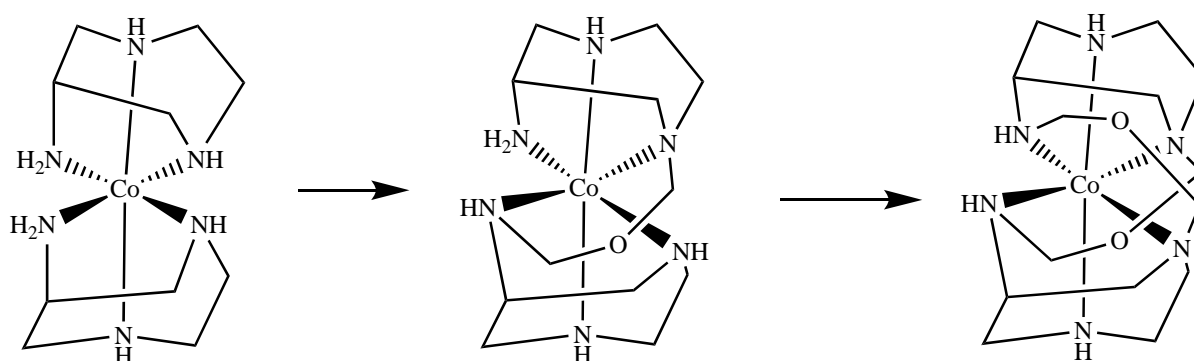


Figure 1.30(a): Oxidimethaneamine bridge formation in prim-sec NH₂ groups of [Co(daza)₂]³⁺.

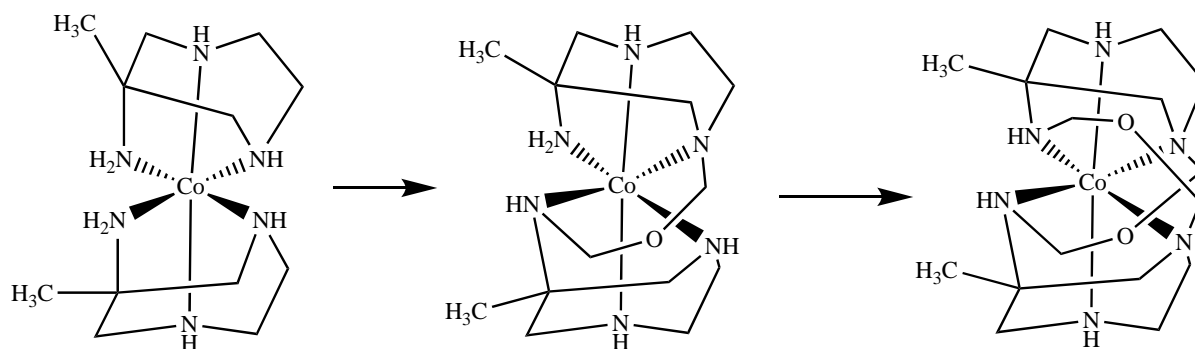


Figure 1.30(b): Oxidimethaneamine bridge formation in prim-sec NH_2 groups of $[\text{Co}(\text{Medaza})_2]^{3+}$.

In case of primary-primary (prim-prim) bridged species, both primary amino groups transform into imines resulting in the formation of diimine species, shown in figure 1.31. Thus, the formation of diimine species inhibits the bridge formation between prim-prim amino groups. Also, the competitive attack of a hemiaminal originating from the secondary amino group would interfere with the formation of a prim-prim bridge derivative. The only way to form the bridge is if one primary NH_2 group completely transforms into an imine and the other remains at the hemiaminal stage, shown in figure 1.32.

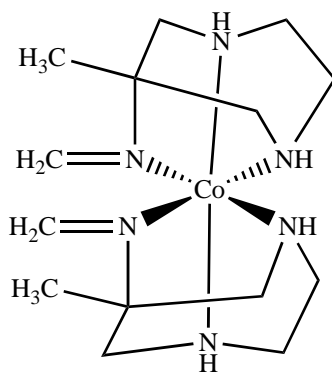


Figure 1.31: Oxidimethaneamine bridge formation in prim-prim NH_2 groups of $[\text{Co}(\text{Medaza})_2]^{3+}$.

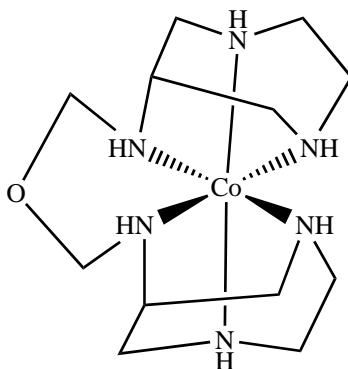


Figure 1.32: Oxidimethaneamine bridge formation in prim-prim NH_2 groups of $[\text{Co}(\text{daza})_2]^{3+}$.

The reactivity of daza and Medaza derivatives toward bridge formation is similar.

The degradation process of the oxidimethaneamine bridge occurred through a base-catalyzed reaction. This took place by an initial protonation of an ether oxygen atom by H^+ followed by an initial deprotonation of an $\text{H}(-\text{N}-\text{Co})$ bridgehead causing a $\text{C}-\text{O}$ bond rupture. The subsequent ring-opening is followed by rapid hydrolysis of the resulting imines and hemiaminals. The first bridge degradation rate is higher, which can be attributed to the enhanced steric strain in the dibridged species.

1.6 AIM

The aim of this thesis is to attempt to prepare new multidentate cage-type amine ligands through the linking of coordinated di- tri- and tetradentate amine ligands. Such an approach appears not to have been hitherto investigated. There are many polydentate N-donor ligands which contain $-\text{NH}_2$ groups, and placing two of these on a single metal ion should then allow them to be linked in a similar process to the ‘capping’ that occurs in, for example $[\text{Co}(\text{sep})]^{3+}$. Linking of these ligands will be achieved using similar condensation reactions to those used in the synthesis of Sargeson cage ligands, namely reaction with formaldehyde and ammonia. The ligands that will be investigated, namely ethylenediamine (en), diethylenetriamine (dien), tris(2-aminoethyl)amine (tren), and 2,6-bis(aminomethyl)pyridine (bamp) are shown in Figure 1.33 and the corresponding cobalt(III) complexes are shown in figure 1.34.

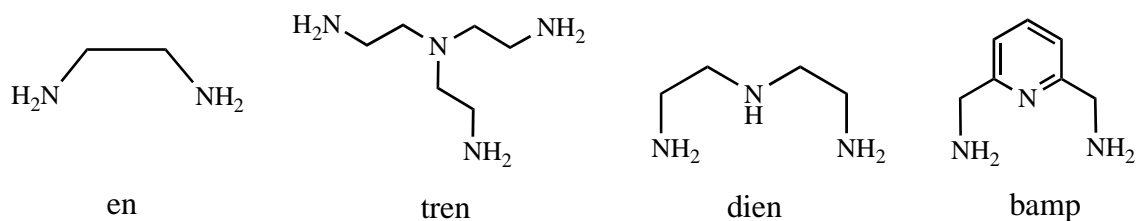


Figure 1.33: NH_2 -containing ligands that will be used to prepare cobalt(III) complexes: ethylenediamine (en), tris(2-aminoethyl)amine (tren), diethylenetriamine (dien), 2,6-bis(aminomethyl)pyridine (bamp).

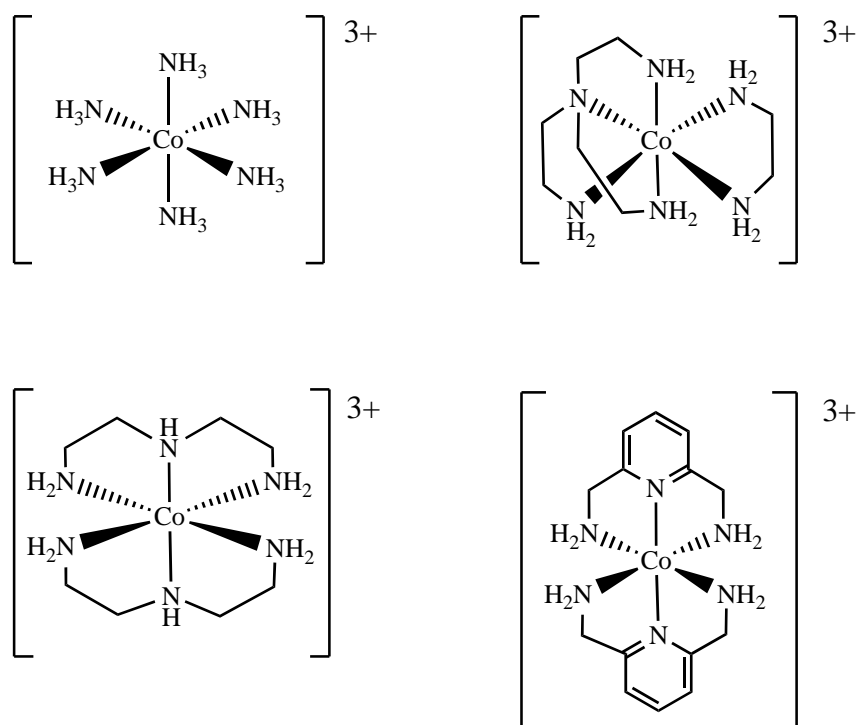


Figure 1.34: Cobalt(III) complexes that will be reacted with formaldehyde and ammonia – $[\text{Co}(\text{NH}_3)_6]^{3+}$, $[\text{Co}(\text{tren})(\text{en})]^{3+}$, $[\text{Co}(\text{dien})_2]^{3+}$, and $[\text{Co}(\text{bamp})_2]^{3+}$.

Sargeson's work with cage compounds showed that reaction with formaldehyde and ammonia resulted in the 'capping' of $[\text{Co}(\text{en})_3]^{3+}$ by an $\text{N}(\text{CH}_2)_3$ unit. Similar reactivity is expected in this case; for example, the NH_2 units in $[\text{Co}(\text{tren})(\text{en})]^{3+}$ should be able to be linked to give a new hexadentate ligand, as should those in $[\text{Co}(\text{bamp})_2]^{3+}$. The presence of both primary and secondary amines in $[\text{Co}(\text{dien})_2]^{3+}$ could result in intraligand condensation reactions with the production of strained small rings.

CHAPTER 2

EXPERIMENTAL

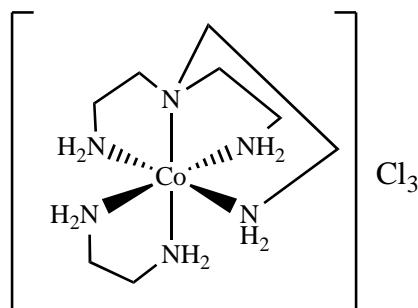
GENERAL METHODS

^{13}C NMR and ^1H NMR were recorded on a Bruker Avance 400 MHz spectrometer at 25.0 ± 0.5 °C. Solutions were made up in D_2O or CDCl_3 using sodium 3-(trimethylsilyl) tetra-deuterio-propionate (NaTSP, ^1H NMR, D_2O , 0.00ppm), CHCl_3 (^1H NMR, CDCl_3 , 7.26 ppm and ^{13}C NMR, CDCl_3 , 77.08 ppm). High-resolution mass spectra were recorded on a Bruker MicrOTOF-Q (Bruker Daltronics, Bremen, Germany) using electrospray ionisation (ESI) in positive mode. SI-MS analyses were conducted using an Agilent 1260 Infinity Quaternary LC System hyphenates to an Agilent 6420 °C Triple Quadruple Mass Spectrometer with electrospray ionisation source (ESI). The following MS ionisation source conditions were used: capillary voltage 4 kV, drying gas temperature 300 °C, drying gas flow 6 L min^{-1} , nebulizer pressure 12 psi. The sample was dissolved in methanol at a concentration of 1 mg/mL and diluted to 5 $\mu\text{g/mL}$ with methanol before directly injecting into the LCMS. A one-minute full scan with a range of 100-1000 m/z was recorded and analysed using Mass Hunter Qualitative analysis software.

Density functional theory (DFT) calculations were performed in Gaussian 16.¹⁶ Geometry optimisations employed the M06 functional¹⁷ and a mixed basis set consisting of LANL2DZ on the metal and 6-31G(d) on other atoms. The ultrafine integration grid of Gaussian 16 was used, as were Cartesian d functions (6D). The calculations were performed in the gas phase.

All reagents and solvents were purchased from sigma-aldrich and were used without further purification.

2.1 Synthesis of $[\text{Co}(\text{tren})(\text{en})]\text{Cl}_3$



2.1.1 Synthesis of $[\text{Co}(\text{tren})(\text{NO}_2)_2]\text{Cl}$

A solution of tren (14.60 g, 0.09716 mol) in 100 mL of ice-cold water was added to 100 mL of an ice-cold aqueous solution of $[\text{Co}(\text{OH}_2)_6]\text{Cl}_2$ (23.80 g, 0.1000 mol) followed by immediate addition of solid NaNO_2 (13.8 g, 0.201 mol) with stirring. The colour of the solution changed from pink to dark green. Air was bubbled through the solution for 3 h, after which time the solution was reduced to dryness (rotavapor) to give a dark brown-red coloured solid. This was recrystallised from hot water to give $[\text{Co}(\text{tren})(\text{NO}_2)_2]\text{Cl}$ as yellowish-greenish crystals (3.20 g, 9.13 % yield). The dark pink coloured mother liquor was retained and treated as described below.

2.1.2 Synthesis of $[\text{Co}(\text{tren})\text{Cl}_2]\text{Cl}$

- The yellowish-greenish crystals of the dinitro compound was treated with conc. HCl (14.5 mL, 10 mole equivalents) to give a parrot green solution. This was evaporated to dryness on a steam bath to give $[\text{Co}(\text{tren})\text{Cl}_2]\text{Cl}$ (3.1 g) as a deep blue powder.
- The mother liquor from the synthesis of $[\text{Co}(\text{NO}_2)_2(\text{tren})]\text{Cl}$ was also treated with conc. HCl (20 mL), resulting in vigorous bubbling and evolution of nitrogen oxides. The colour of the solution changed from orange red to bluish-purple. The solution was evaporated to dryness on a steam bath to give dark-blue $[\text{Co}(\text{tren})\text{Cl}_2]\text{Cl}$ (31.64 g).

2.1.3 Synthesis of $[\text{Co}(\text{tren})(\text{en})]\text{Cl}_3$

- $[\text{Co}(\text{tren})\text{Cl}_2]\text{Cl}$ (3.1 g) was dissolved in water (15 mL), ethylenediamine (0.45 g) was added, and the solution was heated for 30 min on a steam bath, turning orange-red over this time. Following cooling to room temperature, the solution was diluted to 1 L with H_2O , and

sorbed onto a Sephadex SP-C25 cation exchange column. An orange-red band was eluted with 0.2 mol L^{-1} NaCl; this was collected and taken to dryness (rotavap). The orange powder was dissolved in 500 mL H_2O and loaded onto a Dowex 50W X2 cation exchange column. The column was washed with 0.1 mol L^{-1} HCl to remove Na^+ ions and the product was then eluted with 3 mol L^{-1} HCl. The orange eluate collected from this column was then reduced to dryness (rotavap) to give $[\text{Co}(\text{tren})(\text{en})]\text{Cl}_3$ as an orange-yellow powder. ^1H NMR (400 MHz, D_2O): δ 5.2 (br s, 1H), 4.9 (br s, 1H), 4.56 (br s, 1H), 3.5 – 3.21 (m, 2H), 3.15 (d, 1H), 3.0 (t, 1H), 2.80 (s, 1H). ^{13}C NMR (100 MHz, D_2O): δ = 62.82, 61.09, 45.71, 44.95, 44.73, 44.50, 43.82 ppm. ESI-MS: Calcd for $\text{C}_8\text{H}_{24}\text{N}_6\text{Co}^+$, 263.1; found 263.1.

b) The 31.64 g of $[\text{Co}(\text{tren})\text{Cl}_2]\text{Cl}$ from part b) above was dissolved in 300 mL water, ethylenediamine (5.75 g) was added, the solution heated on a steam bath for 30 min and then cooled. The solution was diluted to 2 L with H_2O and loaded onto a Dowex 50W X2 cation exchange column. Red and orange bands were eluted with 1 mol L^{-1} HCl and 6 mol L^{-1} HCl respectively. The orange eluate was then reduced to dryness (rotavap) to give $[\text{Co}(\text{tren})(\text{en})]\text{Cl}_3$ as an orange-yellow solid, which was recrystallised from hot water to give yellow crystals of $[\text{Co}(\text{tren})(\text{en})]\text{Cl}_3$ (5.24 g, 14.74 % yield). These were washed with ice-cold water and isopropanol and air-dried. ^1H NMR (400 MHz, D_2O): δ 5.2 (s, 1H), 4.7 (s, 1H), 3.3 (m, 0.37H), 2.9 (t, 0.08H), 2.7 (m, 0.18H). ^{13}C NMR (100 MHz, D_2O): δ = 62.74, 61.01, 45.44, 44.71, 44.19, 43.49 ppm. ESI-MS: Calcd for $\text{C}_8\text{H}_{24}\text{N}_6\text{Co}^+$, 263.1; found 263.0

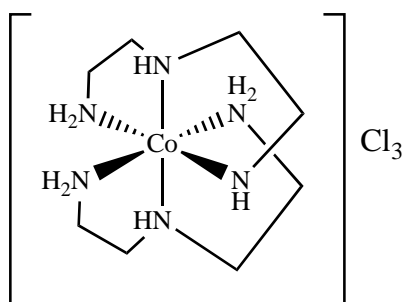
2.1.4. Reaction of $[\text{Co}(\text{tren})(\text{en})]\text{Cl}_3$ with ammonia and formaldehyde

To a stirred yellow solution containing $[\text{Co}(\text{tren})(\text{en})]\text{Cl}_3$ (4.00 g, 0.0150 mol), and Li_2CO_3 (15 g) in 75 mL H_2O were added aqueous NH_3 (99 mL diluted to 300 mL with water) and 37 % aqueous formaldehyde solution (360 mL) simultaneously over an hour with continuous stirring. The colour of the mixture changed to red over this time with the evolution of heat. The mixture was stirred for an additional 30 minutes after the addition of ammonia and formaldehyde. The mixture was filtered to remove unreacted lithium carbonate and the pH of the filtrate was adjusted to approximately 3 using 12 mol L^{-1} HCl. The solution was then diluted to 1 L with water and sorbed onto a Dowex 50W X2 cation exchange column. The column was washed with 1 mol L^{-1} HCl, and a red-orange band was removed with 3 mol L^{-1} HCl; this was reduced to dryness (rotavapor) to give a hygroscopic purplish-pink sticky

material which was washed with isopropanol to obtain a purple powder (1.10 g). This powder was hygroscopic.

^1H NMR (400 MHz, D_2O): δ 7.52 (br s, 1H), 7.02 (br s, 1H), 5.25 (br s, 2H), 4.48-2.60 (br m, 54H). ^{13}C NMR (100 MHz, D_2O): 69.10, 68.72, 67.96, 67.59, 67.17, 60.17, 60.03, 59.56, 58.45, 58.19, 55.33, 54.32, 54.11, 53.25, 52.96, 42.81, 42.59, 42.16, 41.91, 33.49, 33.35 ppm. ESI-MS: Calculated for $\text{CoC}_{12}\text{H}_{30}\text{N}_7\text{Cl}^+$, 366.1580; found 366.1575

2.2 Synthesis of $[\text{Co}(\text{dien})_2]\text{Cl}_3$



2.2.1. $[\text{Co}(\text{NH}_3)_5\text{Cl}]\text{Cl}_2$: Chloropentaamminecobalt(III) chloride was synthesised by the procedure reported in the literature.

Ammonium chloride (25 g, 0.47 mol) was dissolved completely in 150 mL concentrated aqueous ammonia. With continuous stirring, $[\text{Co}(\text{OH}_2)_6]\text{Cl}_2$ (50 g, 0.21 mol) was added in small portions and a pinkish-brown slurry was obtained, to which was added 30% hydrogen peroxide (40 mL) slowly, causing effervescence. When the effervescence stopped, 150 mL concentrated HCl was added slowly. The mixture was heated on a steam bath for 15 minutes, cooled in an ice-bath and the resulting purple precipitate was removed by filtration. The product was washed with ice-cold water (100 mL in portions), followed by 6 mol L^{-1} HCl (100 mL). An ethanol (100 mL) wash was followed by an acetone wash (50 mL) which facilitated drying. The yield of the product was 30.20 g (57.42 % yield).

2.2.2. $[\text{Co}(\text{dien})_2]\text{X}_3$ ($\text{X} = \text{Cl}, \text{Br}$): To a slurry of charcoal (6.04 g) and $[\text{Co}(\text{NH}_3)_5\text{Cl}]\text{Cl}_2$ (30.2 g, 0.120 mol) in 400 mL water, dien (27.37 g, 0.2652 mol) was added with stirring. The mixture was heated on a steam bath for 3 h, and was then filtered through celite to remove the charcoal. The orange-yellow filtrate containing $[\text{Co}(\text{dien})_2]\text{Cl}_3$ was cooled and reduced to dryness (rotavap). The bromide salt of the complex crystallised from hot water on addition of

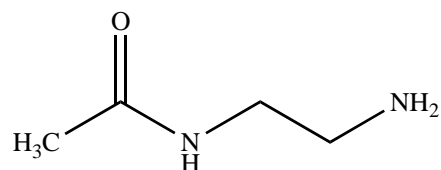
sodium bromide and cooling in an ice-bath. The yellow crystals were removed by filtration, dissolved in water (1000 mL) and the solution was loaded onto a Dowex 50W X2 cation exchange column. The orange-red eluate was collected in fractions of 100 mL and reduced to dryness (rotavap). The fractions which showed similar NMR data to those for the mer-isomer were dissolved in water, combined, reduced to dryness, and washed with ethanol and air-dried to get an orange powder. The yield was 4.80 g. ^1H NMR (400 MHz, D_2O): δ 7.4 (br s, 1H), 4.85 (br s, 1H), 4.48 (br d, 2H), 3.08 (m, 6H), 2.85 (m, 2H). ^{13}C NMR (100MHz, D_2O): δ 50.62, 47.54, 46.25 and small intensity peaks at 55.06, 53.38, 43.77 and 42.54. ESI-MS: Calculated for $\text{CoC}_8\text{H}_{22}\text{N}_5\text{Cl}^+$, 282.1; found 282.2

2.2.3. Reaction of $[\text{Co}(\text{dien})_2]\text{Cl}_3$ with ammonia and formaldehyde

To a stirred mixture of $[\text{Co}(\text{dien})_2]\text{Cl}_3$ (2.03 g, 0.00546 mol) and Li_2CO_3 (5.31 g) in H_2O (26 mL), were added 37 % aqueous formaldehyde solution (128 mL) and concentrated aqueous NH_3 (35 mL diluted to 106 mL with H_2O) simultaneously over 30 min with continuous stirring. The colour of the mixture changed from yellow to orange-red over this time with the evolution of heat. The reaction mixture was stirred for an additional 30 minutes after the addition of ammonia and formaldehyde. The reaction mixture was filtered to remove unreacted Li_2CO_3 and the pH of the filtrate was adjusted to 1.5 using conc. HCl. The solution was then diluted to 1 L with H_2O and sorbed onto a Dowex 50W X2 cation exchange column. The column was washed with 1 mol L^{-1} HCl, then an orange band was eluted with 3 mol L^{-1} HCl; this was collected and reduced to dryness (rotavap) to give a reddish orange material (1.425 g). ^1H NMR (400 MHz, D_2O): δ 7.7 (br m, 1H), 4.9 (br m, 1H), 4.5 (d, 1H), 4.3–3.9 (br m, 2H) 3.7 – 2.5 (br m, 18H) . ^{13}C NMR (100 MHz, D_2O): δ 174.80 ppm, 81.74 – 36.60 ppm. ESI-MS: found 365.1 and 323.0 for $\text{C}_{12}\text{H}_{29}\text{N}_7\text{ClCo}^{+2}$ and $\text{C}_{10}\text{H}_{25}\text{N}_6\text{ClCo}^+$ respectively. Crystallisation of the product was attempted by dissolution in acetonitrile and slow evaporation. This was unsuccessful.

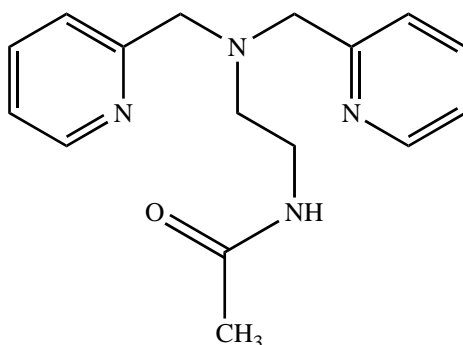
2.3 Attempted synthesis of uns-penp

2.3.1 Synthesis of N-acetylethylenediamine:



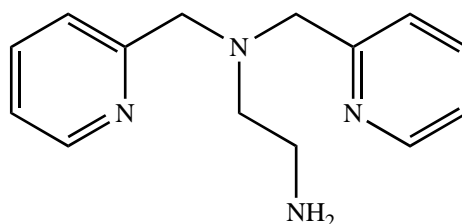
A solution of ethylenediamine (20.1 g, 0.334 mol) and ethyl acetate (7.29 g, 0.0827 mol) was refluxed for 24 h. The solvent was removed (rotavap), and the residue was distilled (130 °C, 3 mmHg) to give the product as a yellow oil (3.90 g, 46.20 % yield). ^1H NMR (400 MHz, D_2O): δ 4.67 (s, 1 H), 3.12 (s, 1 H), 3.06 (t, 1 H), 2.55 (t, 1 H), 1.84 (s, 1 H). ^{13}C NMR (100 MHz, D_2O): δ 173.97, 41.71, 39.66, 38.71, 22.12 ppm.

2.3.2. Synthesis of N-acetyl-uns-penp:



To a solution of N-acetylethylenediamine (1.02 g, 0.00998 mol) and 2-pyridinecarboxyaldehyde (2.14 g, 0.0199 mol) in 1,2-dichloroethane (\approx 20 mL), was added $\text{NaBH}(\text{OAc})_3$ (6.0 g, 0.0283 mol) and the mixture was stirred for 3 h at room temperature. With continuous stirring, 2 mol L^{-1} aq. NaOH (100 mL) was added and the mixture was extracted using CH_2Cl_2 (100 mL x2). The organic fractions were combined, washed with saturated NaCl (100 mL) and dried over Na_2SO_4 before filtering and removing the solvent (rotavap). This procedure was also carried out under nitrogen. Both the crops were combined by dissolution in chloroform and removal of solvent (rotavap), yielding 3.35 g (58.97 %) of N-acetyl-uns-penp. ^1H NMR: δ 9.6 (s, 1H), 8.3 (s, 1H), 8.2 (m, 1H), 7.9 (s, 1H), 7.6 (t, 2H), 7.5 (d, 2H), 7.3 (s, 1H), 7.17 (m, 1H), 4.72 (s, 1H), 4.4 (s, 1H), 3.5 (m, 2H), 3.4 (m, 1H), 3.3 (m, 1H), 3.25 (t, 1H), 3.14 (s, 1H), 1.72 (s, 1H). ^{13}C NMR: δ 194.2, 173.9, 164.03, 152.02, 148.9, 138.55, 126.06, 122.04, 70.94, 69.35, 59.52, 58.00, 44.62, 44.11, 39.41, 21.8 ppm.

2.3.3. Attempted synthesis of Uns-penp:

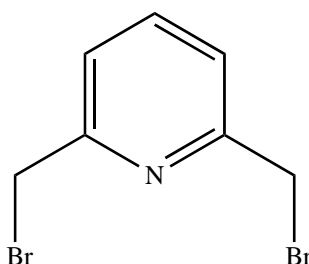


A solution of N-acetyl-uns-penp (2.20 g, 0.00773 mol) dissolved in 5 mol L⁻¹ HCl (50 mL) was refluxed for 24 h at 110 °C. The mixture was then cooled to room temperature, made basic with 2 mol L⁻¹ NaOH, and extracted using CH₂Cl₂ (50 mL x3). The organic fractions were combined and dried over MgSO₄. Following filtration, the resulting solution was reduced to dryness (rotavap). ¹H NMR: δ 8.13 (d, 1H), 7.97 (s, 1H), 7.49 (m, 2H), 7.09 (t, 1H), 4.72 (s, 2H), 3.79 (s, 2H). ¹³C NMR: δ 164.23, 151.7, 148.09, 137.94, 122.92, 122.71, 59.59 ppm along with small intensity peaks over the region δ 194.22 – 57.96 ppm. ESI-MS: Calculated for C₁₄H₁₈N₄⁺, 242.15; found 243.1

Although the mass spec data appeared promising, the NMR of the product obtained from this reaction was not consistent with it being uns-penp¹⁸.

2.4. Synthesis of [Co(bamp)₂]Cl₃

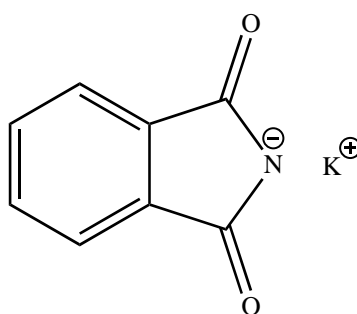
2.4.1. Synthesis of 2,6-dibromomethylpyridine:



A stirred yellow solution of 2,6-pyridinedimethanol (7.0 g, 0.050 mol) and HBr (50 mL, 0.61 mol) was refluxed for 18 h. A white precipitate was formed when the solution was cooled to room temperature in an ice-bath. Excess solvent was removed (rotavap) and HBr (50 mL) was added to the resulting residue. The mixture was again refluxed for 18 h, the solution was

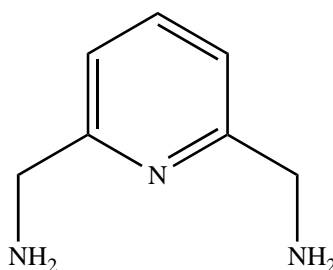
cooled to room temperature in an ice-bath to form a white precipitate, and excess solvent was removed (rotavap). The product was treated with 50 mL NaOH (0.1 mol L⁻¹) and then extracted immediately with chloroform (50 mL x4). The organic fractions were combined and reduced to dryness (rotavap), to obtain the product as a pale pinkish solid (8.20 g, 61.5 % yield). ¹H NMR (400 MHz, CDCl₃): δ 7.7 (t, 1 H), 7.3 (d, 2 H), 4.5 (s, 4 H). ¹³C NMR (100 MHz, CDCl₃): δ 156.73, 138.15, 122.82 (pyridine), 33.42 (methylene) ppm.

2.4.2. Synthesis of potassium phthalimide:



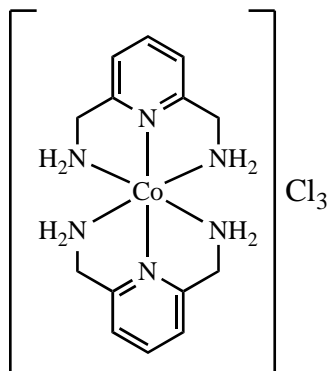
In a small round-bottom flask, a solution of phthalimide (8.0 g, 0.054 mol) in ethanol (160 mL) was refluxed gently for 20 min. The hot solution was decanted from any solid and added to a potassium hydroxide solution (12 mL), which was made by dissolving KOH (6.1 g) in water (6.0 mL) and absolute alcohol (18 mL). The solution was stirred and cooled to room temperature (ice-bath) and the resulting precipitate was filtered and air-dried. The alcoholic mother liquor was used for another crop of potassium phthalimide by repeating the above procedure. The two crops were combined and washed with acetone (200 mL) to get white, shiny, fluffy crystals of potassium phthalimide (11.93 g, 59.08 % yield).

2.4.3. Synthesis of 2,6-diaminomethylpyridine:



A stirred solution of 2,6-dibromomethylpyridine (2.36 g, 0.00890 mol) and potassium phthalimide (3.30 g, 0.0178 mol) in 10 mL DMF was heated to 155 °C under reflux for 48 h. The solution was then cooled to room temperature (ice-bath), water (20 mL) was added, and the resulting white precipitate was removed by filtration. This was then dispersed into 20 mL ethyl alcohol, to which hydrazine hydrate (1.67 mL) was added and the mixture was refluxed for 24 h. A white solid was formed after 15 minutes of refluxing. After the completion of reflux, the mixture was cooled to room temperature (ice-bath) and 6 mol L⁻¹ HCl (20 mL) was added which dissolved the white solid. The solution was then refluxed for 2 h followed by continuous stirring for 10 h at room temperature. The resulting yellow-brown solution was filtered, and the filtrate was made basic using 6 mol L⁻¹ KOH (5-10 mL). This was extracted with chloroform (x3) and the organic fractions were combined and dried over Na₂SO₄. The solid was removed by filtration and the filtrate was reduced to dryness (rotavap) to obtain 2,6-diaminomethylpyridine (0.41 g, 33.6 % yield). ¹H NMR (400 MHz, CDCl₃): δ 7.6 (t, 1 H), 7.1 (d, 2 H), 2.1 (s, 4H). ¹³C NMR (100 MHz, CDCl₃): δ 161.24, 137.03, 136.75, 119.21, 118.90, 118.47, 64.29, 47.60, 47.33 ppm.

2.4.4. Synthesis of [Co(2,6-diaminomethylpyridine)₂]Cl₃:



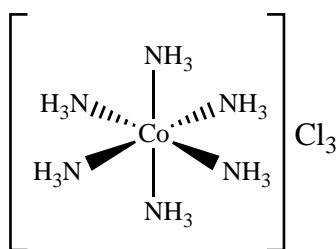
To a stirred solution of 2,6-diaminomethylpyridine (0.41 g, 0.0029 mol) in 40 mL H₂O, was added cobalt(II) perchlorate hexahydrate (0.55 g, 0.00015 mol) and air was bubbled through the solution for an hour. The colour of the orange-brownish solution changed slightly to brown. The solution was then diluted to 50 mL H₂O before loading it onto a Dowex 50W X2 cation exchange column. The column was washed with 1 mol L⁻¹ HCl and a yellow band was eluted with 3 mol L⁻¹ HCl; this was then reduced to dryness (rotavap), yielding orange-brown

solid $[\text{Co}(2,6\text{-diaminimethylpyridine})_2]\text{Cl}_3$ (0.65 g, 100%) as an orange-brown solid. ^1H NMR (400 MHz, D_2O): δ 8.1 (t, 1 H), 7.6 (d, 2H), 5.2 (s, 3 H), 4.6 (t, 4H). ^{13}C NMR (100 MHz, D_2O): δ 162.43, 141.84, 121.41, 51.93, 51.82. ESI-MS calculated for $\text{CoC}_{14}\text{H}_{20}\text{N}_6^+$, 331.10; found 331.1.

2.4.5. Reaction of $[\text{Co}(2,6\text{-diaminomethylpyridine})_2]\text{Cl}_3$ with formaldehyde and ammonia:

To a stirred solution of $[\text{Co}(2,6\text{-diaminimethylpyridine})_2]\text{Cl}_3$ (0.65 g, 0.0014 mol), and Li_2CO_3 (1.01 g) in 5.07 mL H_2O were added a 37 % aqueous formaldehyde solution (24.30 mL) and a concentrated aqueous NH_3 solution (6.70 mL diluted to 20 mL with H_2O) simultaneously dropwise over 30 min with continuous stirring. The colour of the mixture changed from orange to reddish orange with the evolution of heat over this time. The mixture was stirred for an additional 40 minutes after the addition of formaldehyde and ammonia. The mixture was filtered to remove unreacted lithium carbonate and the pH of the filtrate was adjusted to 1.5 with 12 mol L^{-1} HCl. The solution was then diluted to 1 L with water and sorbed onto a Dowex 50W X2 cation exchange column. The column was washed with 1 mol L^{-1} HCl and a yellow band was eluted with 3 mol L^{-1} HCl; this was collected and reduced to dryness (rotavap) to give yellow crystals (0.17 g). ^1H NMR (400 MHz, D_2O): δ 8.39 (t, 1H), 8.31 (t, 2H), 7.84 (d, 2H), 7.78 (d, 1H), 5.39 (s, 4H), 4.27 (s, 2H), 4.0 (m, 10H), 3.85 (m, 7H). ^{13}C NMR (100 MHz, D_2O): δ 174.46, 165.15, 164.63, 162.54, 151.50, 143.81, 143.35, 143.02, 139.01, 124.34, 123.57, 123.29, 122.99, 122.07, 91.15, 78.61, 78.52, 78.46, 78.24, 65.74, 64.57, 64.46, 63.44, 42.65 ppm. ESI-MS: Calculated for $\text{CoC}_{14}\text{H}_{18}\text{N}_5^+$, 315.08; found 315.0.

2.5.1 Synthesis of hexaamminecobalt(III) chloride



To a stirred pink solution of $[\text{Co}(\text{OH}_2)_6]\text{Cl}_2$ (24 g, 0.10 mol) and NH_4Cl (16 g, 0.29 mol) in 20 mL H_2O , was added charcoal (0.4 g) and NH_3 (50 mL), which turned the solution to brownish-red. Air was bubbled through the solution for 3 h, and it was then filtered, and the product crystallised from the filtrate as brown crystals. A yellow-brown slurry of these crystals prepared in 150 mL H_2O containing 2.5 mL HCl was heated for half an hour. The solution was then filtered hot to get brownish yellow filtrate. In the fume hood, a precipitate was formed instantly when concentrated HCl (40 mL) was added slowly to the filtrate kept in an ice-bath and the temperature was reduced slowly to 0° . The precipitate was filtered and washed first with 60 per cent ethanol, followed by 95 per cent and 99 per cent ethanol to obtain yellow crystals of $[\text{Co}(\text{NH}_3)_6]\text{Cl}_3$ (16.15 g, 60 % yield). ^1H NMR (400 MHz, D_2O) δ : 3.5 (s, 1 H). ESI-MS: Calculated for $\text{CoN}_6\text{H}_{18}^+$, 161.09; found 162.0.

2.5.2 Reaction of $[\text{Co}(\text{NH}_3)_6]\text{Cl}_3$ with Ammonia and Formaldehyde:

To a stirred solution of $[\text{Co}(\text{NH}_3)_6]\text{Cl}_3$ (3.35 g, 0.0125 mol), and Li_2CO_3 (12.5 g) in 62.5 mL H_2O were added 37 % aqueous formaldehyde solution (300 mL) and concentrated aqueous NH_3 (82.5 mL diluted to 250 mL with H_2O) simultaneously for a period of 30 minutes with continuous stirring. The mixture warmed and its colour changed from orange to red-brown over this time. The mixture was stirred for an additional 30 minutes after the addition of formaldehyde and ammonia. The mixture was filtered to remove unreacted Li_2CO_3 and the filtrate was adjusted to pH 3 using concentrated HCl (≈ 50 mL). The acidic solution was diluted to 2 L with H_2O and sorbed onto a Dowex 50W X2 cation exchange column. The column was washed with 1 mol L^{-1} HCl , then a red-orange band was removed with 3 mol L^{-1} HCl , which was reduced it to dryness (rotavap) to give a reddish-purple solid (2.22 g, 47.2 % yield). It was not completely soluble in water, so the aqueous solution was filtered to separate the purple powder and the filtrate was reduced to dryness (rotavap) to give a brownish-purple solid (0.62 g). ^1H NMR (400 MHz, D_2O): δ 4.2 (t, 1H), 4.0 (br m, 4H), 3.8-3.4 (br m, 3H), 3.2 - 2.8 (br m, 2H). ^{13}C NMR (100 MHz, D_2O): δ 179.10, 81.77, 69.45, 68.80, 65.72 ppm. ESI-MS calculated for $\text{CoC}_{12}\text{H}_{28}\text{N}_{10}^+$, 371.18; found 371.0.

CHAPTER 3

RESULTS AND DISCUSSION

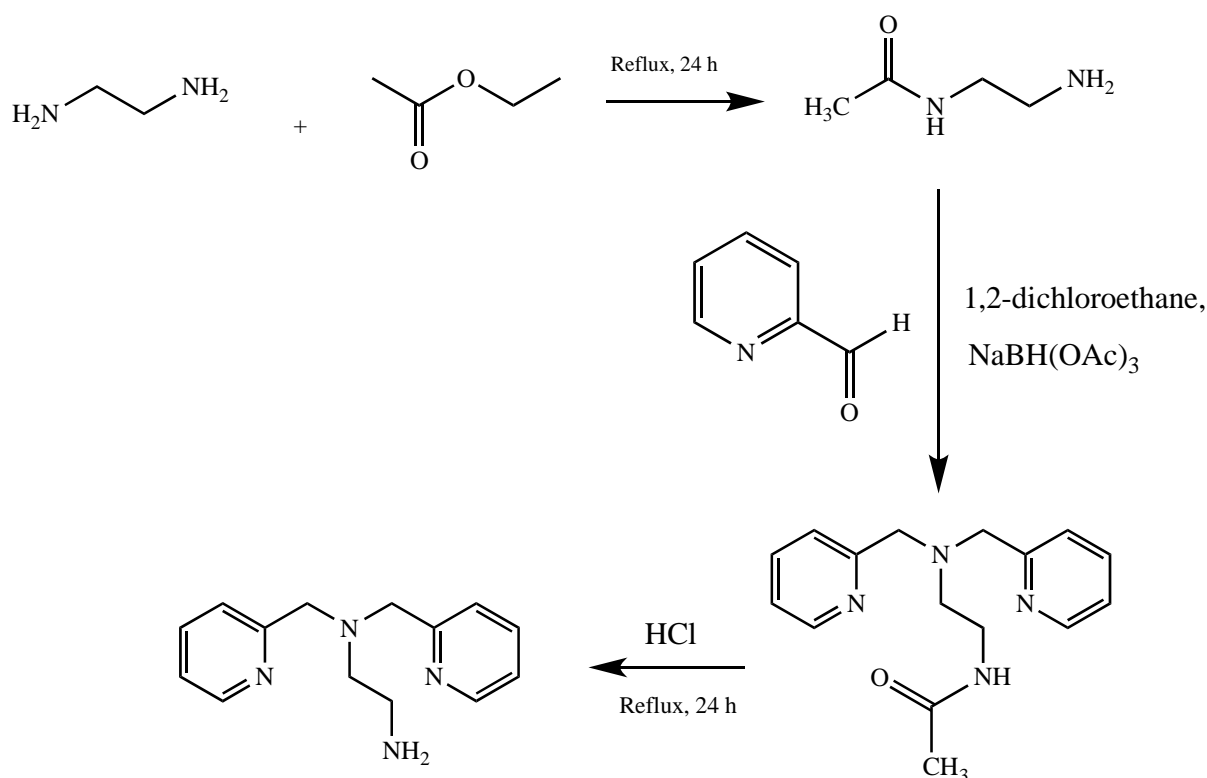
3.1 Preface

The aim of this thesis was to prepare new multidentate amine ligands by linking coordinated -NH₂-containing amine ligands in transition metal complexes through reaction with formaldehyde and ammonia. In order to achieve this, it was first necessary to prepare the appropriate starting complexes, which in some cases required the synthesis of ligands.

3.2 Synthesis and characterisation of ligands

3.2.1 Attempted synthesis of uns-penp

The attempted synthesis of this ligand followed the method of¹⁸ using the reaction of N-acetyleneethylenediamine with 2-pyridinecarboxaldehyde and subsequent deprotection according to the following reaction Scheme 1.



Scheme 1: Synthesis of the ligand uns-penp.

3.2.1.1 Synthesis and characterisation of N-acetythylenediamine.

N-acetythylenediamine was synthesised by refluxing a solution of ethylenediamine and ethyl acetate for 24 h. Excess solvent was removed on the rotavap and the product was isolated as a yellow oil after distillation. N-acetythylenediamine was characterised by ^1H NMR and ^{13}C NMR, shown in figure 3.2(a) and 3.2(b). The ^1H NMR spectrum displayed five signals in the region $\delta = 1.84$ to 3.2 ppm. A singlet peak at 1.84 ppm is due to the protons of **1** NH_2 , a singlet at 2.55 ppm was assigned to the acetyl methyl protons **6**, and a singlet at 4.67 ppm was assigned to the **4** NH protons. Two triplets observed at 3.06 and 3.12 ppm were due to the methylene protons **3** and **2**, figure 3.1. These peaks are in accordance with the number of protons in the ligand N-acetythylenediamine.

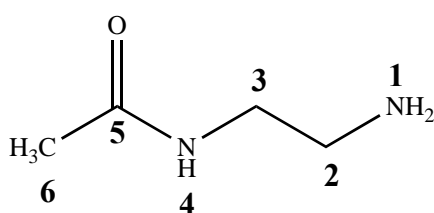


Figure 3.1: N-acetythylenediamine structure.

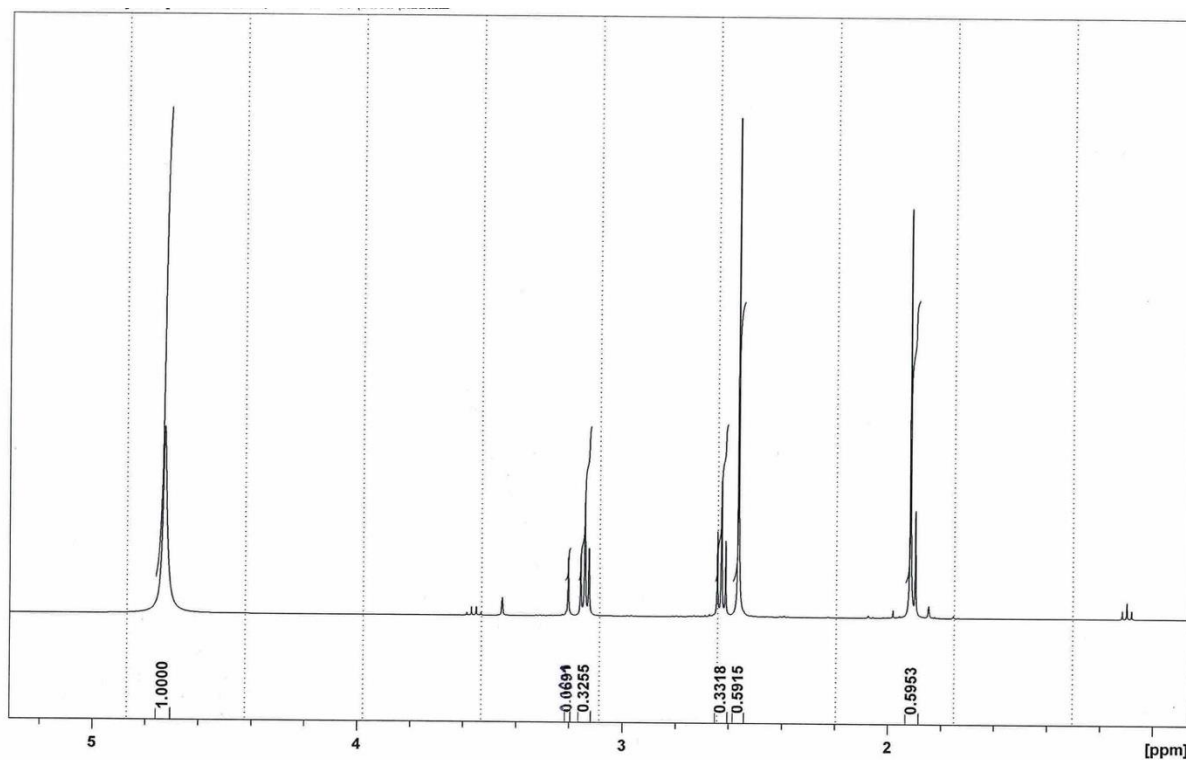


Figure 3.2(a): ^1H NMR spectrum of N-acetythylenediamine.

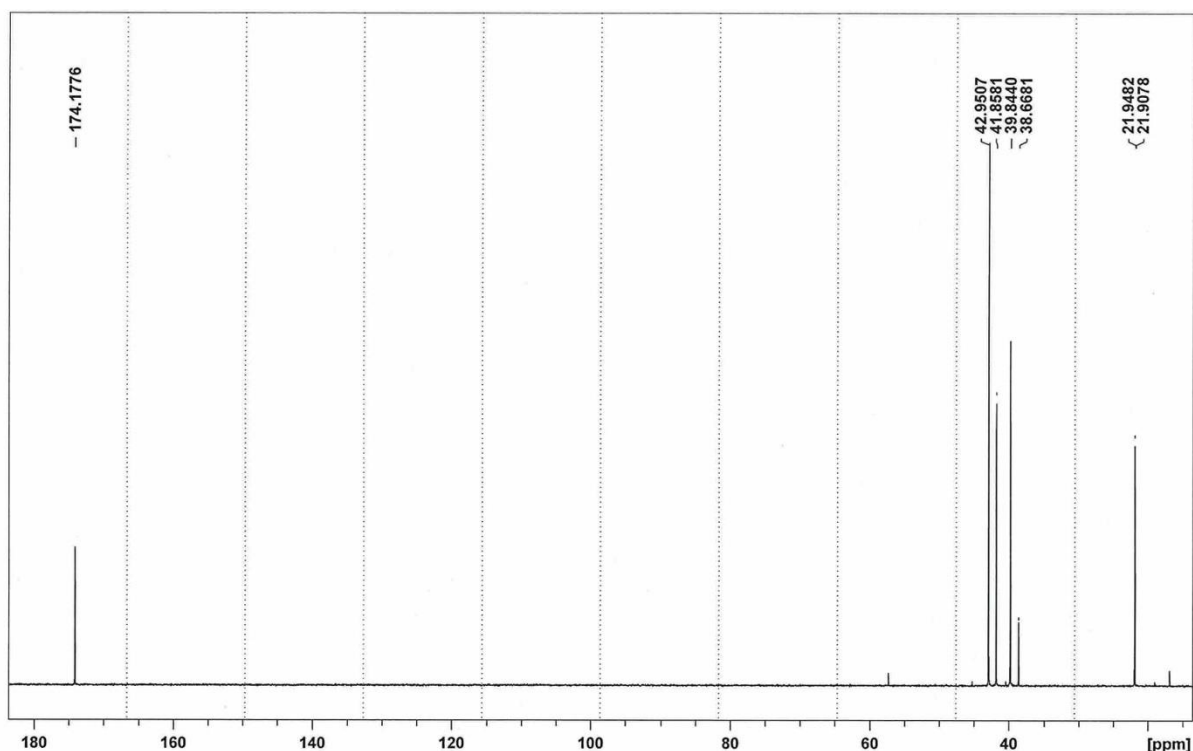


Figure 3.2(b): ^{13}C NMR spectrum of *N*-acetythylenediamine.

The ^{13}C NMR spectrum of *N*-acetythylenediamine displayed five peaks from $\delta = 22.12$ to 173.97 ppm. The peak in the downfield region at $\delta = 173.97$ ppm was assigned to the carbonyl carbon and the peak in the upfield region at $\delta = 22.12$ ppm was assigned to the methyl group. The other peaks can be assigned to the methylene groups.

3.2.1.2 Synthesis and characterisation of *N*-acetyl-uns-penp.

N-acetyl-uns-penp was prepared from the reaction of *N*-acetythylenediamine and 2-pyridinecarboxyaldehyde in 1,2-dichloroethane, and subsequent reduction of the resulting imine using $\text{NaBH}(\text{OAc})_3$. This reaction was carried out both under ambient conditions and under nitrogen. The products from both of these reactions were combined and characterised by ^1H NMR and ^{13}C NMR. The ^1H NMR spectrum, shown in figure 3.3(a) and 3.3(b), displayed a number of multiplets over the region $\delta = 1.5$ to 10.0 ppm, some of which were consistent with the literature data. Similarly, the ^{13}C NMR, shown in figure 3.3(c), of *N*-acetyl-uns-penp more signals than expected, which suggests that the product was impure. The peaks at 171.44, 158.93, 149.66, 137.64, 123.83, 122.49, 59.39, 50.19 and 22.10 ppm

corresponds to N-acetyl-uns-penp¹⁸ but additional signals over the region $\delta = 21.7$ to 194.0 ppm indicates that the product is not pure.

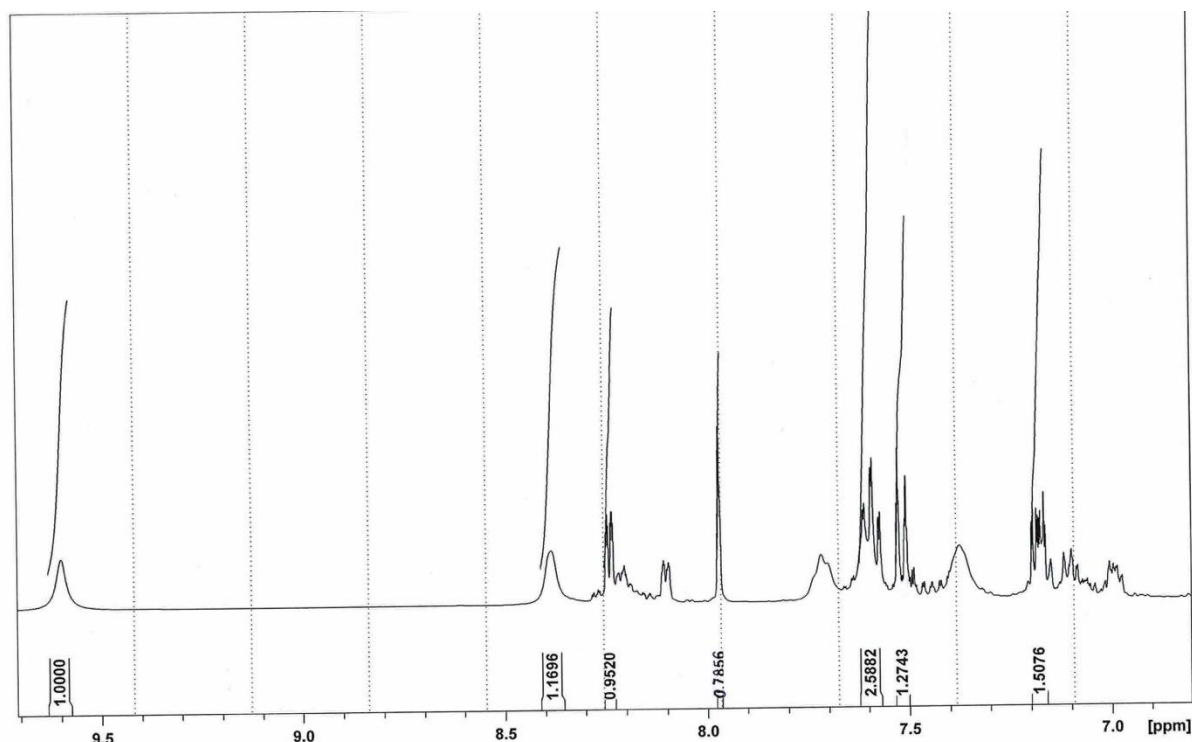


Figure 3.3(a): ¹H NMR spectrum of N-acetyl-uns-penp from $\delta = 9.2$ -6.8 ppm.

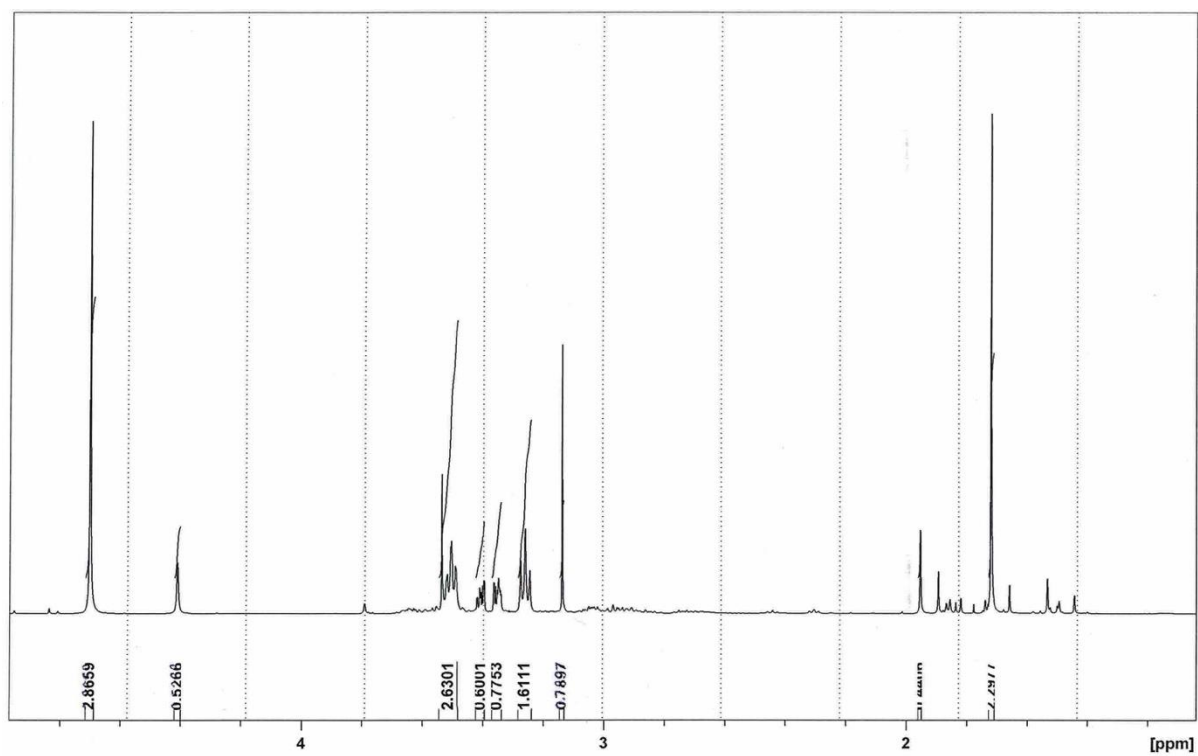


Figure 3.3(b): ¹H NMR spectrum of N-acetyl-uns-penp from $\delta = 5.00$ -1.00 ppm.

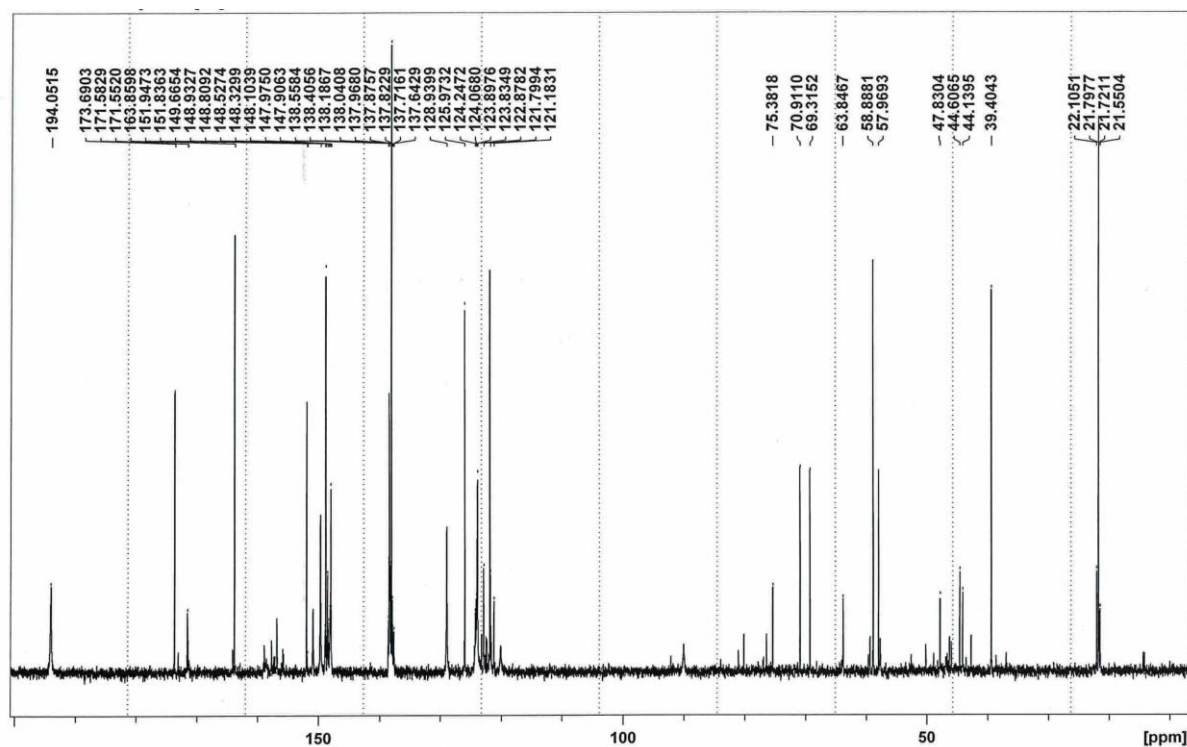


Figure 3.3(c): ^{13}C NMR spectrum of *N*-acetyl-uns-penp.

3.2.1.3 Attempted deprotection of *N*-acetyl-uns-penp.

According to the literature, the uns-penp ligand is obtained from *N*-acetyl-uns-penp by refluxing the latter in HCl for 24 h at 110° C. In our hands, this did not give the expected product, as shown by ^1H NMR, ^{13}C NMR and mass spectrometry. The mass spectrum of uns-penp is shown in figure 3.4. and does seem to at least confirm the presence of uns-penp in the product mixture. The calculated mass for the protonated uns-penp ligand $\text{C}_{14}\text{H}_{19}\text{N}_4^+$ as LH^+ is m/z 243.15 and a peak at m/z 243.1 can be observed in the mass spectrum. A low intensity peak at m/z 152.1 is consistent with a fragment having molecular formula $\text{C}_8\text{N}_3\text{H}_{14}^+$ (calculated m/z 152.1), formed by the loss of pyridine ring and CH_2 and gain one hydrogen to give 1+ charge to the species, figure 3.5(b).

Sample Name	SUKH 40	Position	Vial 41	Instrument Name	QQQ
User Name	QQQ\Agilent	Inj Vol	5	InjPosition	
Sample Type	Sample	IRM Calibration Status	Not Applicable	Data Filename	SUKH 40.d
ACQ Method	FlowInjection no Column ESI SCAN Pos.m	Comment		Acquired Time	29-09-20 10:14:16

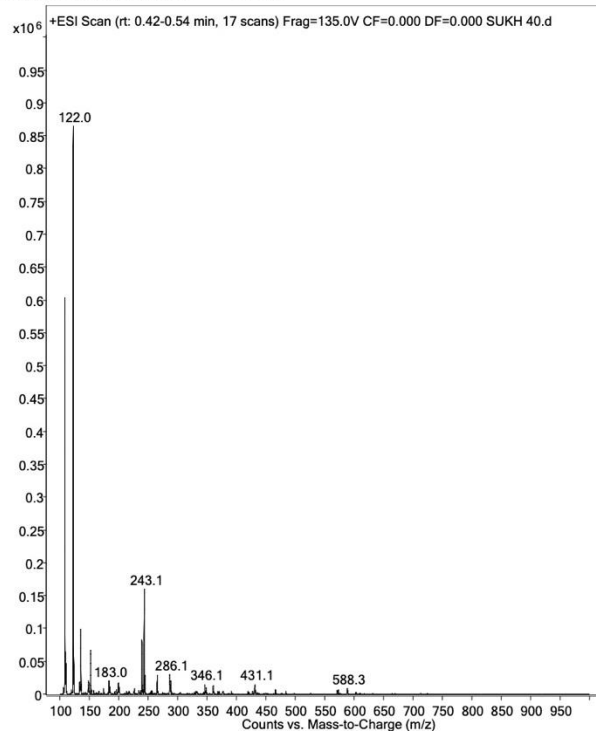


Figure 3.4: Mass spectrum of the product obtained from the synthesis of *uns-penp*.

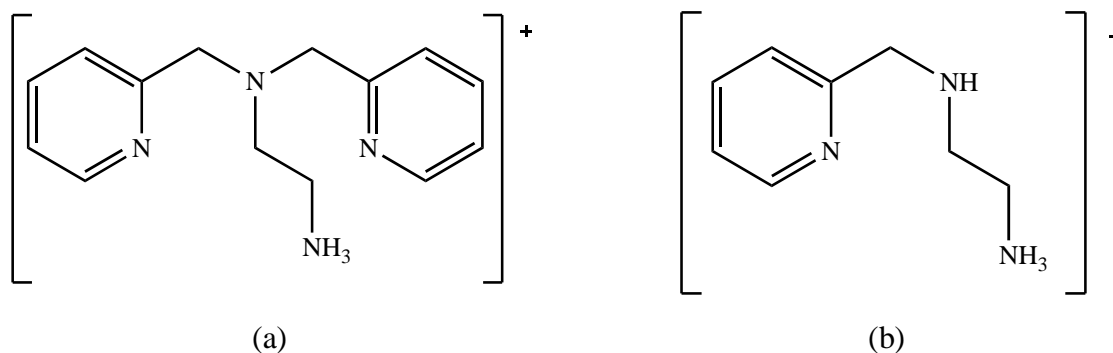


Figure 3.5: (a) Structure of *uns-penp* ligand; (b) Loss of an arm from the ligand to give $C_8H_{14}N_3^+$.

The 1H NMR spectrum, shown in figure 3.6(a) and 36(b), displayed multiplets over the region $\delta = 3.2$ to 9.7 ppm and the ^{13}C NMR spectrum displayed many signals over the region $\delta = 57.96$ to 194.22 ppm. It was difficult to recognise and assign the peaks to the protons and carbons of *uns-penp*. The NMR data were not in accordance with those in the literature¹⁸. The ^{13}C spectrum, shown in figure 3.6(c), displays intense peaks at δ 164.23, 149.64, 148.72, 137.94, 124.07, 122.28, and 59.59 ppm, along with a number of low intensity peaks which

confirm the impurity of the product. The synthesis of uns-penp ligand was unsuccessful, and therefore we did not proceed further to coordinate the ligand to the cobalt(III) ion.

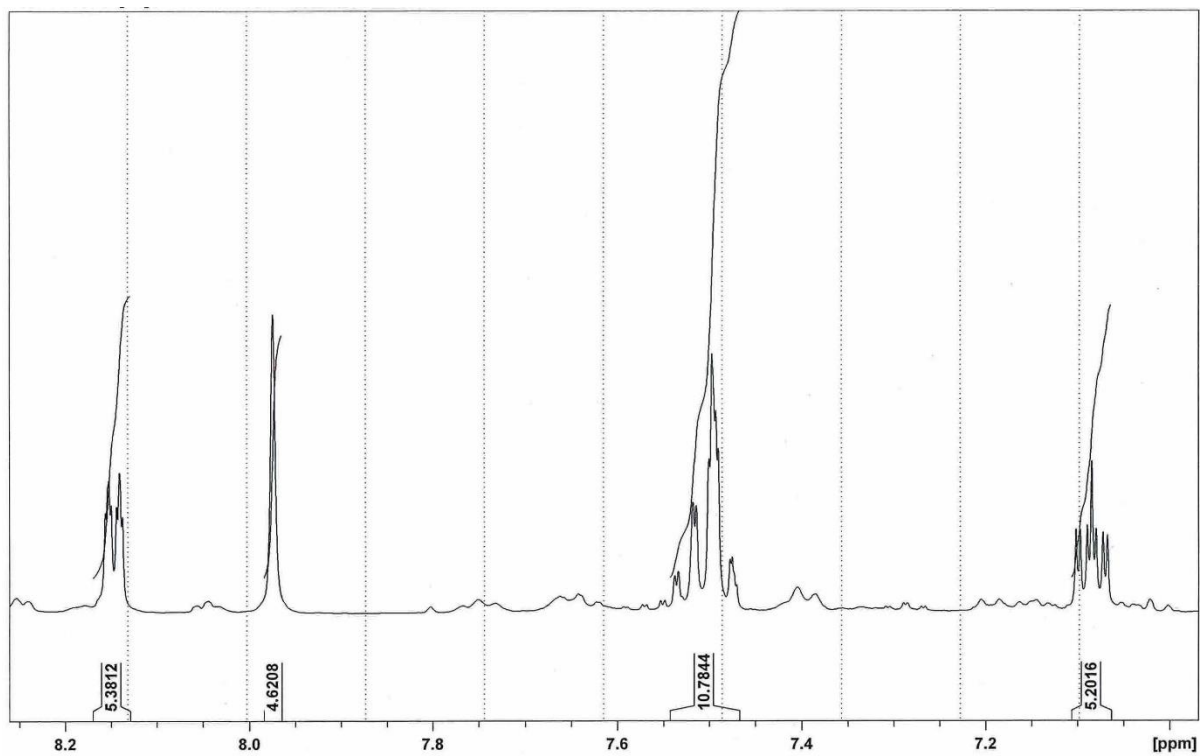


Figure 3.6(a): ^1H NMR spectrum of *uns-penp* from $\delta = 8.2 - 7.1$ ppm.

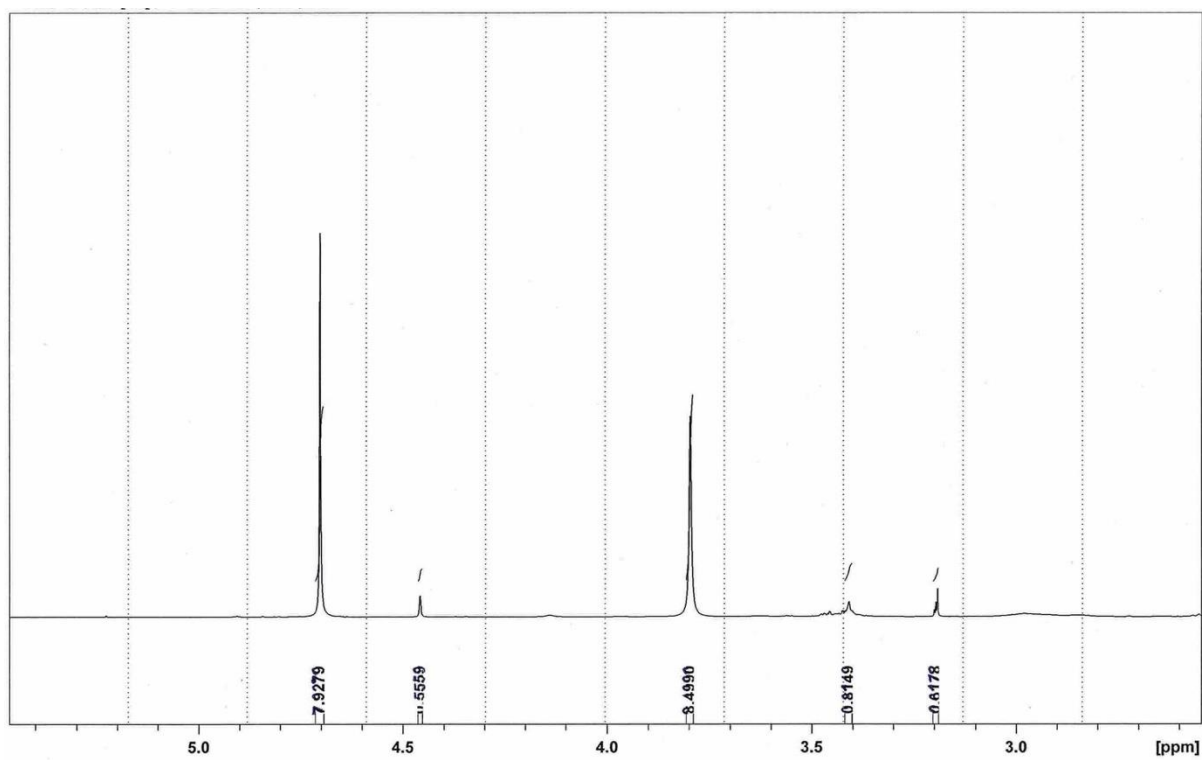


Figure 3.6(b): ^1H NMR spectrum of *uns-penp* from $\delta = 5.0 - 3.0$ ppm.

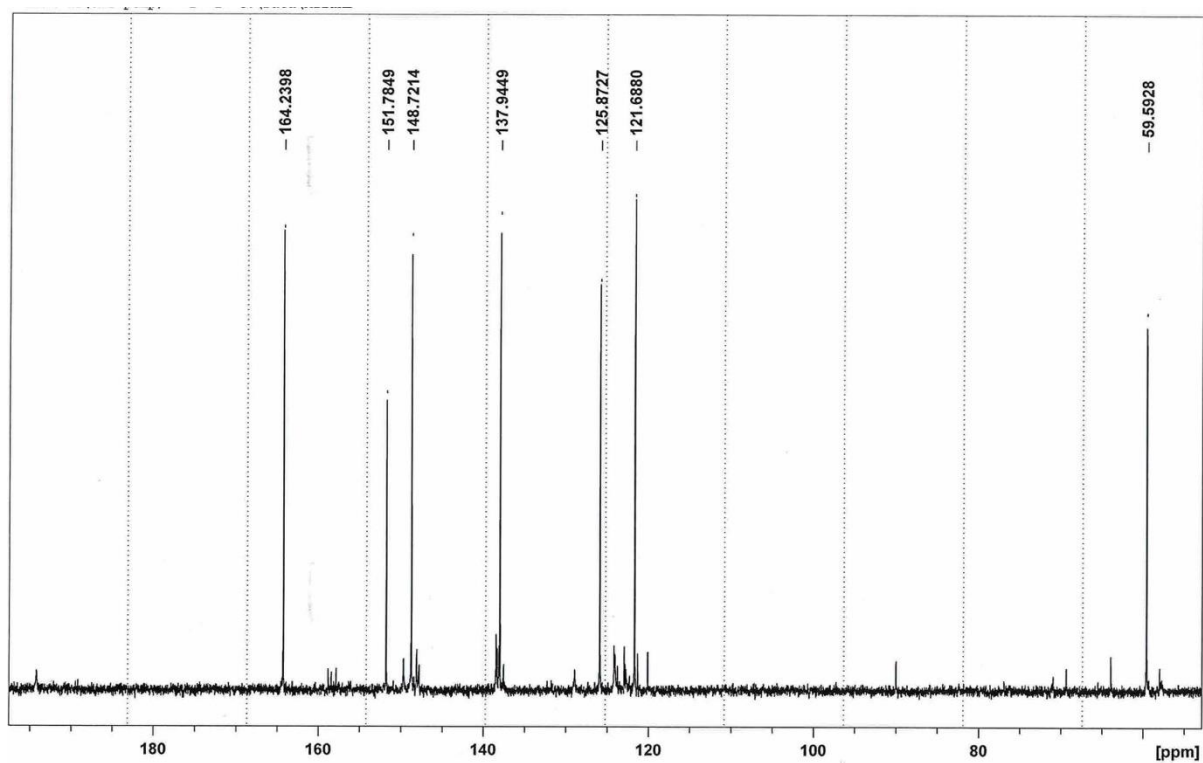
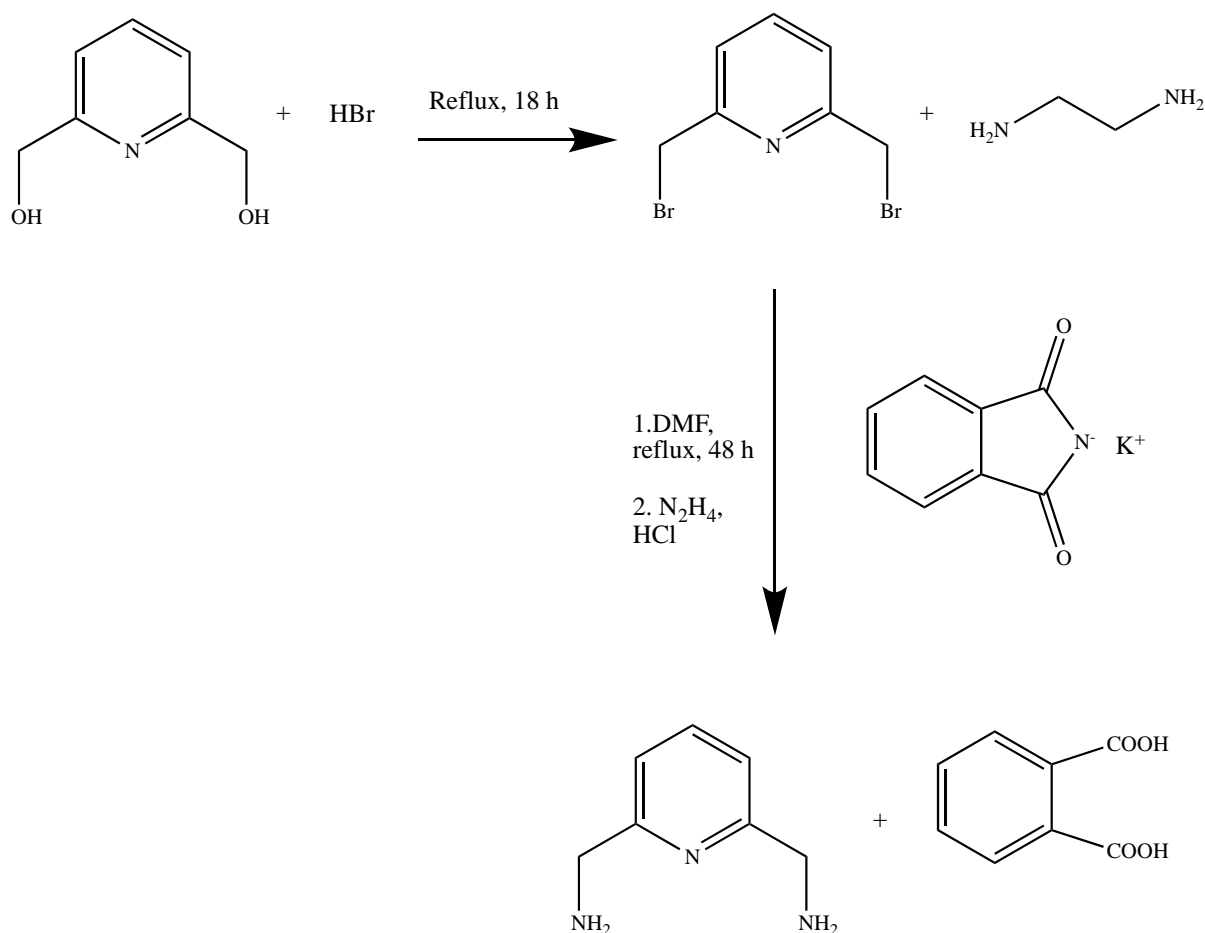


Figure 3.6(c): ^{13}C NMR spectrum of uns-penp.

3.2.2 Synthesis of 2,6-di(aminomethyl)pyridine

2,6-di(aminomethyl)pyridine was synthesised from the reaction of 2,6-di(bromomethyl)pyridine with potassium phthalimide and subsequent deprotection. The former was prepared by the reaction of 2,6-pyridinedimethanol with HBr. The overall reaction is shown in Scheme 2 below.



Scheme 2: Synthesis of 2,6-di(aminomethyl)pyridine.

3.2.2.1 Synthesis of potassium phthalimide

Potassium phthalimide was synthesised according to the literature method¹⁹, by the reaction of phthalimide in ethanol with potassium hydroxide solution.

3.2.2.2 Synthesis and characterisation of 2,6-di(bromomethyl)pyridine.

2,6-di(bromomethyl)pyridine was synthesised²⁰ by the reaction of 2,6-pyridinedimethanol and HBr. The pale pinkish coloured product was isolated and characterised by ¹H and ¹³C NMR, shown in figure 3.7(a) and 3.7(b).

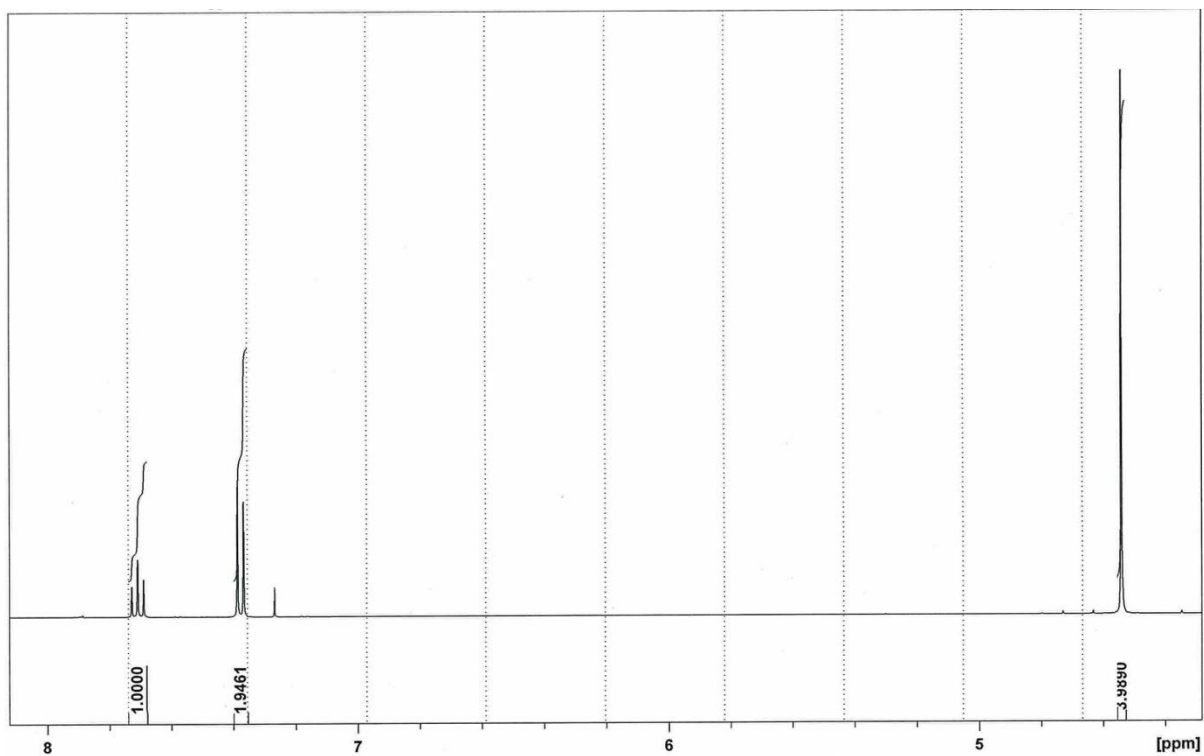


Figure 3.7(a): ^1H NMR spectrum of 2,6-di(bromomethyl)pyridine.

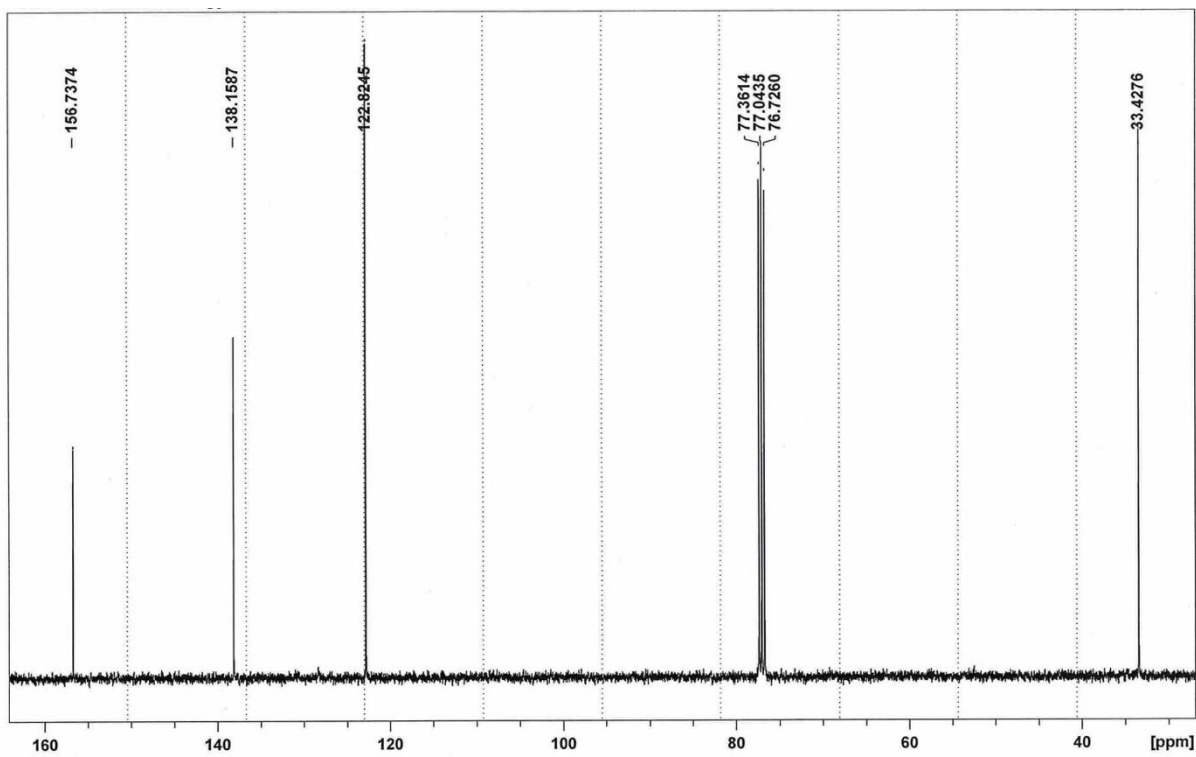


Figure 3.7(b): ^{13}C NMR spectrum of 2,6-di(bromomethyl)pyridine.

The ^1H NMR spectrum of 2,6-dibromomethylpyridine in CDCl_3 displays three signals in the range $\delta = 4.5$ to 7.7 ppm. The singlet in the upfield region is due to the methylene hydrogens. The other two signals, a doublet and a triplet, in the downfield region are due to the hydrogens of the pyridine ring. The triplet may be assigned to the hydrogen atom attached to the carbon *para* to the nitrogen of the pyridine ring, while the doublet can be assigned to the other two equivalent *meta* protons. The ^{13}C NMR spectrum of 2,6-dibromomethylpyridine displays four signals over the region $\delta = 156.73$ to 33.42 ppm. The one upfield signal can be attributed to the equivalent methylene carbon atoms. The other three signals in the downfield region are due to the carbons in the pyridine ring. The signal at 156.73 ppm is most likely due to the equivalent *ortho* carbon atoms owing to its low intensity; this is indicative of a carbon atom having no attached protons. The highest intensity signal at 122.82 ppm is due to the two *meta* carbons of the pyridine ring.

3.2.2.3 Synthesis and characterisation of 2,6-di(aminomethyl)pyridine.

2,6-di(aminomethyl)pyridine was synthesised according to the literature method²⁰, by reacting 2,6-di(bromomethyl)pyridine with potassium phthalimide in DMF under reflux, and deprotection with hydrazine hydrate under reflux in ethanol. 2,6-di(aminomethyl)pyridine was isolated and characterised by ^1H and ^{13}C NMR spectroscopy. The ^1H NMR spectrum, shown in figure 3.8(a), displays three signals in the region $\delta = 2.1$ to 7.1 ppm. The singlet in the upfield region is due to the equivalent methylene hydrogen atoms. The triplet at 7.6 ppm is due to the hydrogen attached to the carbon atom *para* to the nitrogen of the pyridine ring. The doublet at 7.1 ppm is due to the hydrogen atoms at *meta* positions to the nitrogen of the ring. The ^{13}C NMR spectrum of 2,6-diaminopyridine, shown in figure 3.8(b), displays four signals in the range $\delta = 47.60$ ppm to 161.24 ppm. The upfield signal is due to the equivalent methylene carbon atoms attached to the amino group. The other signals are due to the pyridine carbons. The ^1H and ^{13}C NMR spectra of the ligand 2,6-diaminomethylpyridine are consistent with those in the literature²⁰.

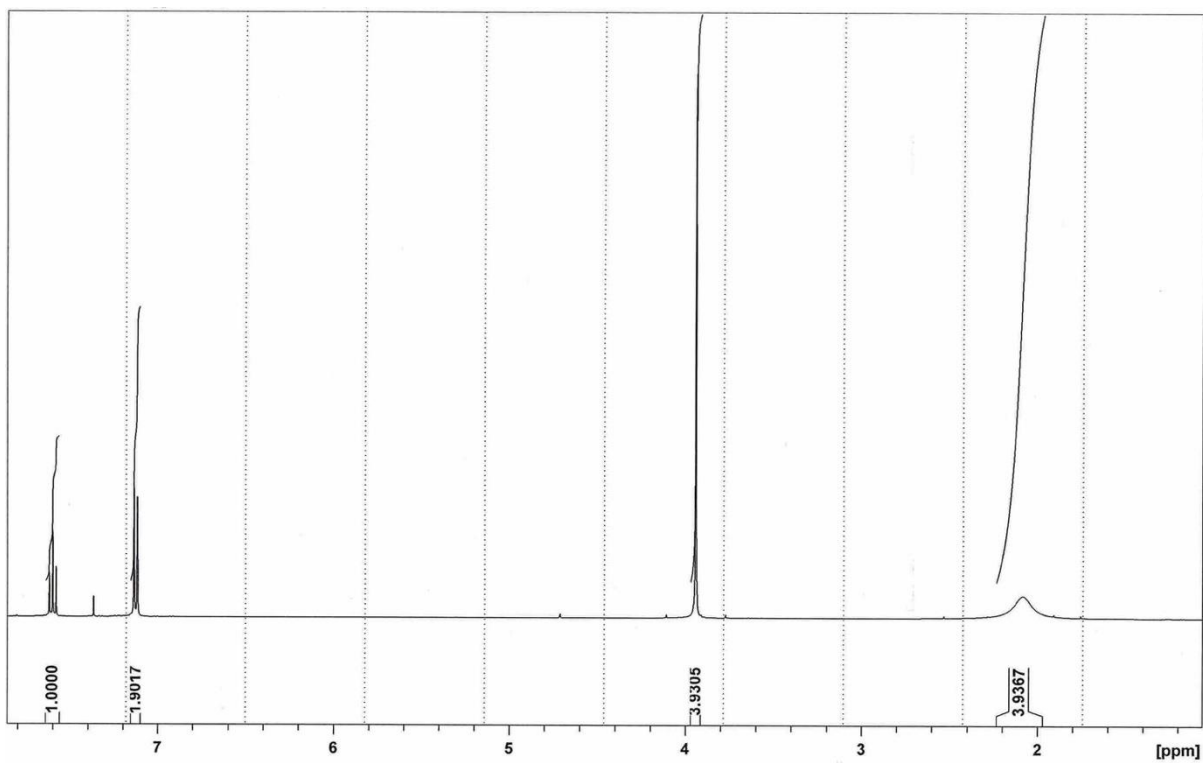


Figure 3.8(a): ^1H NMR spectrum of 2,6-di(aminomethyl)pyridine.

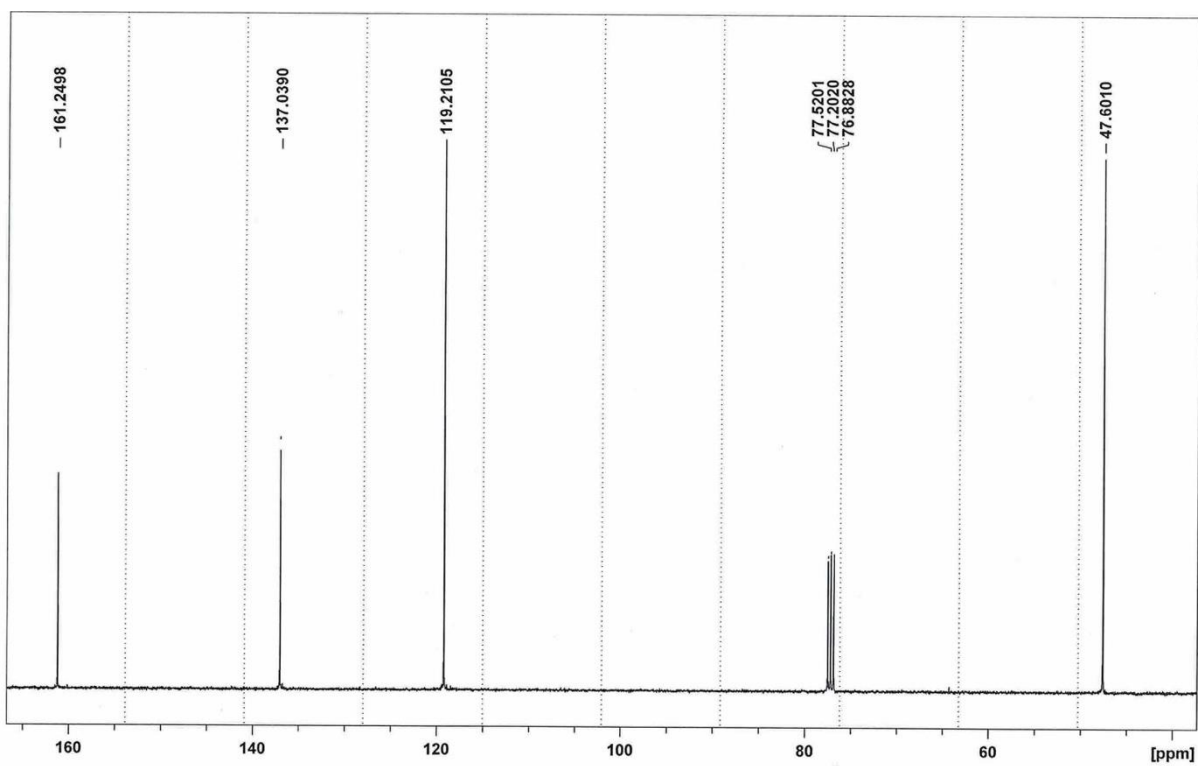


Figure 3.8(b): ^{13}C NMR spectrum of 2,6-di(aminomethyl)pyridine.

3.3 Synthesis and characterisation of the precursor complexes

3.3.1 Synthesis and characterisation of $[\text{Co}(\text{tren})(\text{en})]\text{Cl}_3$.

$[\text{Co}(\text{tren})(\text{en})]\text{Cl}_3$ was synthesised according to the method described in the literature, by the reaction of $[\text{Co}(\text{tren})\text{Cl}_2]\text{Cl}$ with ethylenediamine in water on a steam bath. The crude product was purified by column chromatography on both Sephadex SP-C25 and Dowex 50Wx2 cation exchange columns. The yellow-orange product was isolated as the chloride salt following recrystallisation from hot water.

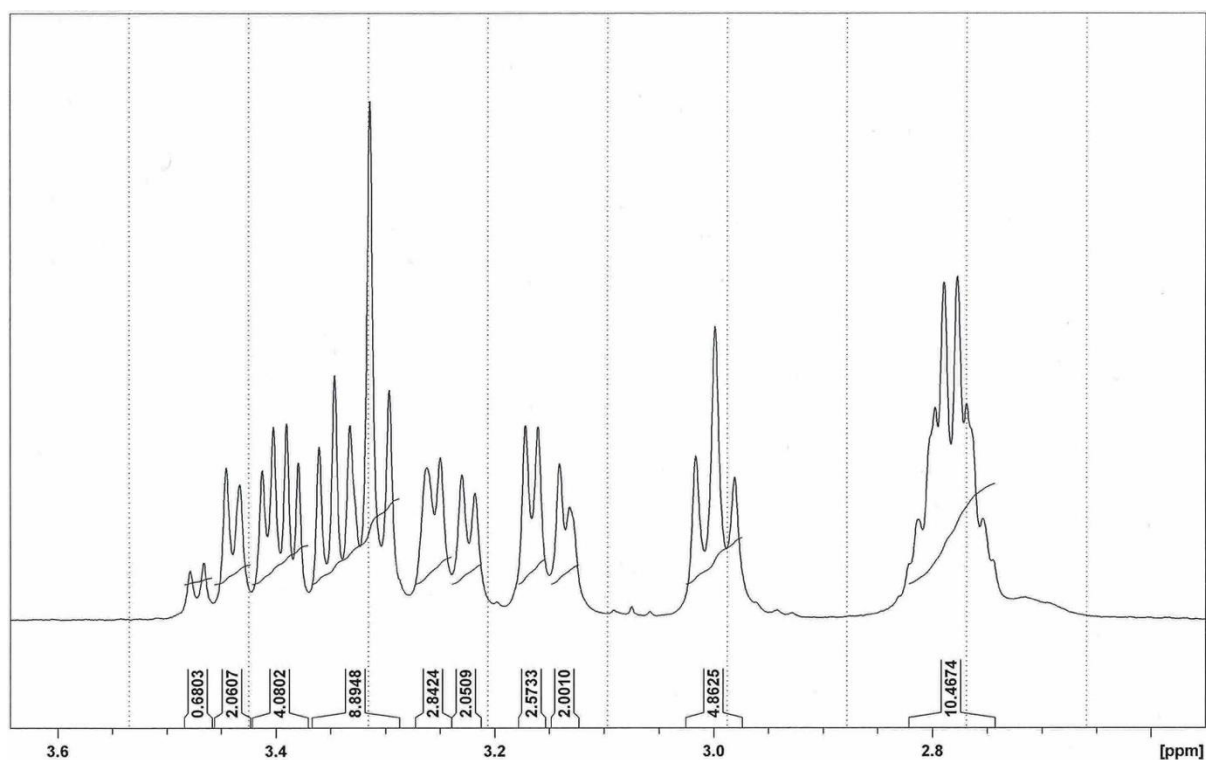


Figure 3.9(a): ^1H NMR spectrum of $[\text{Co}(\text{tren})(\text{en})]\text{Cl}_3$.

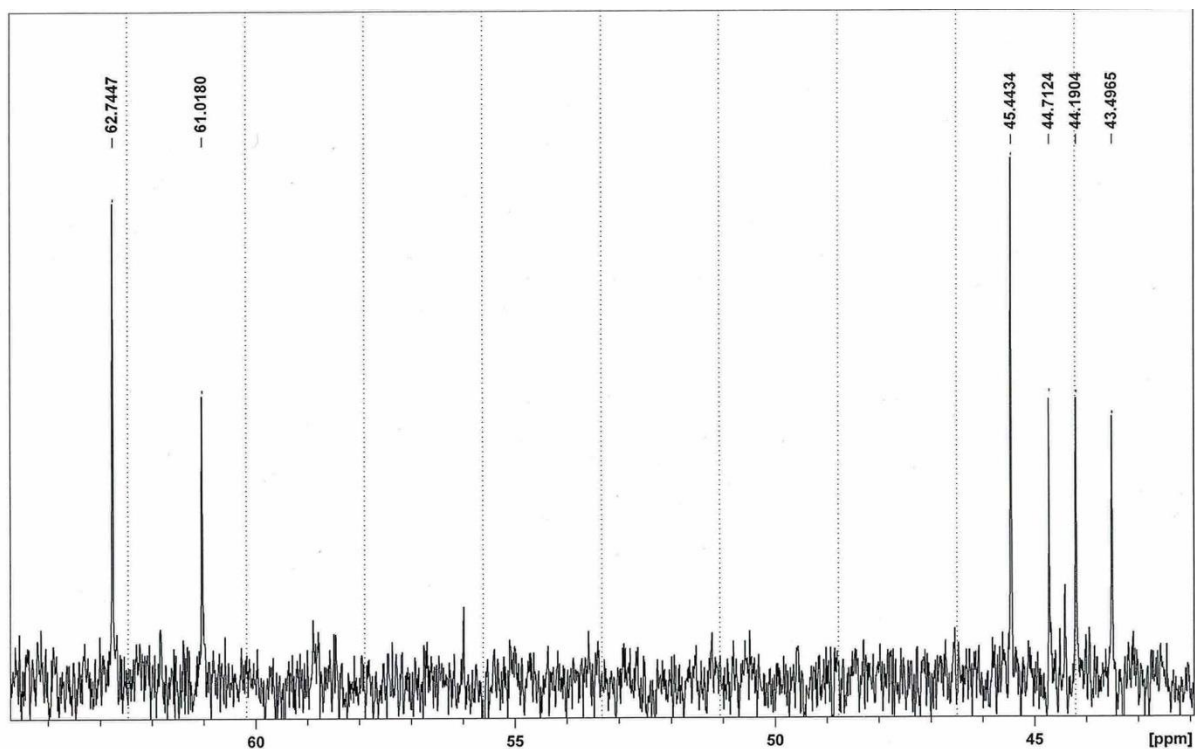


Figure 3.9(b): ^{13}C NMR spectrum of $[\text{Co}(\text{tren})(\text{en})]\text{Cl}_3$.

$[\text{Co}(\text{tren})(\text{en})]\text{Cl}_3$ was characterised by ^1H and ^{13}C NMR, and mass spectrometry. The ^1H NMR spectrum of $[\text{Co}(\text{tren})(\text{en})]\text{Cl}_3$ in D_2O , shown in figure 3.9(a), comprises 8 signals in the region $\delta = 2.9 - 5.2$ ppm. The three lowest field signals are all broad, strongly suggesting that these signals are due to the NH protons on both the tren and en ligands. The CH_2 protons on the tren and en ligands give rise to complex multiplets. The integrals of these signals are consistent with the proposed formula of the complex. The ^{13}C NMR spectrum, shown in figure 3.9(b), displays six signals over the range $\delta = 43.49$ to 62.74 ppm, which is typical of CH_2 carbon atoms. The signals at 62.74 and 45.44 ppm are approximately twice the intensity of the other four, suggesting these are due to 2 carbon atoms, while the remaining four are due to individual carbon atoms in different chemical environments. According to the literature²¹, the higher intensity signals at 62.74 ppm and 45.44 ppm can therefore be assigned to carbons C2 and C1 respectively, the signal at 61.01 ppm is due to C4, while the remainder are due to C3 and the en carbon atoms, as shown in figure 3.10.

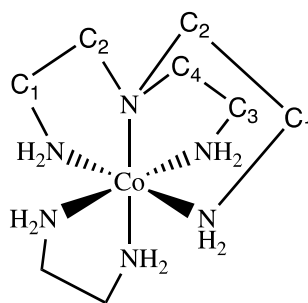


Figure 3.10: The structure of $[\text{Co}(\text{tren})(\text{en})]^{3+}$.

The fact that only 6, rather than 8, signals are observed implies that rapid chelate ring inversion must be occurring, which then results in an apparent mirror plane being present in the molecule on the NMR timescale. The HSQC NMR of $[\text{Co}(\text{tren})(\text{en})]\text{Cl}_3$, figure 3.9(c), shows that carbon atoms labelled C2 are attached to the hydrogen atoms which display multiplet signals at δ 3.36 and 3.15 ppm. This shows then that the attached H atoms are inequivalent, and are probably coupled to each other. Hence, there are a total of 4 hydrogens attached to the two equivalent carbons of the tren ligand. Similarly the carbon atoms labelled C1 are coupled to the hydrogen atoms which display doublet of doublets signals at δ 3.4 and 3.2 ppm. This again shows that these hydrogen atoms are inequivalent and probably geminally coupled. Again there are total of four hydrogens attached to symmetrically disposed carbon atoms of the tren ligand. The rest of the coupling is between the individual carbons of the arm of tren ligand and the ethylenediamine ligand.

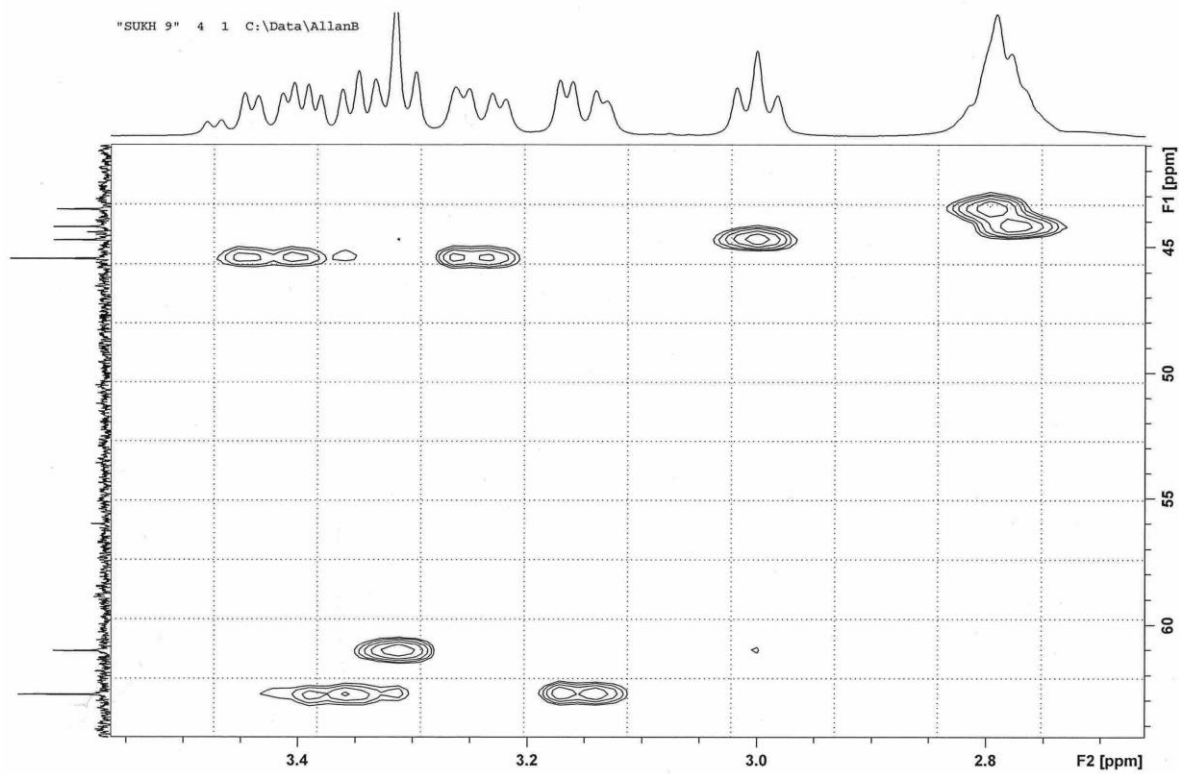


Figure 3.9(c): HSQC NMR spectrum of $[\text{Co}(\text{tren})(\text{en})]\text{Cl}_3$.

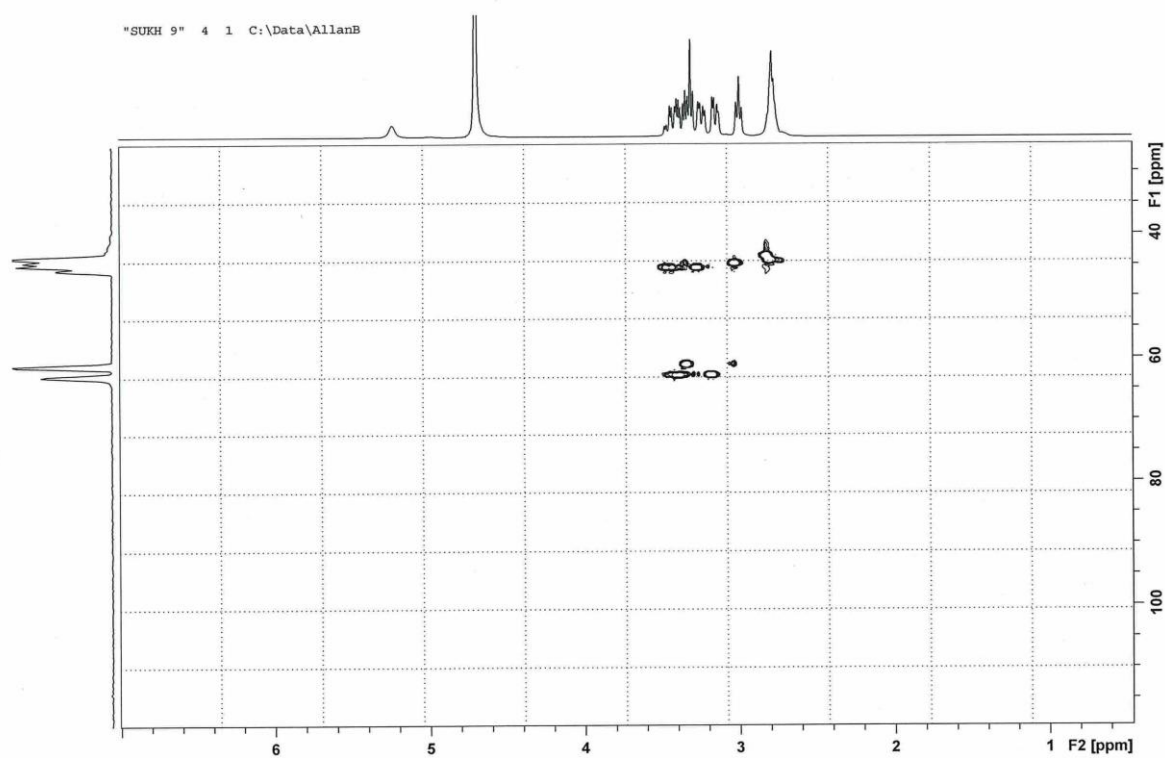


Figure 3.9(d): HMBC NMR spectrum of $[\text{Co}(\text{tren})(\text{en})]\text{Cl}_3$.

According to the HMBC, shown in figure 3.9(d), it can be said that C2 carbons correlate with the hydrogens of C1 and C4, the C4 carbon correlates with the hydrogens of the two C2 carbons. The C1 carbons correlate with the hydrogens of C2 and C4 while the C3 carbons correlate with the hydrogens of C2. On the basis of the data obtained, the C1 and C2 carbons can be assigned to the four carbons of the two arms of the tren ligand which display intense signals, and the C3 and C4 carbons of the other arm can be assigned to the peaks δ 44.95 and 61.09 ppm respectively. The other two peaks can be assigned to the carbons of the en ligand. Thus, the NMR data are consistent with the structure of the $[\text{Co}(\text{tren})(\text{en})]\text{Cl}_3$.

Two mass spectra of $[\text{Co}(\text{tren})(\text{en})]\text{Cl}_3$ are shown in figure 3.11a and 3.11b. These spectra correspond to the products obtained from the two syntheses of the complex and although there are some differences between the spectra, some of the peaks are the same.

Sample Name	Co(trisen)(en) 4	Position	Vial 53	Instrument Name	QQQ
User Name	QQQ\Agilent	Inj Vol	10	InjPosition	
Sample Type	Sample	IRM Calibration Status	Not Applicable	Data Filename	Co(trisen)(en) 4.d
ACQ Method	FlowInjection no Column ESI SCAN Pos.m	Comment		Acquired Time	28-01-20 10:56:35

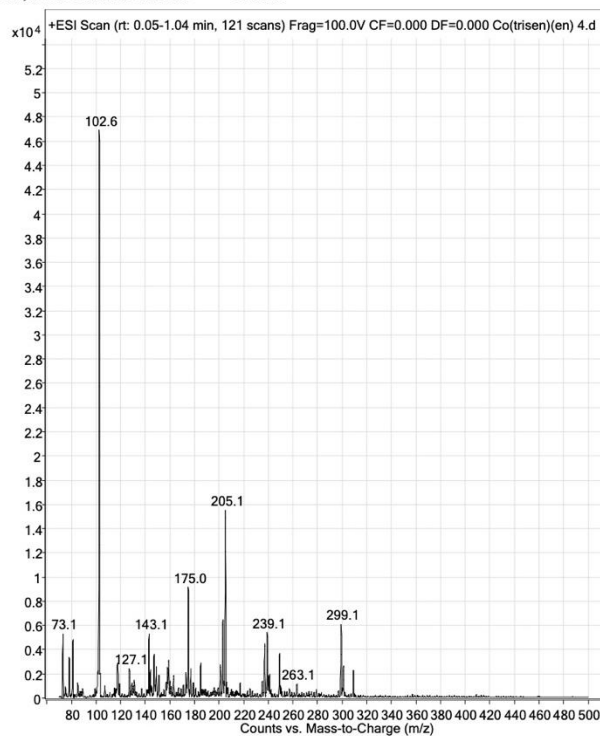


Figure 3.11a: Mass spectrum of $[\text{Co}(\text{tren})(\text{en})]\text{Cl}_3$ obtained from the first synthesis.

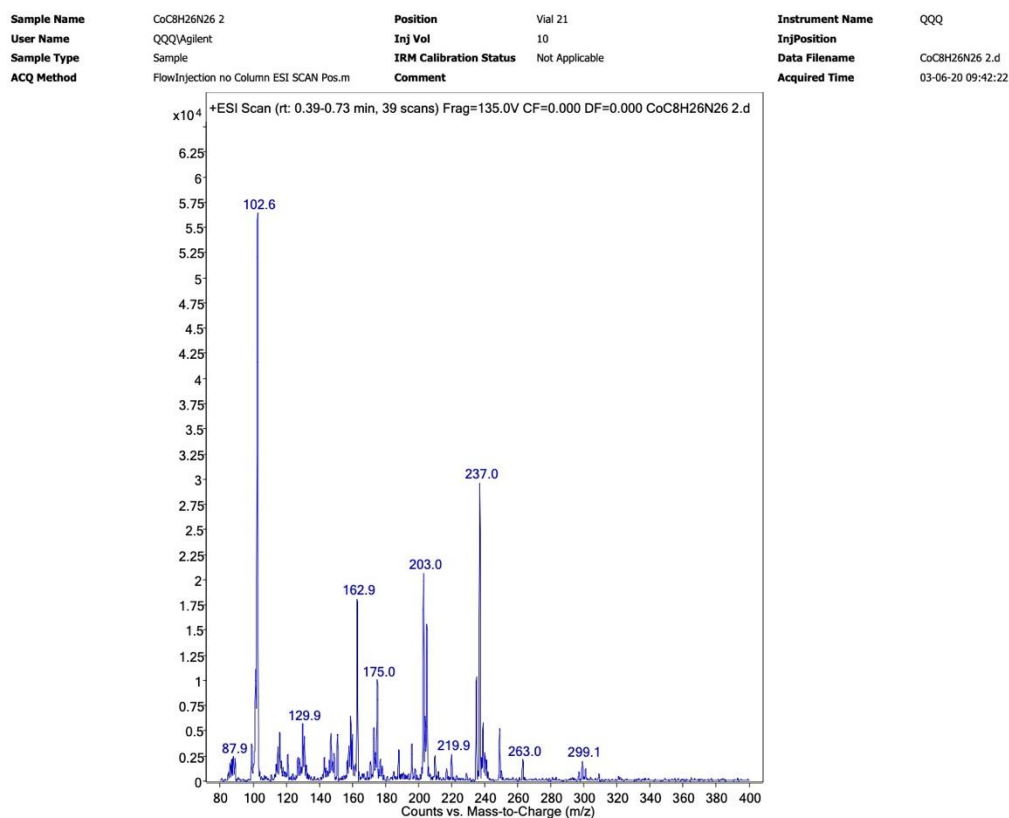


Figure 3.11b: Mass spectrum of $[Co(tren)(en)]Cl_3$ obtained from the second synthesis.

The monoisotopic mass for the expected parent ion $C_8H_{26}N_6Co$ is 265.1. However, no peak for a singly charged species at this m/z value is observed in either spectrum. However, both show a very small peak at m/z 263.1/263.0 which can be assigned to the loss of two protons from $C_8H_{26}N_6Co$ to give a singly charged ion having the formula $C_8H_{24}N_6Co^+$ (Calc m/z : 263.1; found 263.1/263.0). In both spectra, the most intense peak occurs at $m/z = 102.6$. This is consistent with a singly charged ion having the formula $C_2H_6NCo^+$, (Calc m/z : 102.9; found 102.6). This could be rationalised in terms of loss of the tren ligand and fragmentation of the en ligand to give a 4-membered chelate ring²² containing cobalt(II), as shown in figure 3.12. Such complexes have been previously observed in the literature²².

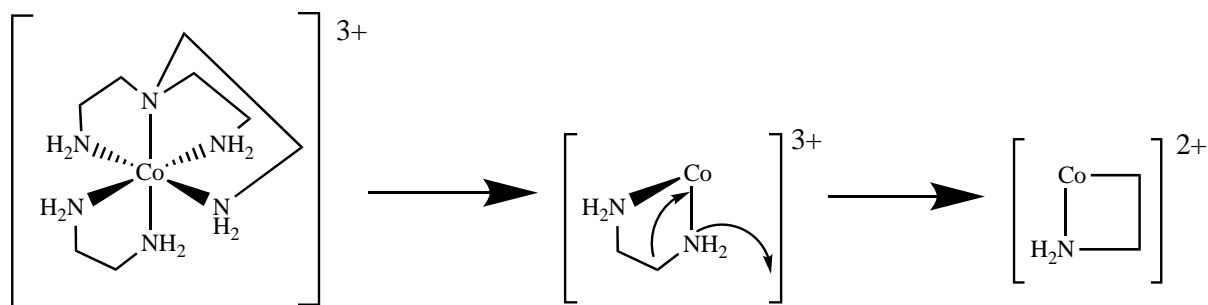


Figure 3.12: Loss of the tren ligand and fragmentation of the en ligand to form a 4-membered chelate ring.

In both spectra, a prominent peak at m/z 205.1 is observed. This is consistent with loss of the en ligand and reduction of cobalt(III) to cobalt(I) to give a singly charged fragment having the molecular formula $C_6H_{18}N_4Co^+$ (calculated m/z 205.08). This would thus correspond to $[Co(tren)]^+$. A peak at m/z 203.0 in Figure 3.13(a), can therefore be ascribed to $[Co(tren-2H)]^+$, where the required 1+ charge is obtained through two proton loss from a Co(III) species. The peak at $m/z = 239.1$ arises due to the loss of two carbon and two hydrogen atoms from the parent ion to give $C_6H_{24}N_6Co^+$ (calculated m/z 239.13) and the cobalt(III) is reduced to cobalt(I). The possible product of this process is shown in figure 3.13(b).

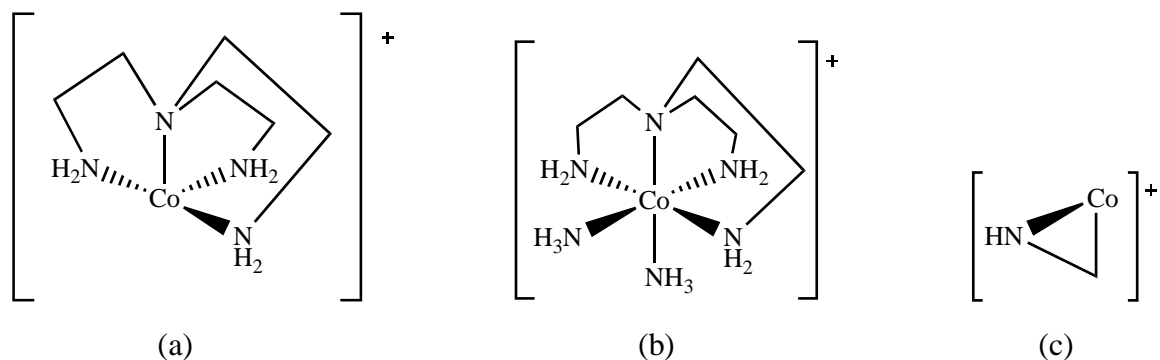


Figure 3.13: Mass spectral fragments obtained from (a) loss of the en ligand and reduction of Co(III) to Co(I) to give $C_6H_{18}N_4Co^+$; (b) loss of ethene from the en ligand and reduction to Co(I) to give $C_6H_{24}N_6Co^+$; (c) three-membered ring formed along with reduction of Co(III) to Co(II).

The mass spectrum 3.2b also shows peaks at m/z 102.6 and m/z 263.0 which is due to the same fragments as explained above. One prominent peak is observed at m/z 237.0 which is

due to the loss of ethene from the en ligand along with loss of two protons to give a 1+ Co(III) species of molecular formula $C_6H_{22}N_6Co^+$ (calculated m/z 237.13). A very small intensity peak at m/z 87.9 is consistent with the three-membered ring, shown in figure 3.13 (c), formed by the loss of tren ligand and $-NH_2CH_2$ from en ligand. the loss of a proton give 1+ charge to the fragment having molecular formula CH_3NCo^+ (calculated m/z 87.9). This requires the reduction of Co(III) to Co(II). Such three-membered ring has been observed in literature²².

3.3.2 Synthesis and characterisation of $[Co(dien)_2]Cl_3$.

$[Co(dien)_2]Cl_3$ was synthesised according to the method of Keene and Searle, by the reaction of $[Co(NH_3)_5Cl]Cl_2$ with dien in a slurry of charcoal on a steam bath. $[Co(NH_3)_5Cl]Cl_2$ was prepared according to the literature²³. The product $[Co(dien)_2]Cl_3$ was filtered and recrystallised from hot water using sodium bromide and was then further purified by chromatography on Dowex 50Wx2 resin, eluting with HCl. The coordination complex $[Co(dien)_2]Cl_3$ consists of a cobalt(III) ion surrounded by six nitrogen atoms of two diethylenediamine ligands in a distorted octahedral geometry. This complex has three isomers; s-fac, u-fac and mer, which are shown in figure 3.14. The mer-isomer was separated from the s-fac and u-fac isomers in fractions on a Dowex 50Wx2 cation exchange column, being isolated from the last fractions.

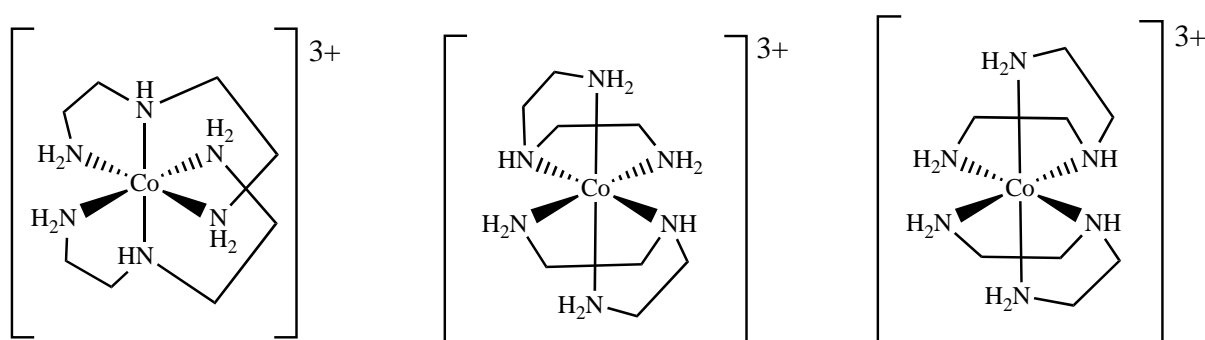


Figure 3.14: Isomers of $[Co(dien)_2]^{3+}$; (from left to right) mer, s-fac and u-fac.

$[Co(dien)_2]Cl_3$ was characterised by 1H and ^{13}C NMR, and mass spectrometry. The 1H NMR spectrum of $[Co(dien)_2]Cl_3$ in D_2O , shown in figure 3.15(a), comprises five signals in the region $\delta = 7.4$ to 2.83 ppm. The three lowest field signals are broad, suggesting that these signals are due to secondary and primary NH protons on both dien ligands. The CH_2 protons on these ligands give rise to complex multiplets in the upfield region.

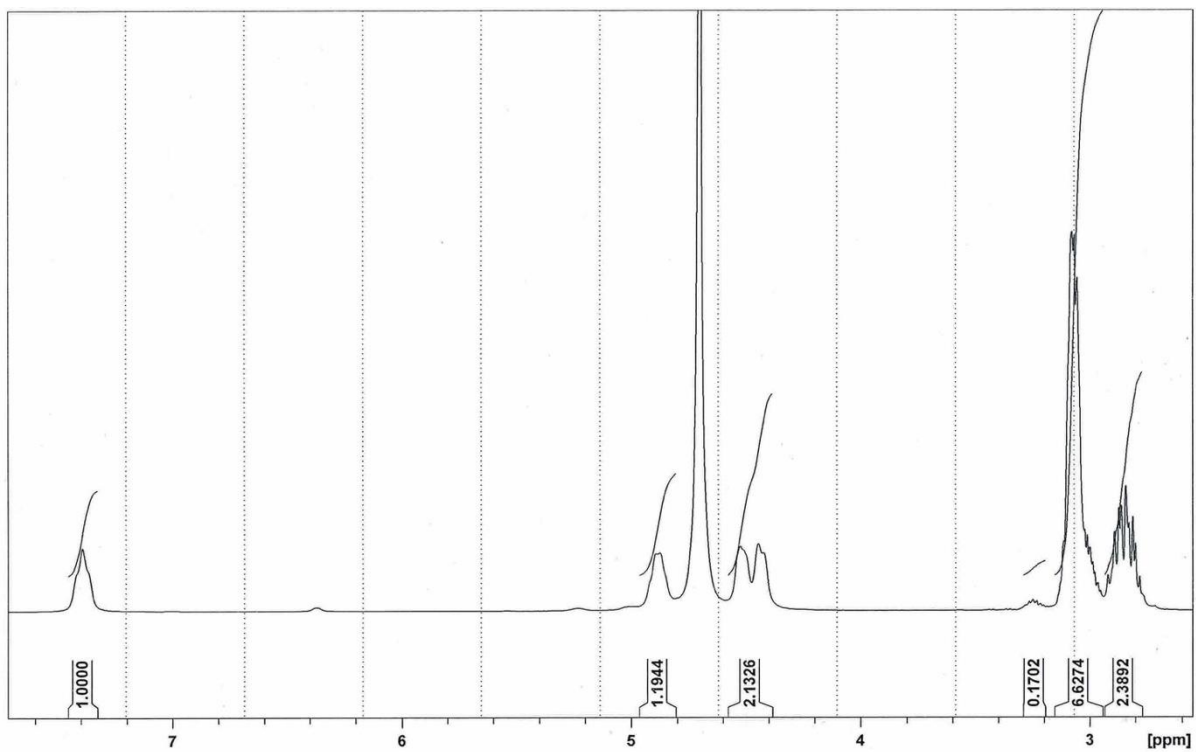


Figure 3.15(a): ^1H NMR spectrum of $[\text{Co}(\text{dien})_2]\text{Cl}_3$.

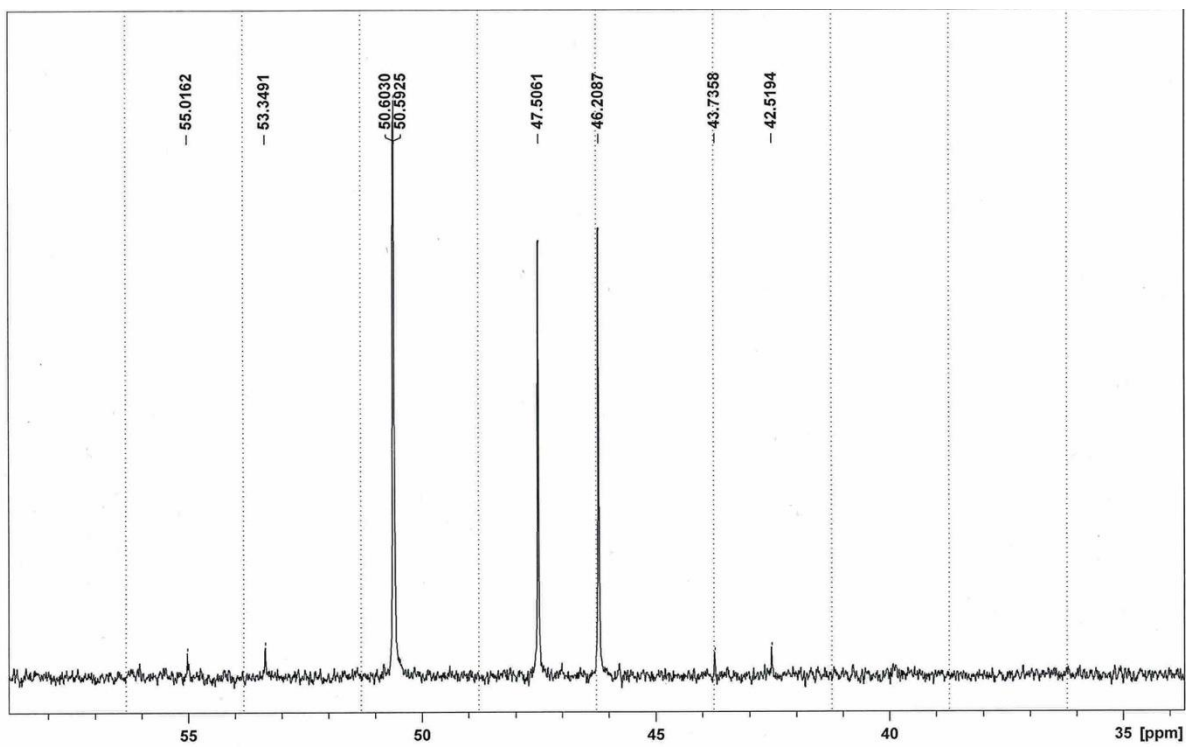


Figure 3.15(b): ^{13}C NMR spectrum of $[\text{Co}(\text{dien})_2]\text{Cl}_3$.

The ^{13}C NMR spectrum, shown in figure 3.15(b), displays three signals over the range $\delta = 50.60$ to 46.20 ppm with intensity ratios 2:1:1. Literature data assigns the signal at $\delta = 50.60$ ppm to two CH_2 carbons attached to the secondary N atom and the other two signals at $\delta = 47.50$ and 46.20 ppm to individual carbons attached to primary N atoms. The meridional configuration has been assigned to this complex by the similarity of its NMR spectrum with the literature²⁴.

The mass spectrum of $[\text{Co}(\text{dien})_2]^{3+}$ is shown in figure 3.16.

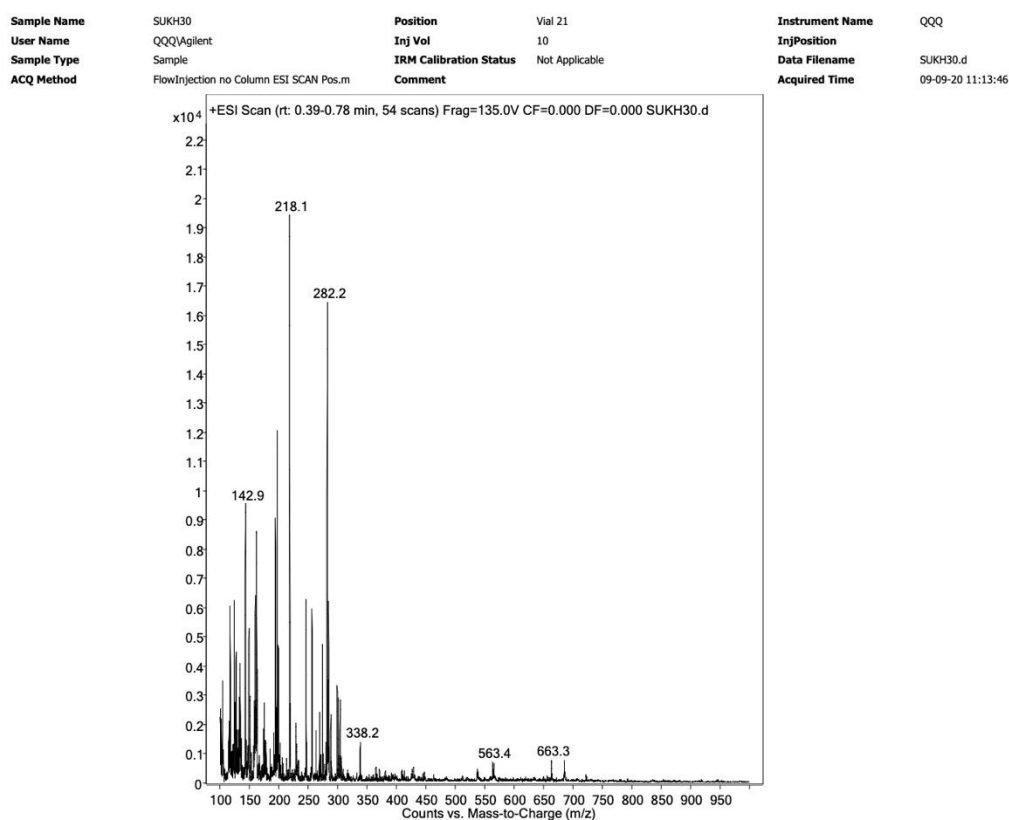


Figure 3.16a: The mass spectrum of $[\text{Co}(\text{dien})_2]\text{Cl}_3$.

Sample Name	SUKH30	Position	Vial 21	Instrument Name	QQQ
User Name	QQQ\Agilent	Inj Vol	10	InjPosition	
Sample Type	Sample	IRM Calibration Status	Not Applicable	Data Filename	SUKH30.d
ACQ Method	FlowInjection no Column ESI SCAN Pos.m	Comment		Acquired Time	09-09-20 11:13:46

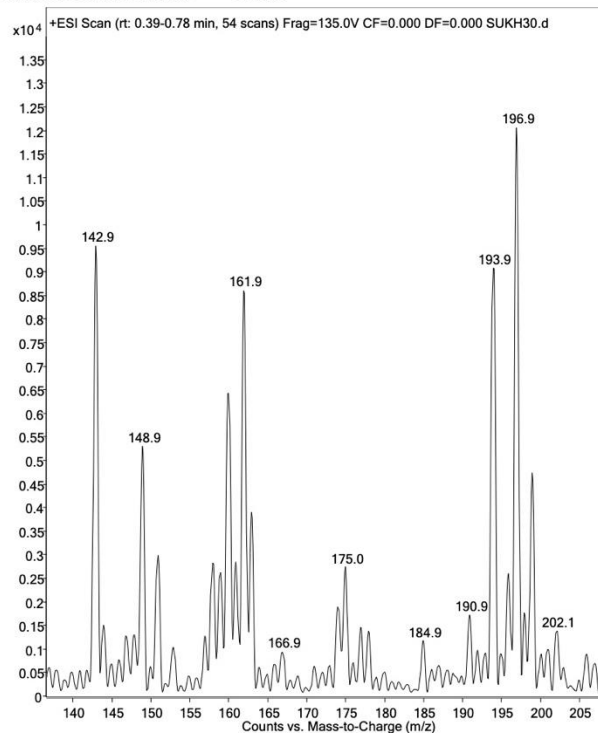


Figure 3.16b: The mass spectrum of $[\text{Co}(\text{dien})_2]\text{Cl}_3$ showing m/z region 205-140.

The calculated monoisotopic mass of $[\text{Co}(\text{dien})_2]^{3+}$ ($\text{CoC}_8\text{H}_{26}\text{N}_6$) is 265.16, but there is no peak observed in the spectrum at this m/z value, which would require reduction of the metal centre to Co(I). The intact ion could also lose two protons in order to obtain the necessary 1+ charge, in which case a peak at m/z 263.14 would be expected, but is not observed. A small peak observed at m/z 299.0 is consistent with the formula $\text{C}_8\text{H}_{25}\text{N}_6\text{ClCo}^+$ (calculated m/z 299.11) formed by the gain of a chloride ion and loss of a proton to give a +1 charge to the complex. However, the two major peaks observed in the spectrum occur at m/z 282.2 and m/z 218.1, with the latter being the base peak. There are two possibilities for the peak at m/z 282.2. This could be due to a singly charged fragment having the molecular formula $\text{C}_8\text{H}_{27}\text{N}_6\text{CoO}^+$ (calculated m/z 282.26), figure 3.17(a). This could result from a complex having the formulation $[\text{Co}(\kappa^3\text{-dien})(\kappa^2\text{-dien})(\text{OH})]^+$ in which one of the dien ligands binds in a hypodentate fashion to allow coordination of a hydroxide ligand, alongside reduction of Co(III) to Co(II). An equivalent formulation would be $[\text{Co}(\kappa^3\text{-dien})(\kappa^2\text{-dien-H})(\text{OH}_2)]^+$, in

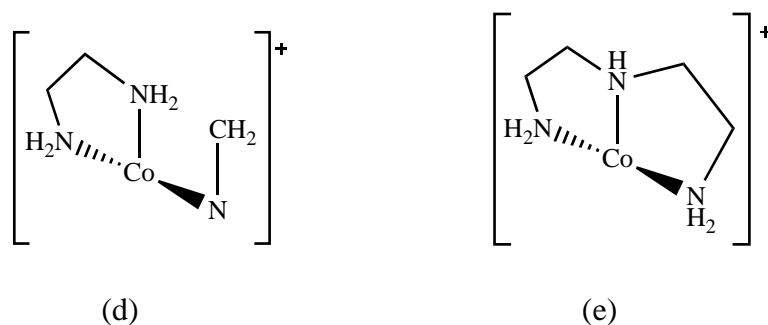


Figure 3.17: (d) Loss of one dien ligand and loss of $-CH_2NH_2$ arm of the other dien ligand to give $C_3H_{10}N_3Co^+$, (e) Loss of one dien ligand to give $C_4H_{13}N_3Co^+$.

3.3.3 Synthesis and Characterisation of $[Co(2,6\text{-di(aminomethyl)pyridine})_2]Cl_3$.

$[Co(2,6\text{-di(aminomethyl)pyridine})_2]Cl_3$ was synthesised by reacting 2,6-di(aminomethyl)pyridine with cobalt(II) perchlorate while air was bubbled through the reaction mixture to effect the oxidation of Co(II) to Co(III). The product was purified by column chromatography using a Dowex 50Wx2 cation exchange column, and was isolated as the chloride salt. The product was characterised by 1H and ^{13}C NMR spectroscopy, and mass spectrometry.

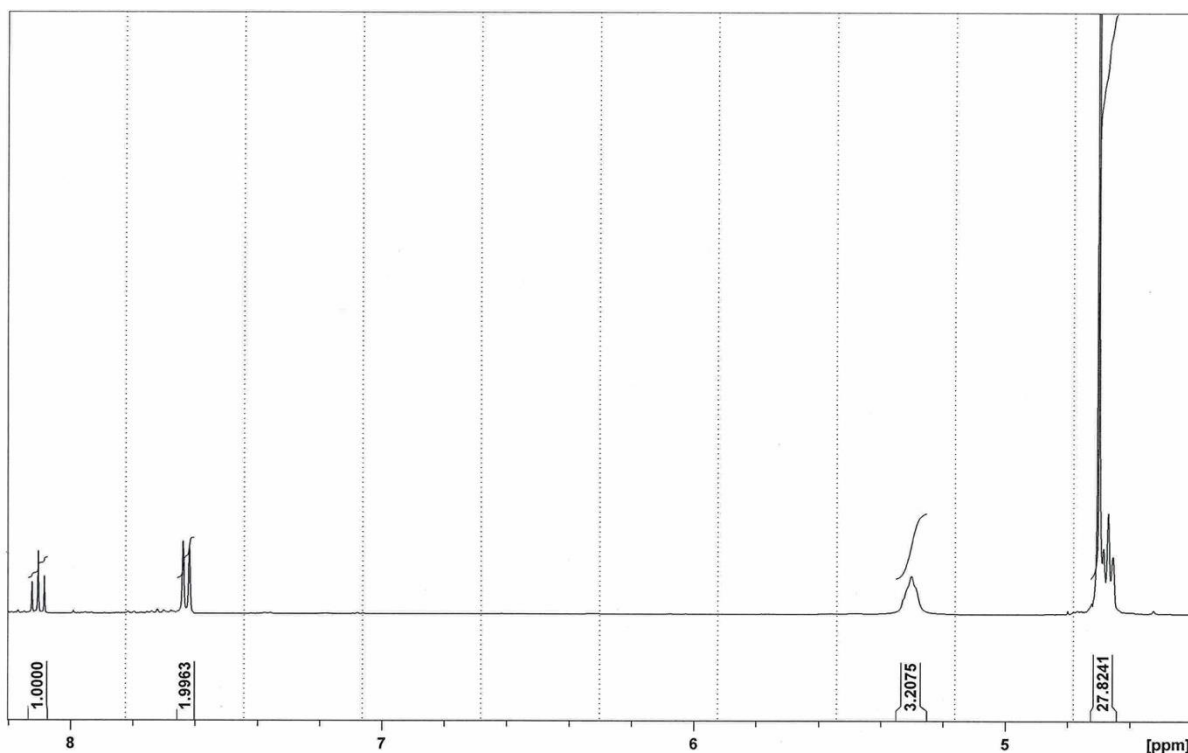


Figure 3.18(a): 1H NMR spectrum of $[Co(2,6\text{-di(aminomethyl)pyridine})_2]Cl_3$.

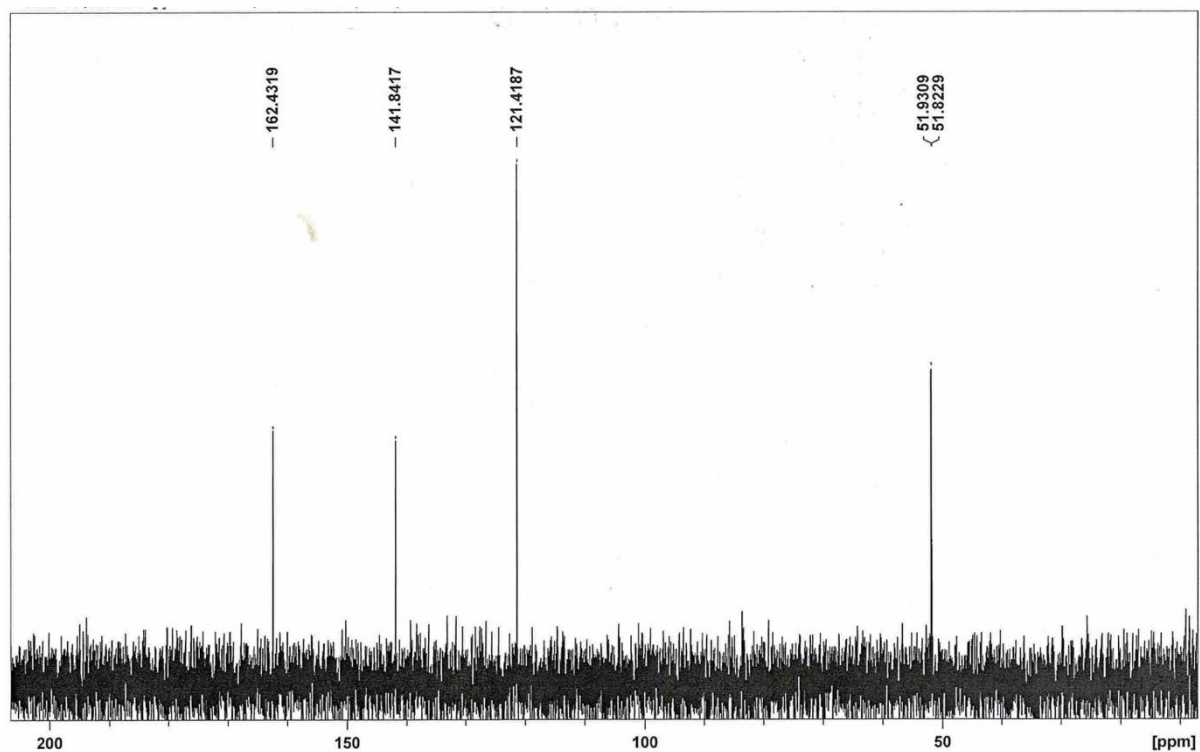


Figure 3.18(b): ^{13}C NMR spectrum of $[\text{Co}(2,6\text{-di}(\text{aminomethyl})\text{pyridine})_2]\text{Cl}_3$.

The ^1H NMR spectrum of $[\text{Co}(2,6\text{-di}(\text{aminomethyl})\text{pyridine})_2]\text{Cl}_3$, figure 3.18(a), displays three signals in the range $\delta = 5.2$ to 8.2 ppm in the ratio 3:2:1. The ^{13}C NMR spectrum, shown in figure 3.18(b), displays four prominent peaks in the region $\delta = 47.70 - 160.73$ ppm, which are in accordance with the structure of the ligand described above.

The mass spectrum of the complex is shown in figure 3.19.

Sample Name	SUKH 45	Position	Vial 62	Instrument Name	QQQ
User Name	QQQ\Agilent	Inj Vol	5	InjPosition	
Sample Type	Sample	IRM Calibration Status	Not Applicable	Data Filename	SUKH 45.d
ACQ Method	FlowInjection no Column ESI SCAN Pos.m	Comment		Acquired Time	29-10-20 14:25:03

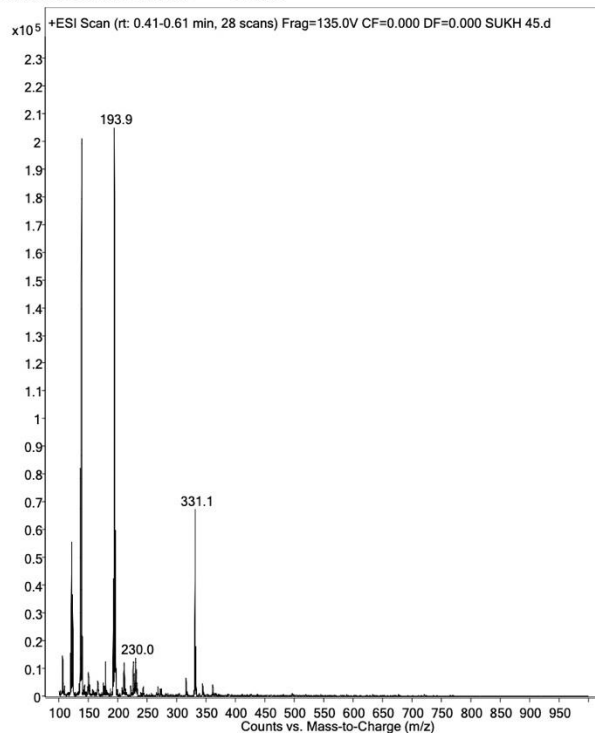


Figure 3.19: Mass spectrum of of $[\text{Co}(2,6\text{-diaminimethylpyridine})_2]^{3+}$.

The monoisotopic mass of $[\text{Co}(2,6\text{-diaminomethylpyridine})_2]^{3+}$ ($\text{CoC}_{14}\text{H}_{22}\text{N}_6$) is 333.12. The peak at m/z 331.1 can be assigned to a fragment having the molecular formula $\text{C}_{14}\text{H}_{20}\text{N}_6\text{Co}^+$ (calculated m/z 331.10), and this may be formed by the loss of two protons from the parent complex, shown in figure 3.20(a). The base peak is at m/z 193.9 which corresponds to a fragment having the molecular formula $\text{C}_7\text{H}_9\text{N}_3\text{Co}^+$ (calculated m/z 194.01); this may be formed by the loss of one ligand and two protons to give a 1+ charge to the fragment, figure 3.20(b). A high intensity peak is observed at m/z 138.0 and this can be assigned to the protonated ligand $\text{C}_7\text{H}_{12}\text{N}_3$ as LH^+ , figure 3.20(c). Another possibility for this peak is the pyridine ring attached to the cobalt ion by the loss of two CH_2 and two NH_2 groups to give the fragment $\text{C}_5\text{H}_5\text{NCo}^+$ (calculated m/z 137.9) and the cobalt(III) is reduced to cobalt(I), figure 3.20(d).

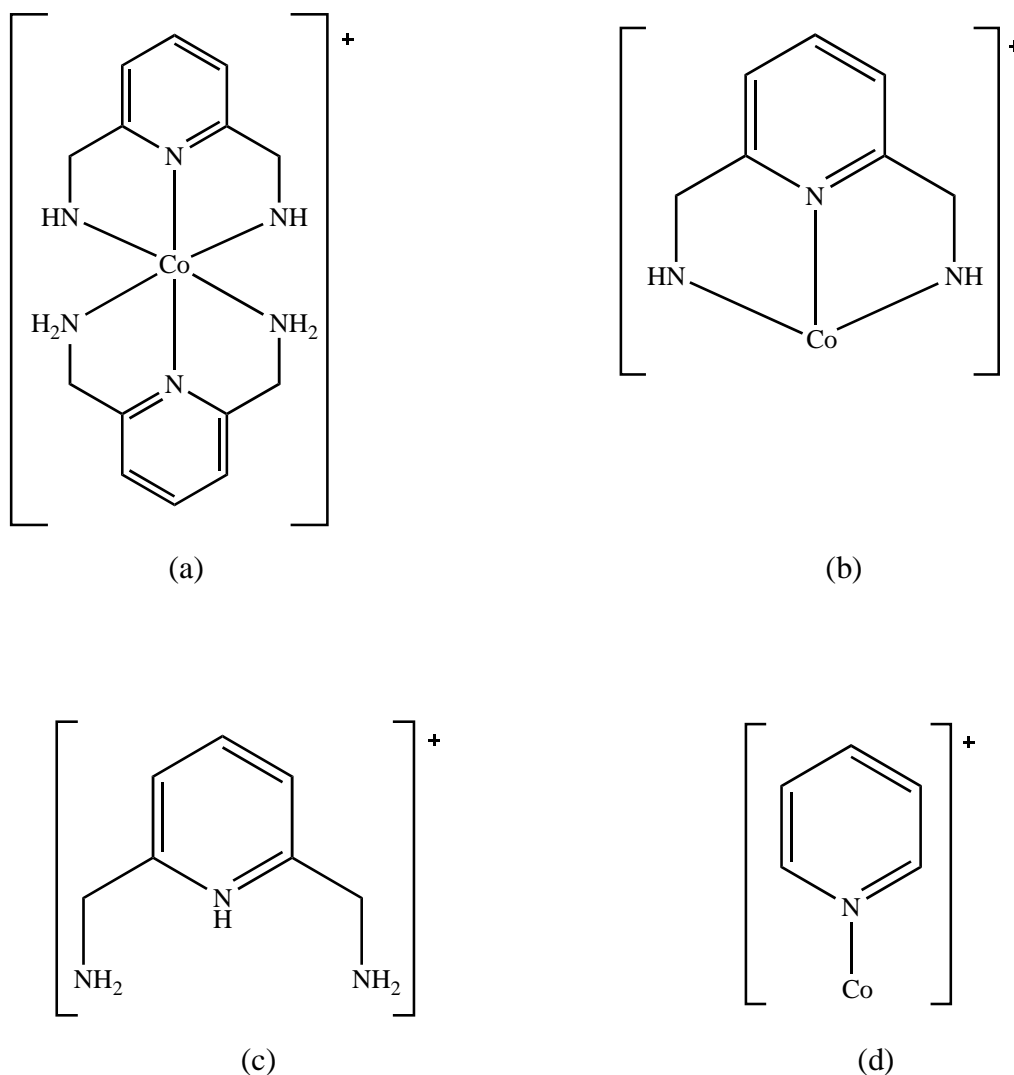


Figure 3.20: (a) Structure of $C_{14}H_{20}N_6Co^+$ formed by the loss of two protons, (b) Loss of one bamp ligand and two protons from the parent complex, (c) Protonated bamp ligand itself, (d) Loss of one bamp ligand and two $-CH_2NH_2$ arms from the other bamp ligand.

3.3.4 Synthesis and Characterisation of $[Co(NH_3)_6]Cl_3$.

$[Co(NH_3)_6]Cl_3$ was synthesised according to the literature method²⁵ through the aerial oxidation of a solution of $[Co(OH_2)_6]Cl_2$ and ammonium chloride/ammonia in water in the presence of charcoal. The yellow product was obtained in good yield. $[Co(NH_3)_6]Cl_3$ was characterised by 1H NMR spectroscopy and mass spectrometry.

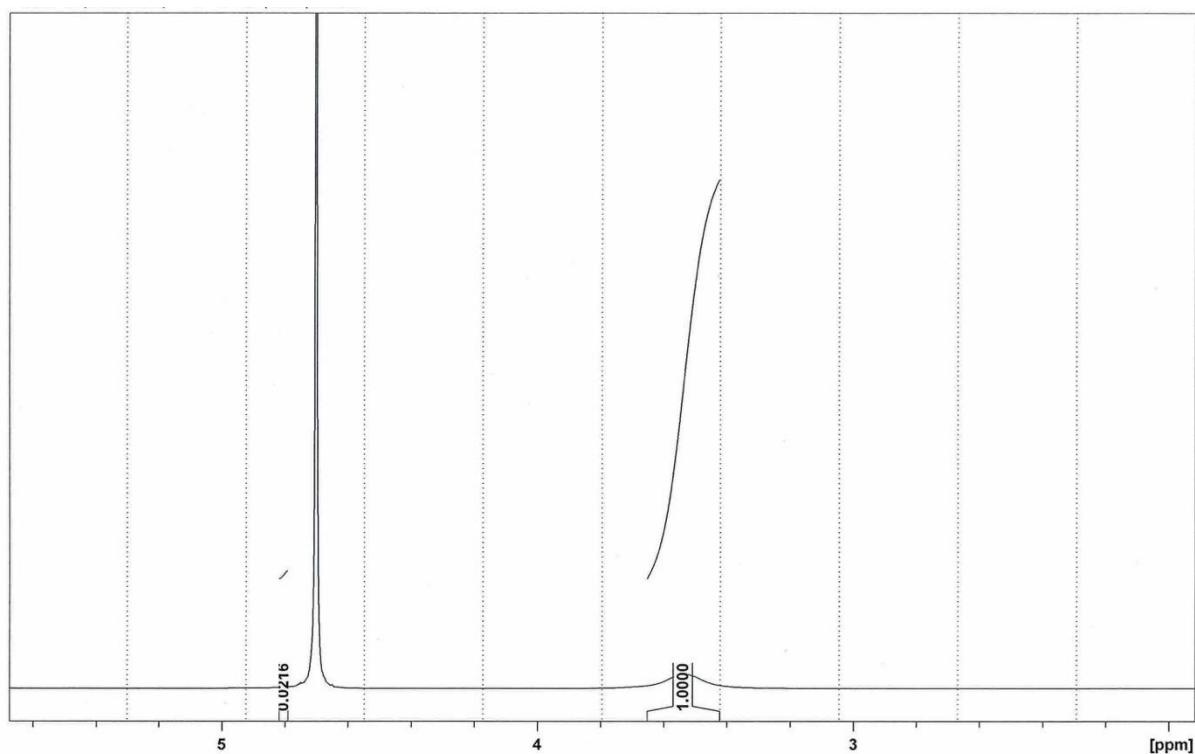


Figure 3.21(a): ^1H NMR spectrum of $[\text{Co}(\text{NH}_3)_6]\text{Cl}_3$.

The ^1H NMR spectrum of $[\text{Co}(\text{NH}_3)_6]\text{Cl}_3$, shown in figure 3.21, displays one singlet at $\delta = 3.5$ which is due to the N-H hydrogen atoms, with all the H atoms being in the same chemical environment. The mass spectrum of $[\text{Co}(\text{NH}_3)_6]^{3+}$ is shown in figure 3.22.

Sample Name	SUKH47 2	Position	Vial 72	Instrument Name	QQQ
User Name	QQQ\Agilent	Inj Vol	5	InjPosition	
Sample Type	Sample	IRM Calibration Status	Not Applicable	Data Filename	SUKH47 2.d
ACQ Method	FlowInjection no Column ESI SCAN Pos.m	Comment		Acquired Time	05-11-20 15:05:06

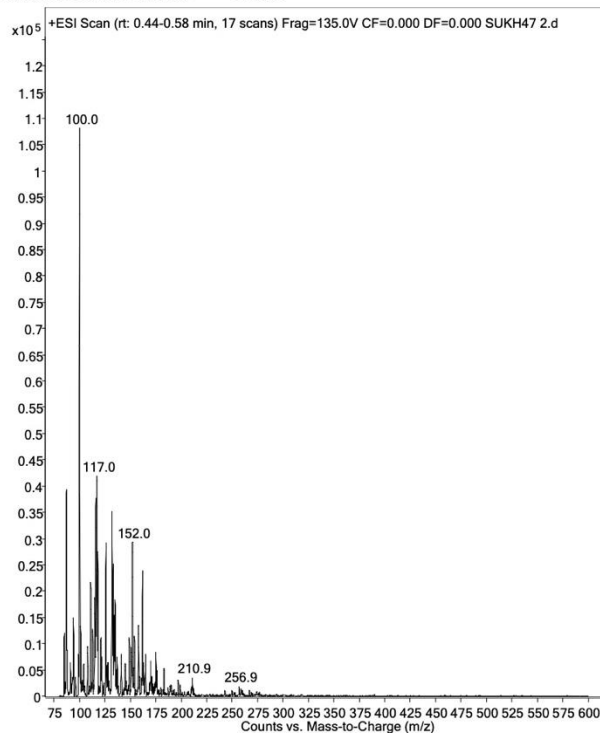


Figure 3.22: Mass spectrum of $[Co(NH_3)_6]^{3+}$.

The expected mass calculated for $[Co(NH_3)_6]^{3+}$ ($N_6H_{18}Co$) is 161.09, but no peak is observed at this value of m/z . A small peak is observed in the mass spectrum of $[Co(NH_3)_6]^{3+}$ at m/z 162.0 which could be due to the gain of a proton and reduction to Co(I) to give $CoN_6H_{19}^+$ (calculated m/z 162.09) but this appears chemically unreasonable as there is no obvious site for protonation. Another possibility for this peak is the loss of two NH_3 groups and gain of a chloride ion along with reduction of cobalt(III) to cobalt(II) to give $N_4H_{12}ClCo^+$ (calculated m/z 162.00), figure 3.23(a). The other high intensity peaks are difficult to interpret. However, there are some low intensity peaks which can be assigned to the fragments. For example, the peak at m/z 108.0 is due to the fragment having molecular formula $N_3H_7Co^+$ (calculated m/z 107.99), which is formed due to the loss of three amine ligands and loss of two protons to give a 1+ charge, figure 3.23(b). The peak at m/z 91.0 can be due to the fragment having

$[\text{Co}(\text{CN})_6]^{3-}$, while the solvents used were acetonitrile and water; vapour diffusion with diethylether was also used with the former solvent. The failure to obtain crystals may well be due to the probability that a large number of isomers can potentially be formed in these reactions.

3.4.1 Reaction of $[\text{Co}(\text{NH}_3)_6]\text{Cl}_3$ with formaldehyde and ammonia.

$[\text{Co}(\text{NH}_3)_6]\text{Cl}_3$ was reacted with formaldehyde and concentrated aqueous ammonia in the presence of lithium carbonate with continuous stirring for an hour. Both the change in the colour of the solution from orange to red-brown and the evolution of heat indicated a reaction had occurred. The product was purified by column chromatography using a Dowex 50Wx2 cation exchange column. The product was isolated as the chloride salt and characterisation was attempted by ^1H and ^{13}C NMR, and mass spectrometry.

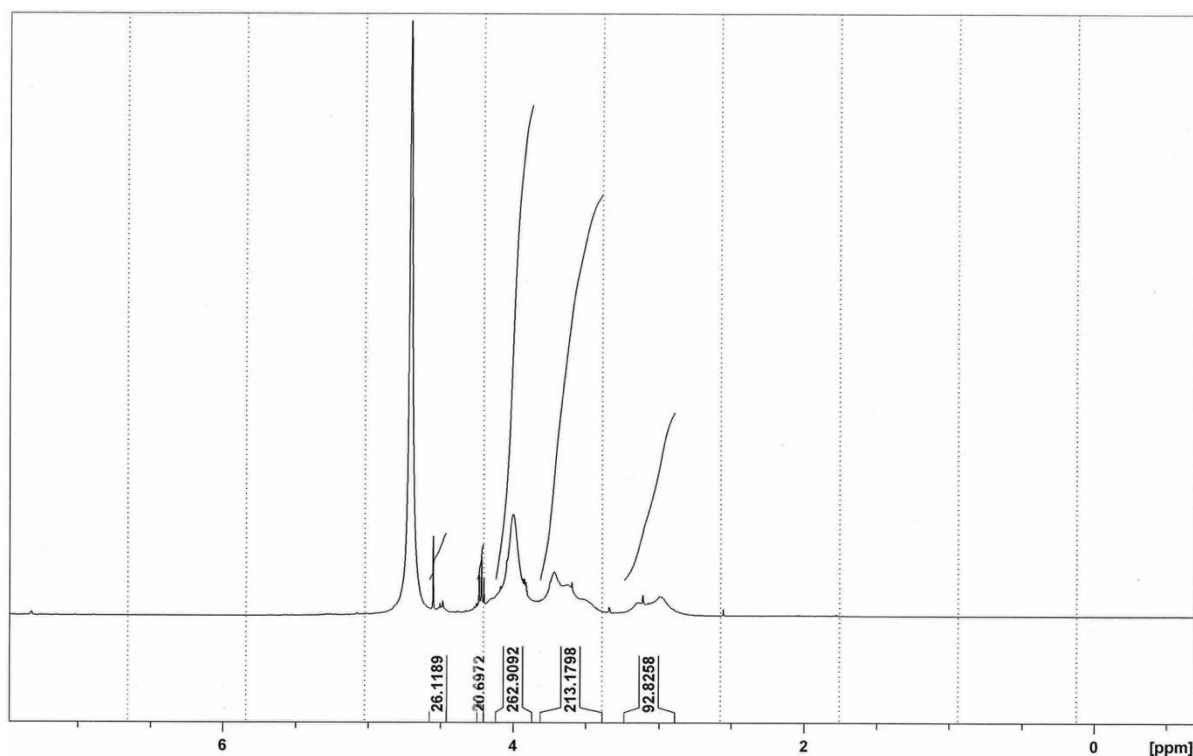


Figure 3.24(a): ^1H NMR spectrum of the complex formed by reacting $[\text{Co}(\text{NH}_3)_6]\text{Cl}_3$ with formaldehyde and ammonia.

The ^1H NMR spectrum, shown in figure 3.24(a), of the product confirmed that incorporation of one or more H-containing moieties had occurred, as the spectrum of the starting material, which contained only a single peak, was altered to give a triplet at 4.2 ppm and three broad multiplets in the region 4.0 – 2.8 ppm. These signals are in the ratio 1:3:3:2.

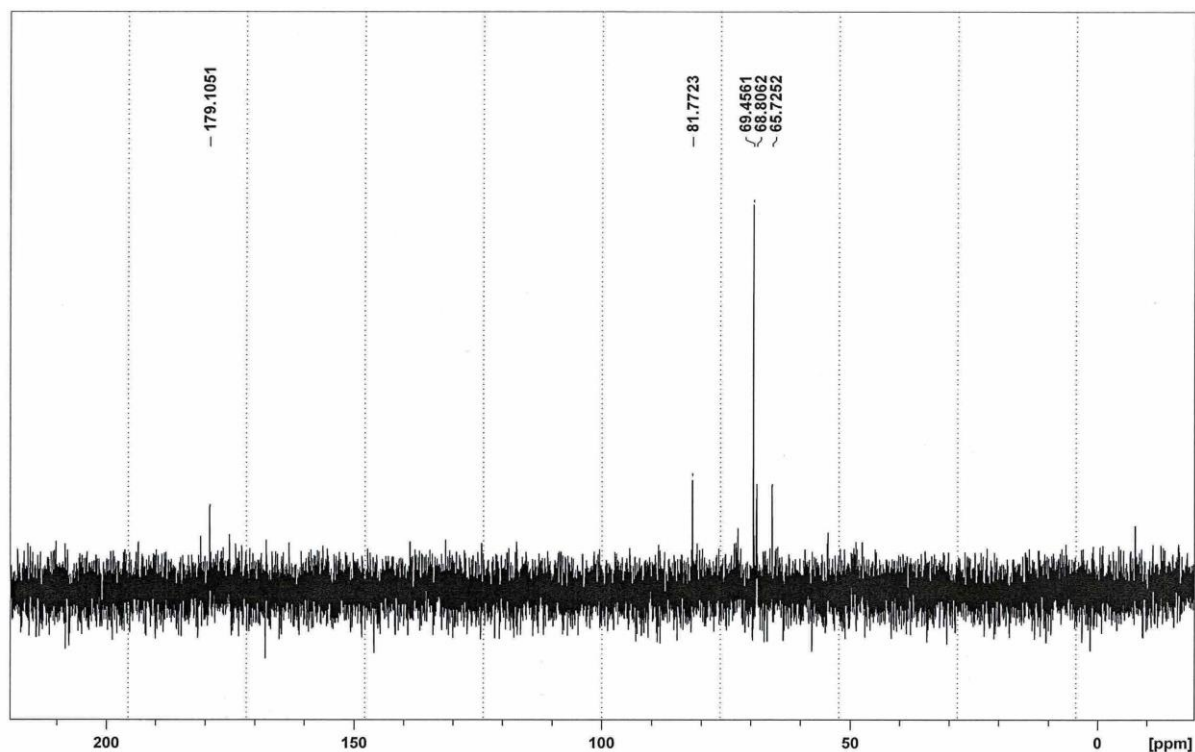


Figure 3.24(b): ^{13}C NMR spectrum of the complex formed by reacting $[\text{Co}(\text{NH}_3)_6]\text{Cl}_3$ with formaldehyde and ammonia.

The ^{13}C NMR spectrum, shown in figure 3.24(b), of this compound similarly showed that reaction had taken place, with peaks observed at δ 179.10, 81.77, 69.45, 68.80, and 65.72 ppm. No peaks were observed in the parent complex because there were no carbons. The peak at $\delta = 69.45$ ppm is of significantly higher intensity than the other peaks, and perhaps suggests that the isolated complex is impure. The chemical shift of this peak strongly suggests that it corresponds to a N-C-N carbon atom of a ‘capping’ $\text{N}(\text{CH}_2)_3$ -unit, given its similarity to the chemical shifts of analogous peaks in the ^{13}C NMR spectrum of $[\text{Co}(\text{sep})]^{3+}$. The peak at 179.10 is consistent with the presence of an imine carbon atom.

The mass spectrum of the newly formed complex is shown in figures 3.25a and 3.25b.

Sample Name	Unavailable	Position	Unavailable	Instrument Name	Unavailable
User Name	Unavailable	Inj Vol	Unavailable	InjPosition	Unavailable
Sample Type	Unavailable	IRM Calibration Status	Not Applicable	Data Filename	SUKH 49 A 3.d
ACQ Method		Comment	Sample information is unavailable	Acquired Time	Unavailable

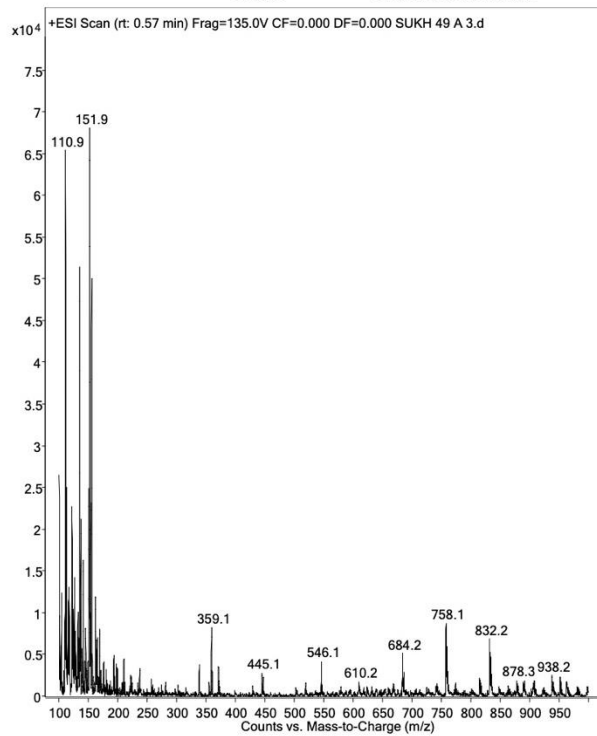


Figure 3.25a: Mass spectrum of the new cage complex formed after reaction with formaldehyde and ammonia .

Sample Name	Unavailable	Position	Unavailable	Instrument Name	Unavailable
User Name	Unavailable	Inj Vol	Unavailable	InjPosition	Unavailable
Sample Type	Unavailable	IRM Calibration Status	Not Applicable	Data Filename	SUKH 49 B 3.d
ACQ Method		Comment	Sample information is unavailable	Acquired Time	Unavailable

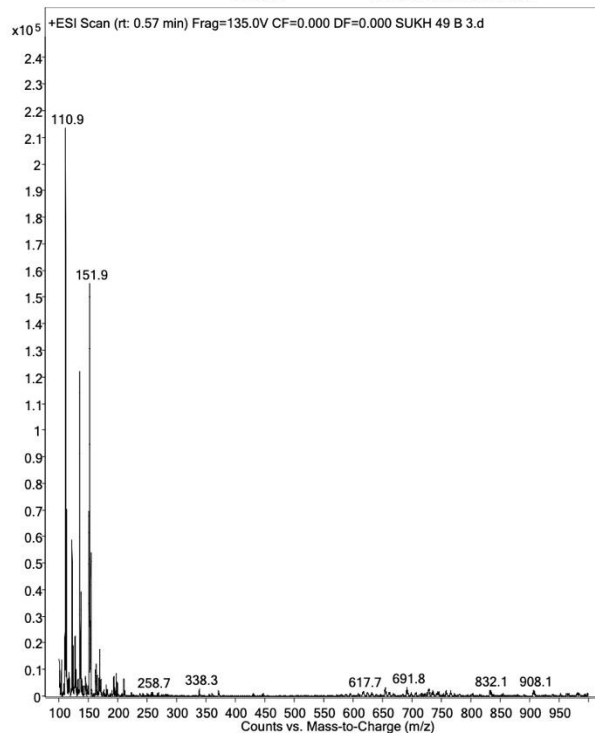


Figure 3.25b: Mass spectrum of the new cage complex formed after reaction with formaldehyde and ammonia .

Two mass spectra were obtained for the same product. Three prominent peaks in both spectra were observed at m/z 110.9, m/z 134.9 and m/z 151.9, but these proved difficult to assign in a chemically sensible manner. All other peaks were of low intensity and based on these, assumed structure possibilities for the new cage complex is shown in figure 3.26. A very low intensity peak is observed in both the spectra at m/z 371.0 is consistent with the molecular formula $C_{12}H_{28}N_{10}Co^+$ (calculated m/z 371.18) formed by the loss of two protons to give 1+ charge to the complex. This complex has four apical N atoms bonded to the coordinated ammonia ligands through carbon atoms, shown in figure 3.26(a). A small intensity peak at m/z 161.9 in spectrum 3.15a is consistent with the half cage structure of the complex, shown in figure 3.26(b), with the loss of three amine ligands and a proton to give the fragment having molecular formula $C_3H_{11}N_4Co^+$ (calculated m/z 162.03) where cobalt(III) is reduced to cobalt(II). The peak at m/z 162.9 in spectrum 3.15b is consistent with the $C_3H_{12}N_4Co^+$ (calculated m/z 163.03) where cobalt(III) is reduced to cobalt(I) along with the loss of three

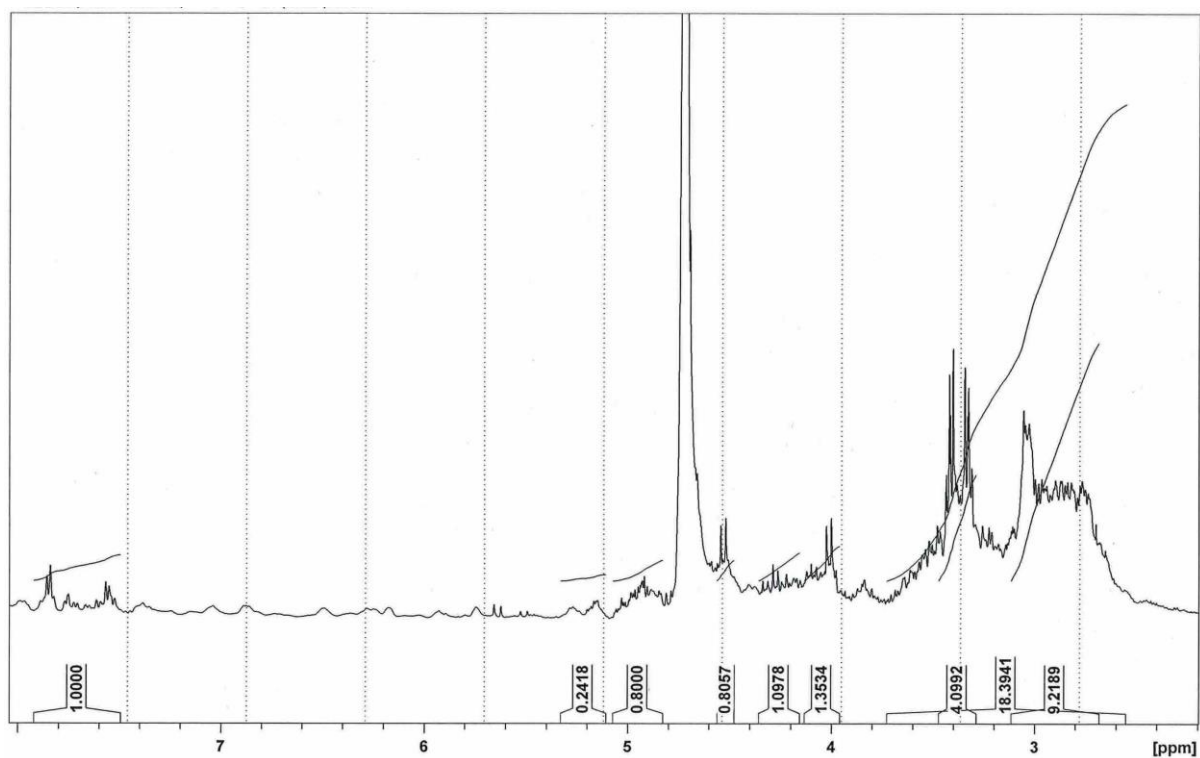


Figure 3.27(a): ^1H NMR spectrum of the complex formed by reacting $[\text{Co}(\text{dien})_2]\text{Cl}_3$ with formaldehyde and ammonia.

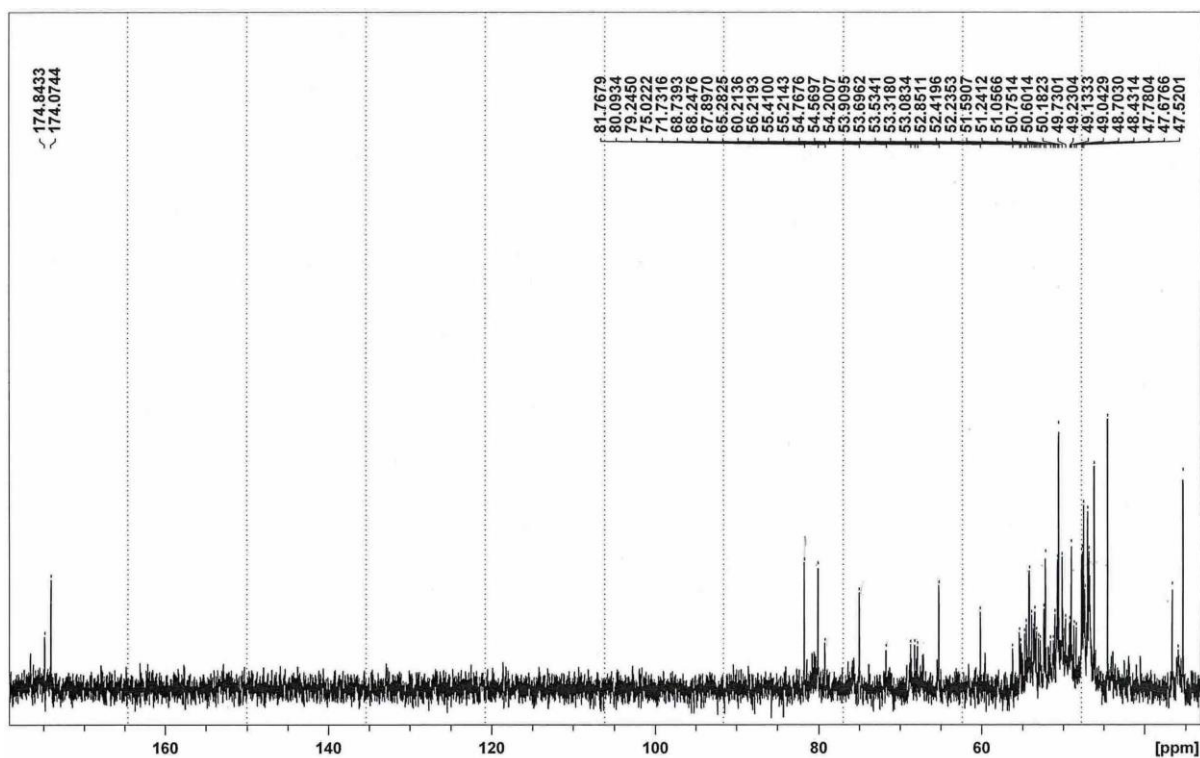


Figure 3.27(b): ^{13}C NMR spectrum of the complex formed by reacting $[\text{Co}(\text{dien})_2]\text{Cl}_3$ with formaldehyde and ammonia.

The ^1H NMR spectrum of the complex in D_2O , shown in figure 3.27(a), displays a number of multiplets in the region $\delta = 8.0$ to 1.53 ppm. The singlet peaks in the spectrum of parent complex are altered to broad multiplets in the new complex with a slight shift of the signals to downfield region. The ^{13}C NMR spectrum of the complex in D_2O , shown in figure 3.27(b), display many signals over the region $\delta = 174.8$ to 35.34 ppm. These signals could be due to the impurities or due to the formation of isomers. The NMR of the new complex consists the peaks of the parent complex but in low intensities. The presence of many different signals which were of high intensity comparatively, can therefore suggest that the reaction with formaldehyde and ammonia has resulted in the inclusion of different carbons that link the coordinated N of the parent complex. The NMR was noisy and it was difficult to interpret each signals at that stage.

The mass spectrometry of the newly formed complex, figure 3.28, shows some of the same peaks as seen in the mass spectrum of the parent complex. It is also rather noisy, perhaps suggesting the presence of a number of isomers which fragment in different ways.

The prominent peaks at m/z 162.0 and 196.9 are already explained above in section 3.2, the latter being the base peak in this spectrum. The former peak is due to the fragment having one dien ligand attached to the reduced cobalt(I) from cobalt(III), i.e. $[\text{Co}(\text{dien})]^+$ ($\text{C}_4\text{H}_{13}\text{N}_3\text{Co}^+$, calculated m/z 162.04), figure 3.29(a) and the peak at 196.9 is due to the same fragment but with one chloride attached, and Co(III) reduced to Co(II), $[\text{Co}(\text{dien})\text{Cl}]^+$. The isotopic ratio for the latter peak (peaks 2 m/z units apart, in a 3:1 ratio) is indicative of the presence of chlorine. Other possibility for this peak is the fragment having molecular formula $\text{C}_3\text{H}_{11}\text{N}_4\text{ClCo}^+$ (calculated m/z 197.00), figure 3.29(b) which derives from loss of a proton from a half-cage structure and reduction to Co(II) to give an overall 1+ charge. The peaks at m/z 246.0, 274.2, 299.0 and one small peak at 663.4 were also similar to those observed in the parent complex, but again proved difficult to assign. One prominent peak at m/z 365.1 is consistent with a species having the molecular formula $\text{C}_{12}\text{H}_{29}\text{N}_7\text{ClCo}^+$ (calculated m/z 365.15), figure 3.29(c). This is formed through capping the dien ligands with a $\text{N}(\text{CH}_2)_3^-$ unit, and formation of an imino moiety, both of which have precedence in the literature, along with reduction to Co(II).

Sample Name	SUKH32 3	Position	Vial 93	Instrument Name	QQQ
User Name	QQQ\Agilent	Inj Vol	10	InjPosition	
Sample Type	Sample	IRM Calibration Status	Not Applicable	Data Filename	SUKH32 3.d
ACQ Method	FlowInjection no Column ESI SCAN Pos.m	Comment		Acquired Time	03-09-20 14:20:10

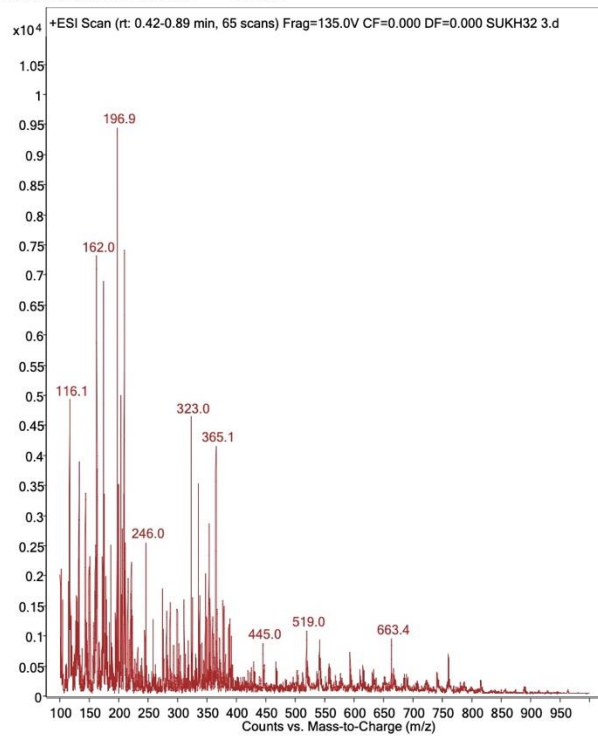


Figure 3.28: a) Full mass spectrum of the new complex formed by the reaction of $[\text{Co}(\text{dien})_2]\text{Cl}_3$ with formaldehyde and ammonia.

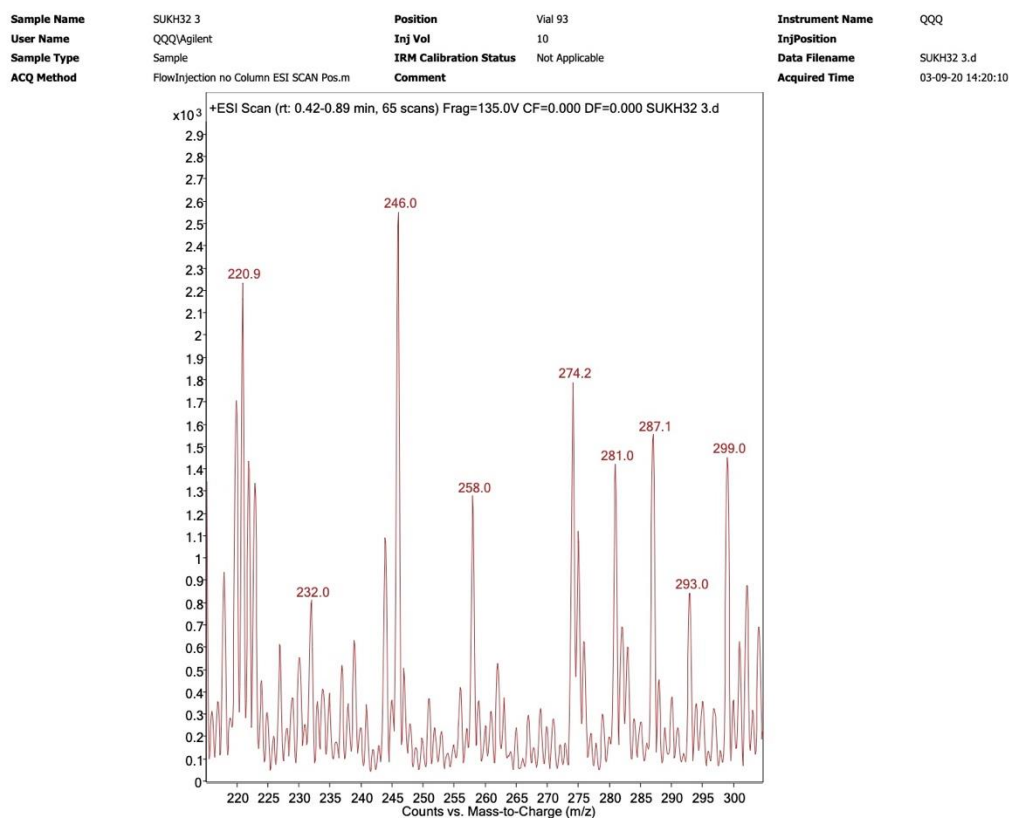


Figure 3.28: a) Full mass spectrum and b) mass spectrum (m/z 215-305) of the product formed by the reaction of $[Co(dien)_2]Cl_3$ with formaldehyde and ammonia.

The peak of approximately 1/3 the intensity at m/z 367 implies the presence of chlorine. A peak at m/z 353.0 is consistent with a species having molecular formula $C_{11}H_{29}N_7ClCo^+$ (calculated m/z 353.15), figure 3.29(d), where an incomplete cap is formed, along with a four-membered $Co(N-C-N)$ ring. Reduction of cobalt(III) to cobalt(II) also occurs. A prominent peak at m/z 208.9 is consistent with the fragment having the molecular formula $C_4H_{18}N_6Co^+$ (calculated m/z 209.09) where two incomplete cages have formed, figure 3.29(e). Another possible cage formation process in which the dien ligands are linked by single carbon bridges can give rise to a macrocyclic fragment having the molecular formula $C_{10}H_{24}N_6Co^+$ figure 3.29(f). This is consistent with the peak observed at m/z 287.1 (calculated m/z 287.13). A prominent peak at m/z 323.0 appears to be closely related to this, being consistent with a fragment having the molecular formula $C_{10}H_{25}N_6ClCo^+$ (calculated m/z 323.11) which can be formed from the above intact macrocycle by the addition of one chloride, loss of a proton and reduction to $Co(II)$ to give the fragment a +1 charge. The

presence of chlorine is indicated by the peak at m/z 325.0 which is approximately 1/3 of the intensity of the parent.

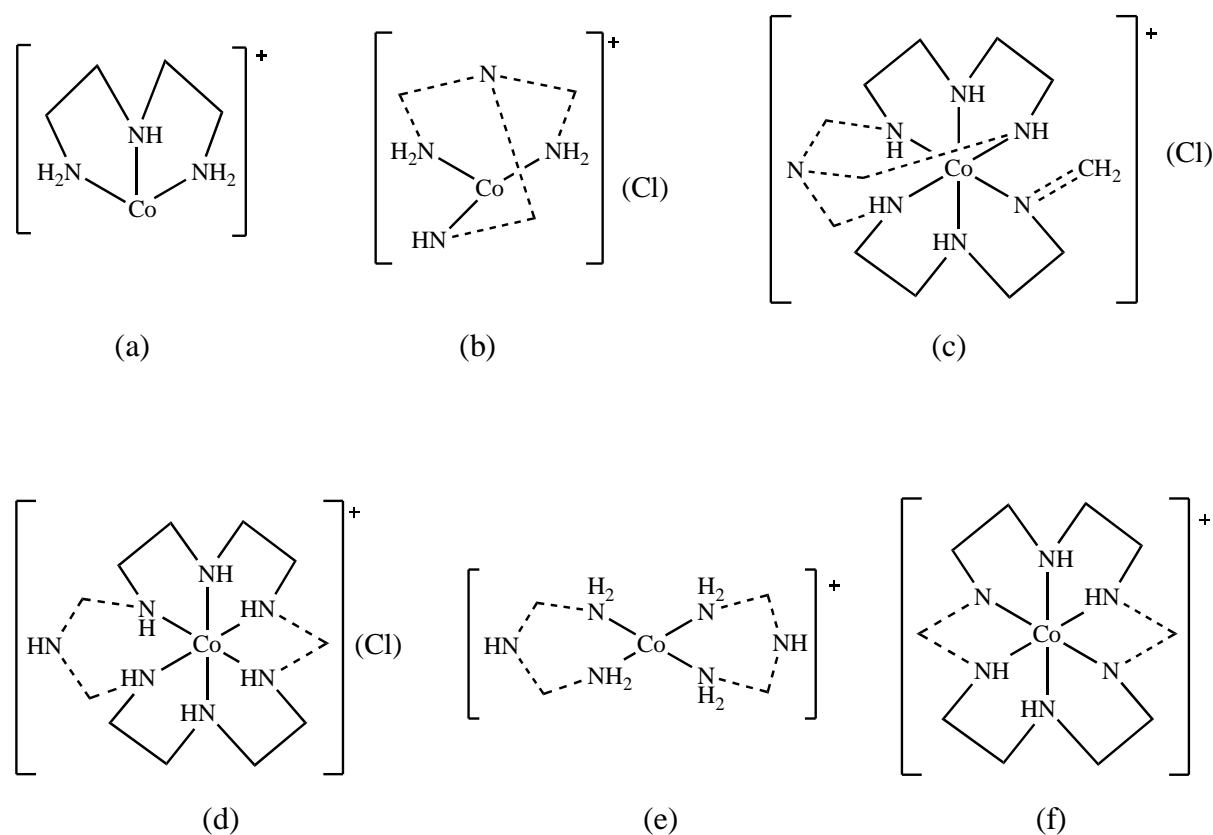


Figure 3.29: (a) Fragment formed by the loss of one dien ligand and loss of any cage formed; (b) Fragment consisting of N atoms only that are involved in the formation of cage structure; (c) Possible cage structure that involve three coordinated N atoms bonded to apical N atom through carbon atoms and the formation of imine bond to one coordinated N atom; (d) Another possible cage structure formed by apical N atom involving two N atoms coordinated to cobalt and the other two NH_2 groups linked through carbon atom; (e) Fragment involving only those coordinated N atoms which are linked to two apical N atoms through carbon atoms to form cage structure; (f) Another possible cage structure formed by $\text{NH-CH}_2\text{-NH}$ link.

According to the fragments and peaks observed in the mass spectrum, the structures of the possible cage complexes and their possible isomers, are shown in figure 3.30.

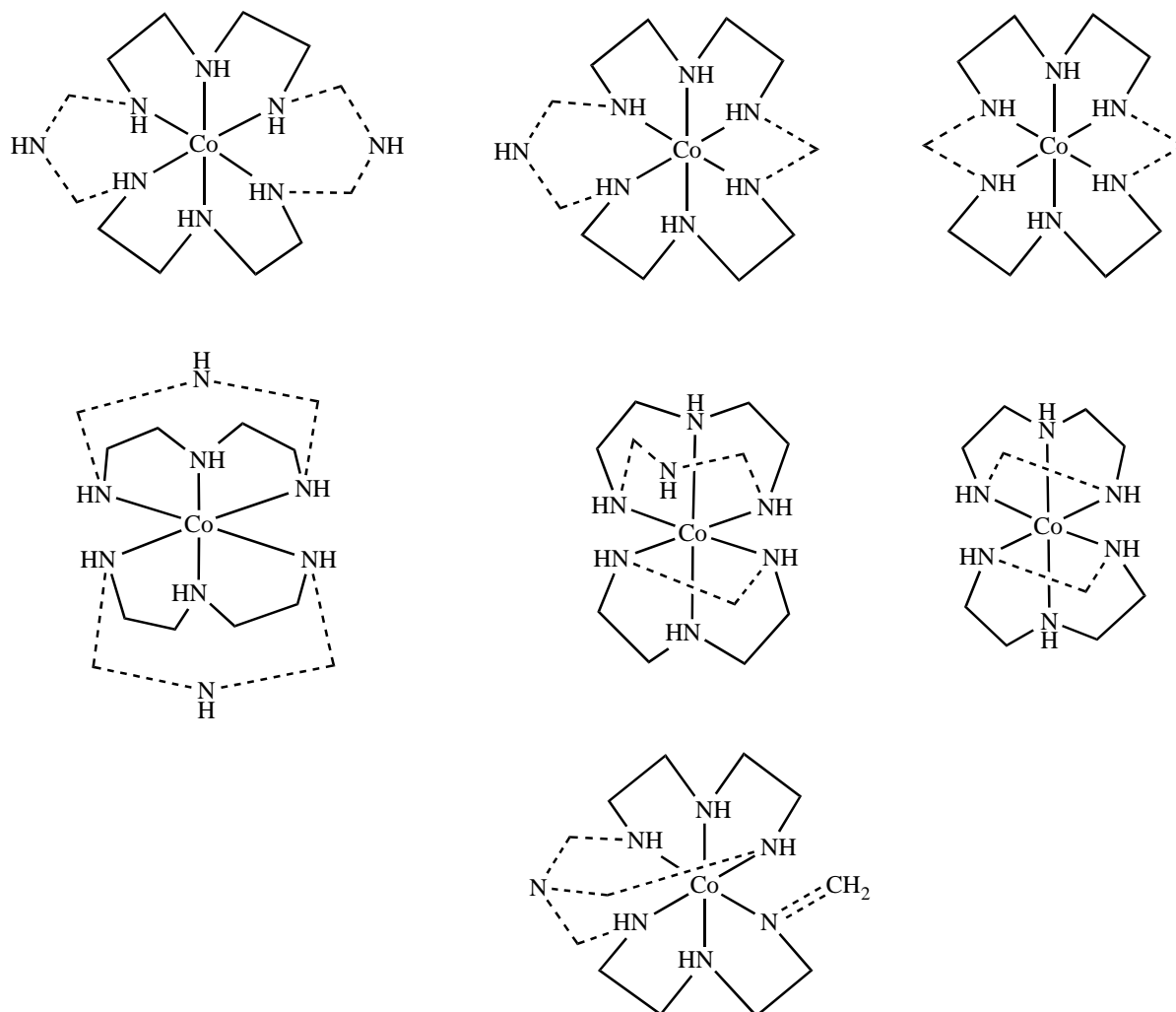


Figure 3.30: Assumed cage structure of the newly formed cage complex and the possible isomers which may arise due to the cages formed within the same ligand or between two ligands.

3.4.2 Reaction of $[\text{Co}(2,6\text{-di(aminomethyl)pyridine})_2]\text{Cl}_3$ with formaldehyde and ammonia.

$[\text{Co}(2,6\text{-di(aminomethyl)pyridine})_2]\text{Cl}_3$ was reacted with formaldehyde and conc. aqueous ammonia in the presence of lithium carbonate with continuous stirring for an hour. The colour of the solution changed from light orange to orange-red on the addition of formaldehyde and ammonia, with the evolution of heat. The product was purified by column chromatography using a Dowex 50Wx2 cation exchange column and then isolated as a chloride salt of greenish-yellow colour. Characterisation of the product was attempted using ^1H NMR, ^{13}C NMR and mass spectrometry.

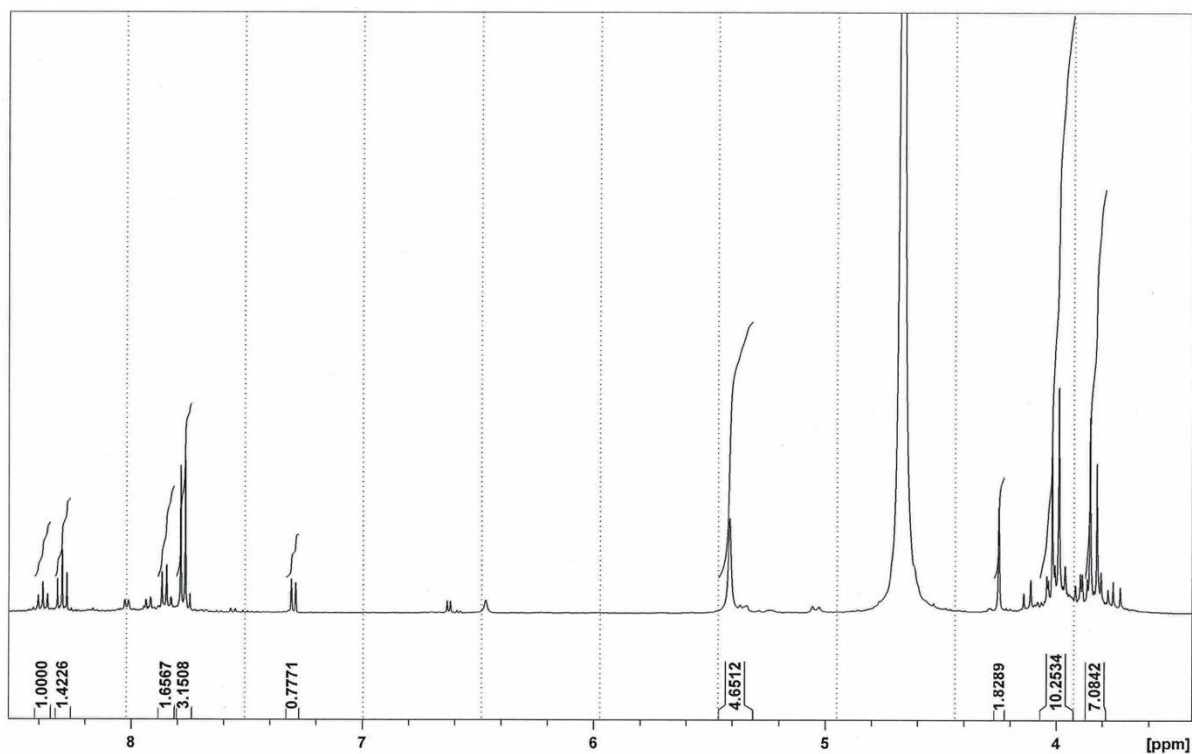


Figure 3.31(a): ^1H NMR spectrum of the complex formed by reacting $[\text{Co}(2,6\text{-di(aminomethyl)pyridine})_2]\text{Cl}_3$ with formaldehyde and ammonia.

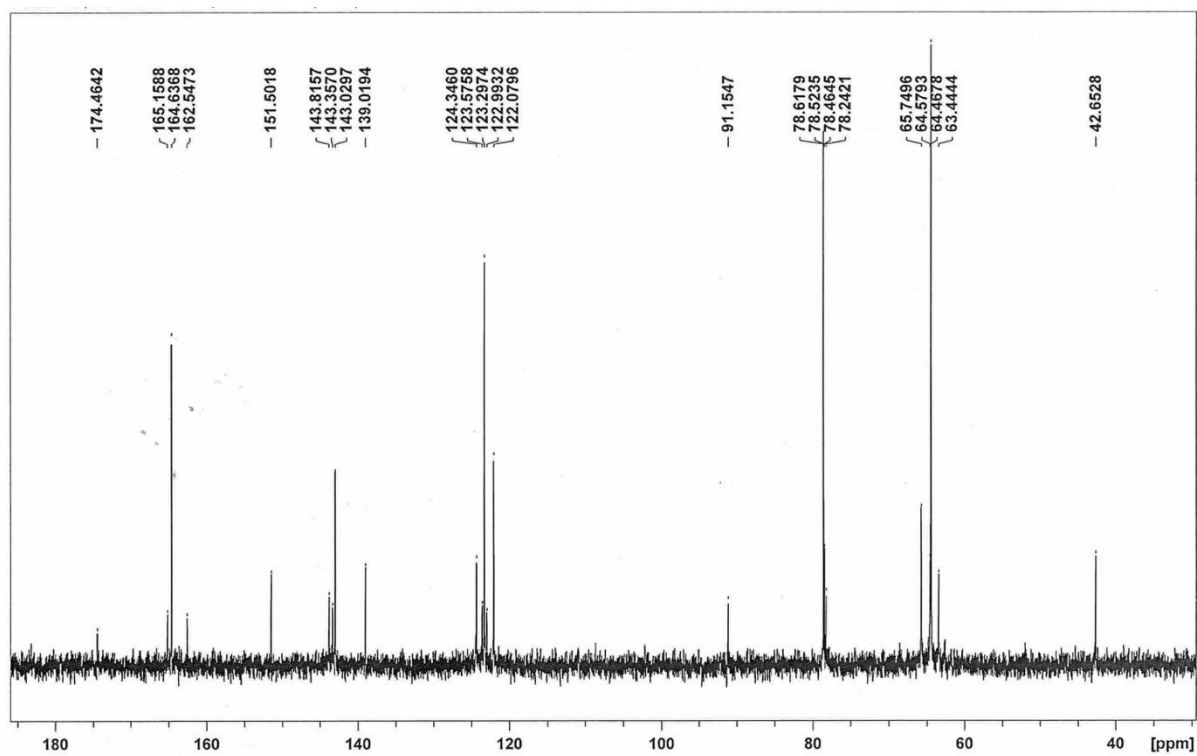


Figure 3.31(b): ^{13}C NMR spectrum of the complex formed by reacting $[\text{Co}(2,6\text{-di(aminomethyl)pyridine})_2]\text{Cl}_3$ with formaldehyde and ammonia.

The ^1H NMR spectrum, shown in figure 3.31(a), displays signals in the region $\delta = 3.7$ to 8.5 ppm. It consists of two multiplets, two singlets, two triplets and three doublets. Four additional peaks were observed when compared with the ^1H NMR spectrum of the parent complex. The broad multiplets observed in the upfield region can be assigned to the methylene carbons that link the neighbouring N of the complex. The ^{13}C NMR spectrum of the newly formed cage complex, shown in figure 3.31(b), display 8 signals in the region $\delta = 42.64$ to 164.6 ppm. Three peaks in the downfield region, are close to the peaks observed in the parent complex and also the intensity of the leftmost peak is slightly greater than the parent complex. There are two high intensity peaks at $\delta = 64.46$ ppm and $\delta = 78.45$ ppm which suggests the inclusion of carbons that form the cage structure. However, the intensity of the most upfield peak is low as compared to the other peaks of the complex as well as compared to that in the NMR spectrum of parent complex. There are two more peaks at $\delta = 65.74$ ppm and 122.07 ppm.

The mass spectrum of this complex is shown in figure 3.32. The base peak m/z 138.0 is similar to that found for the parent complex which is consistent with a pyridine ring bonded to a Co(I) ion, giving a fragment having molecular formula $\text{C}_5\text{H}_5\text{NCo}^+$ (calculated m/z 137.97), figure 3.33(a). A medium intensity peak is observed at m/z 315.0 which is consistent with the parent complex losing two arms of one of the bamp ligands, intramolecular half-capping of the other bamp ligand, along with loss of a proton and reduction of cobalt(III) to cobalt(II), giving a fragment having molecular formula $\text{C}_{14}\text{H}_{18}\text{N}_5\text{Co}^+$ (calculated m/z 315.08), figure 3.33(b). Another prominent peak observed at m/z 236.0 can be formed from the m/z 315 peak by loss of pyridine and a proton, to give a fragment having the molecular formula $\text{C}_9\text{H}_{13}\text{N}_4\text{Co}^+$ (calculated m/z 236.04), figure 3.33(c). this requires the reduction of cobalt(III) to cobalt(II).

Sample Name	SUKH46	Position	Vial 71	Instrument Name	QQQ
User Name	QQQ\Agilent	Inj Vol	5	InjPosition	
Sample Type	Sample	IRM Calibration Status	Not Applicable	Data Filename	SUKH46.d
ACQ Method	FlowInjection no Column ESI SCAN Pos.m	Comment		Acquired Time	05-11-20 15:00:09

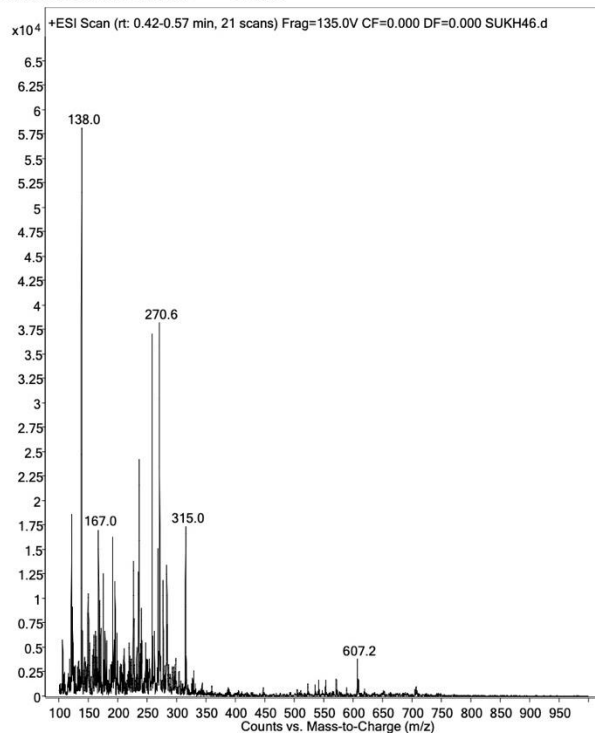


Figure 3.32: Mass spectrum of the product formed after reaction of $[\text{Co}(2,6\text{-di}(\text{aminomethyl})\text{pyridine})_2]\text{Cl}_3$ with formaldehyde and ammonia.

The peak at m/z 167.0 is consistent with a fragment in which half capping has taken place along with loss of a proton, having the molecular formula $\text{C}_2\text{H}_{14}\text{N}_5\text{Co}^+$ (calculated m/z 167.05) where cobalt(III) is reduced to cobalt(II), figure 3.33(d). The peak at m/z 149.0 is due to the N-C-N linking of the coordinated amines and the loss of two protons give a 1+ charge to $\text{C}_2\text{H}_{10}\text{N}_4\text{Co}^+$ (calculated m/z 149.02), figure 3.33(e). A fragment formed by losing one proton, one CH_2 and one NH_2 and reduction of cobalt(III) to cobalt(II) to give $\text{CH}_8\text{N}_3\text{Co}^+$ (calculated m/z 121.00), figure 3.33(f), is consistent with the peak observed at m/z 121.0. The peak observed at m/z 191.0 is consistent with a fragment having the molecular formula $\text{C}_4\text{H}_{14}\text{N}_5\text{Co}^{+2}$, which can be formed by the loss of both the pyridine rings of the ligands along with a proton to give a 2+ charged complex (calculated m/z 191.07), figure 3.33(g), which then requires reduction of cobalt(III) to cobalt(II).

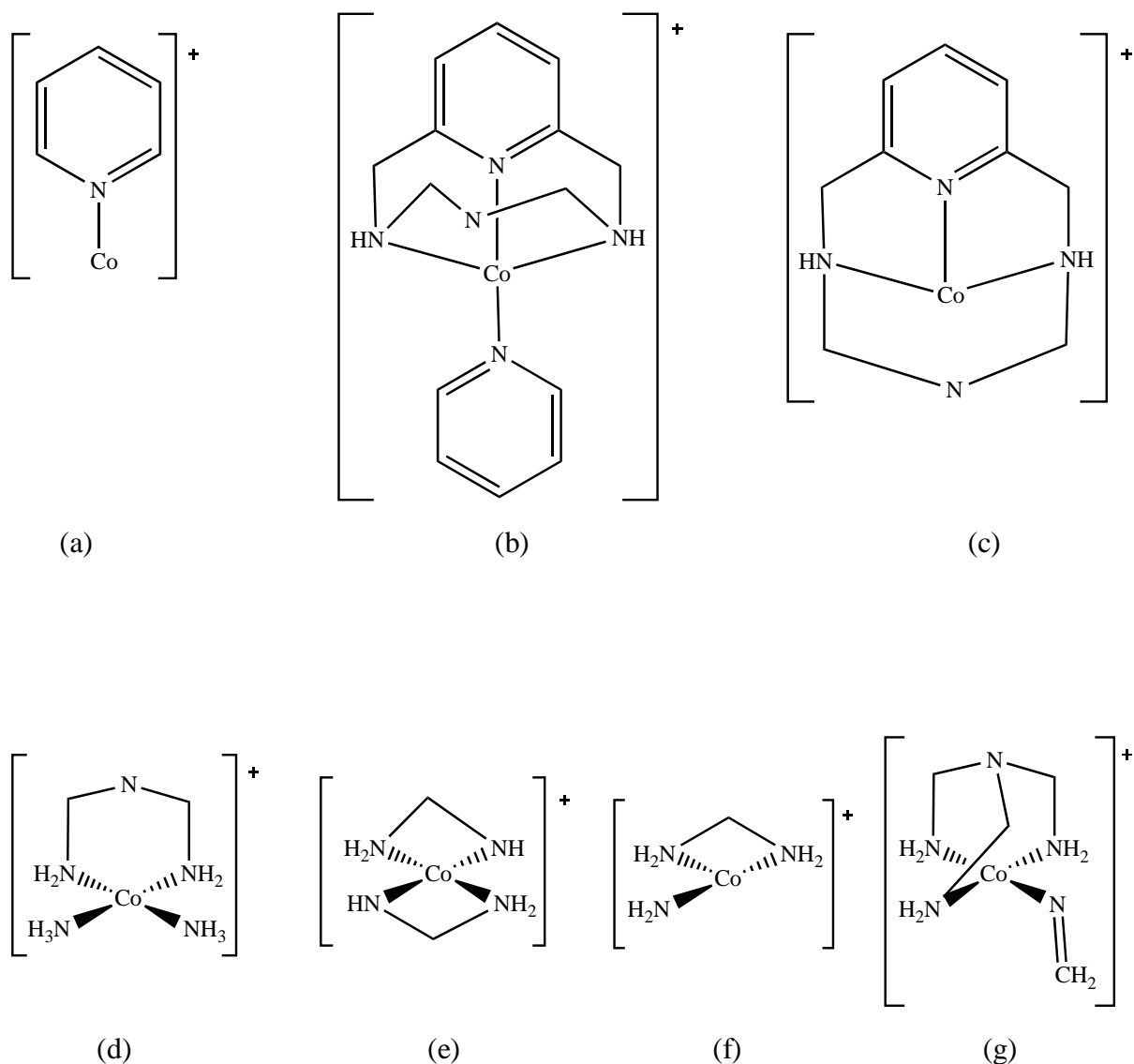


Figure 3.33: (a) A fragment same as observed in the mass spectrum of parent complex; (b) Assumed cage formed around N atoms of one ligand and the fragment formed by the loss of two arms of other bamp ligand; (c) Fragment formed by the loss of one ligand and structure consisted of cage around the other ligand attached to cobalt; (d) Fragment consisting of one cage and is formed by the loss of both ligands except the NH_2 coordinated to cobalt; (e) Fragment consisting of N atoms that are involved in the cage structure; (f) Fragment formed by the loss of both ligands except the N atoms that are involved in the cage formation and except one amine ligand that may have broken from the arm of the bamp ligand; (g) Fragment consisting of N atoms that are involved in the cage formation through another possibility.

There are some other peaks which are difficult to interpret without the actual crystal structure. The possible fragments observed in the mass spectrometry can therefore be formed from the possible structures of the new cage complex, shown in figure 3.34. However, no peaks were observed in the mass spectrum of the cage complex which can confirm these structures.

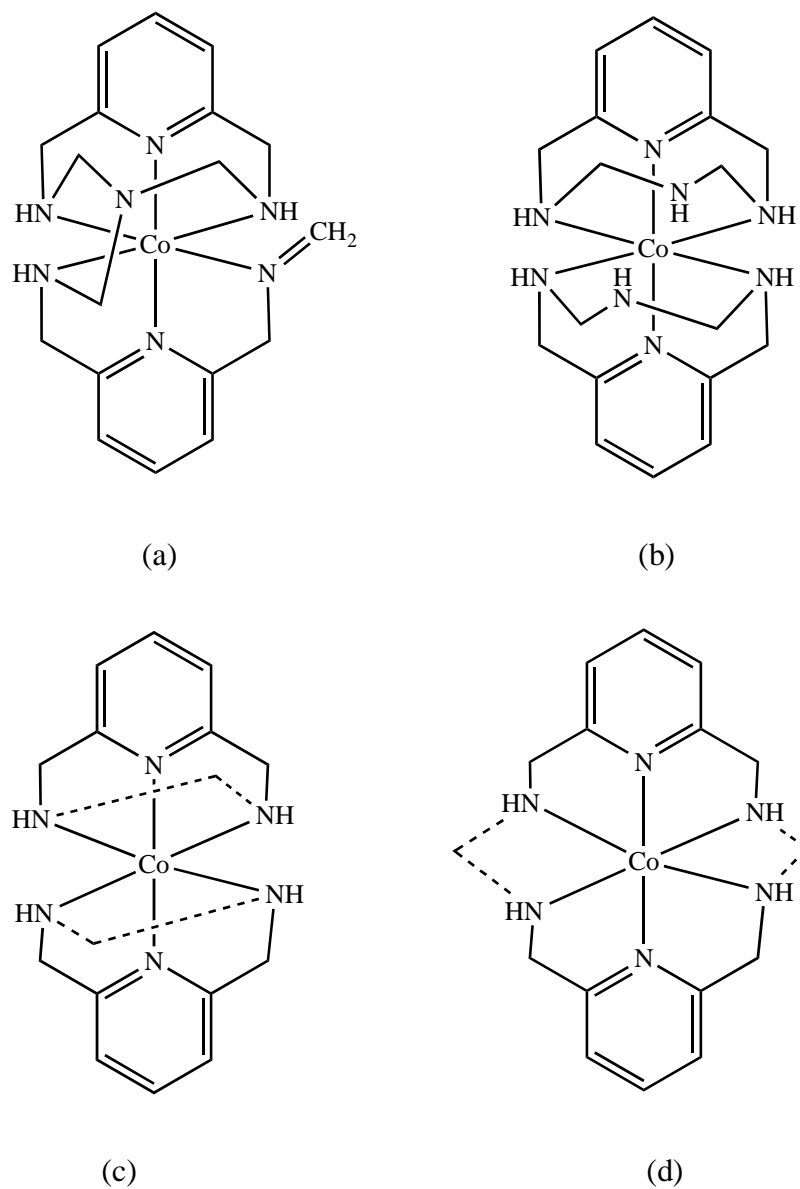


Figure 3.34: The four possibilities assumed for the formation of cage structure around the $[Co(bamp)]^{3+}$ complex. In (a), the cage structure involves three N atoms of both ligands to form bond with apical N atom through carbons, while one coordinated N atom is involved in the formation of imine. While in (b), two apical N atoms are forming cages with four coordinated N atoms of the ligand separately through carbon atoms. In (c) and (d), the cage structure is formed via carbons only which can link the coordinated N atoms of the same ligand or can link the N of two ligands.

3.4.4 Reaction of $[\text{Co}(\text{tren})(\text{en})]\text{Cl}_3$ with formaldehyde and ammonia.

$[\text{Co}(\text{tren})(\text{en})]\text{Cl}_3$ was reacted with formaldehyde and ammonia with continuous stirring for an hour, using an adaptation of the literature method for the synthesis of cage complexes²⁷. The colour of the solution changed from orange to red and heat was evolved. The complex was purified by column chromatography on a Dowex 50Wx2 cation exchange column. A red-orange band was observed on the column and was collected using HCl as described in the experimental section. After removal of the solvent, the purple hygroscopic product was isolated as the chloride salt following washing with isopropanol and air-drying. Characterisation of the complex was attempted by ^1H and ^{13}C NMR spectra, shown in figure 3.35(a) and 3.35(b), and mass spectrometry.

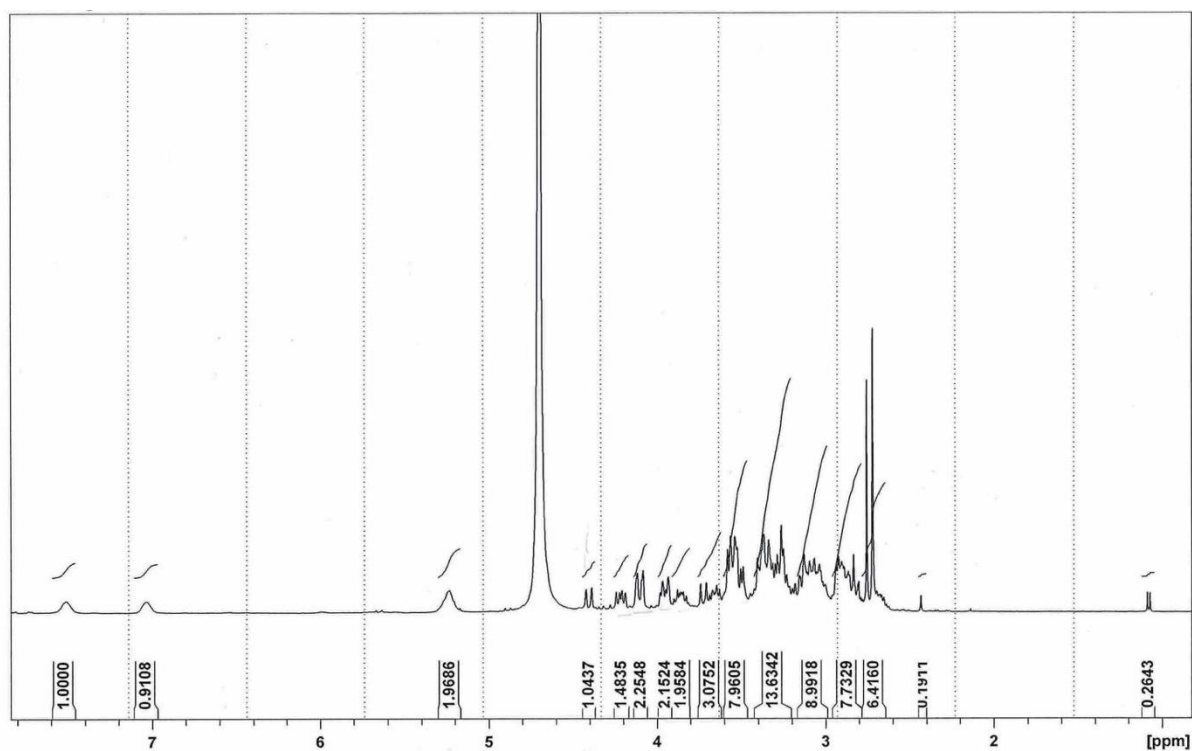


Figure 3.35(a): ^1H NMR spectrum of the complex formed by reacting $[\text{Co}(\text{tren})(\text{en})]\text{Cl}_3$ with formaldehyde and ammonia.

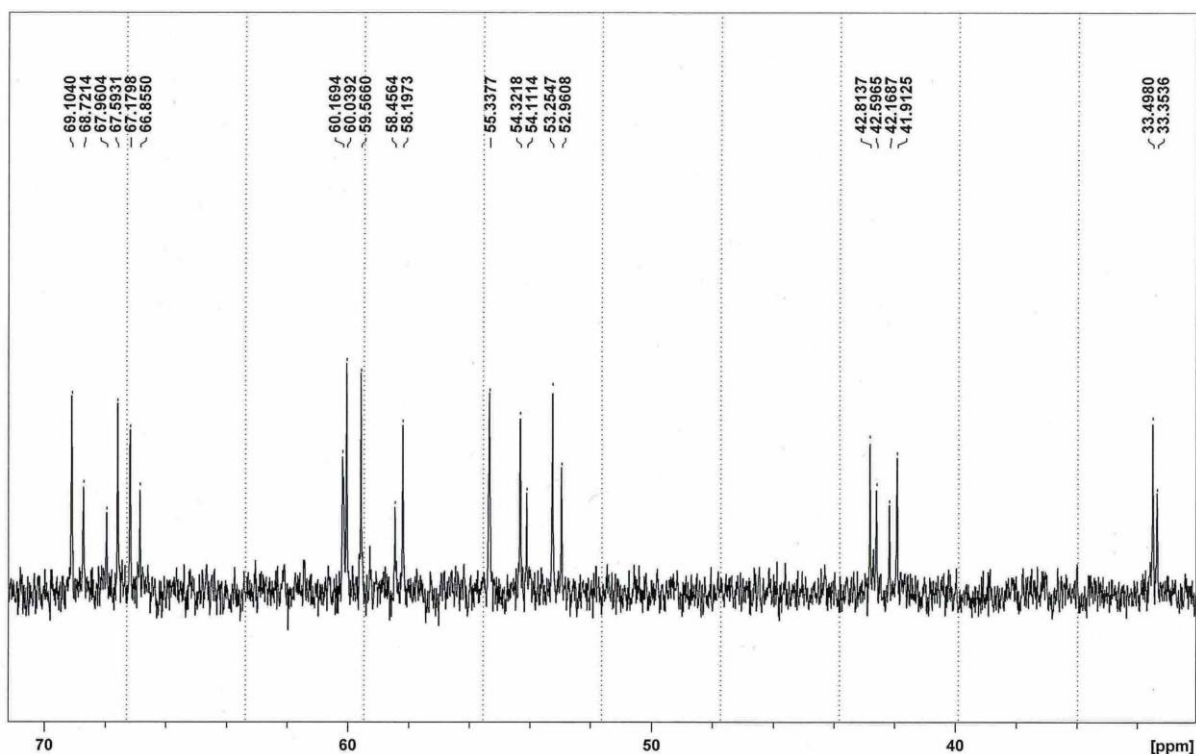


Figure 3.35(b): ^{13}C NMR spectrum of the complex formed by reacting $[\text{Co}(\text{tren})(\text{en})]\text{Cl}_3$ with formaldehyde and ammonia.

The ^1H NMR spectrum of the complex in D_2O displays a methylene envelope over the region $\delta = 2.7$ ppm to 4.5 ppm. Three broad singlets of low intensity are observed at lower field, and these are undoubtedly due to N-H protons. In comparison to the ^1H NMR of the starting material, the methylene signals are less well defined and the peaks are situated over a wider chemical shift range. It is difficult to make any assignment of the protons in this spectrum, other than the N-H protons.

The ^{13}C NMR spectrum displays 22 peaks over the region $\delta = 33.31$ to 69.11 ppm. This compares to that of the starting material which shows 6 peaks over the range $\delta = 43.50$ to 62.74 ppm. The spectrum of the product shows the peaks to occur in pairs, strongly suggesting the product to be a mixture of at least two isomers. Groups of new peaks are present in the product in the regions 67-69 ppm, 53-55 ppm and 33 ppm, none of which are present in the starting material. It is instructive to note that the ^{13}C NMR spectrum of $[\text{Co}(\text{sep})]^{3+}$ shows only 2 signals, one at 67.0 ppm and the other at 53.3 ppm, while $[\text{Co}(\text{en})_3]^{3+}$, from which it is prepared, shows a single peak around 46 ppm. It is therefore reasonable to assign the group of peaks at 53-55 ppm in the product to 'en-type' carbon atoms, while those at 67-69 ppm are very probably due to 'N-C-N-type' carbon atoms, of the

type adjacent to the 'cap' N atoms in $[\text{Co}(\text{sep})]^{3+}$. It has been shown¹¹ that the carbon atom in four-membered $\text{Co}(\text{N}-\text{C}-\text{N})$ chelate rings exhibits a relatively high field signal in the ^{13}C NMR spectrum (a range of $\delta = 50\text{-}20$ ppm), and so the peaks around $\delta = 33$ ppm could well be due to such carbon atoms.

The high resolution mass spectrum of the product is shown in figure 3.36.

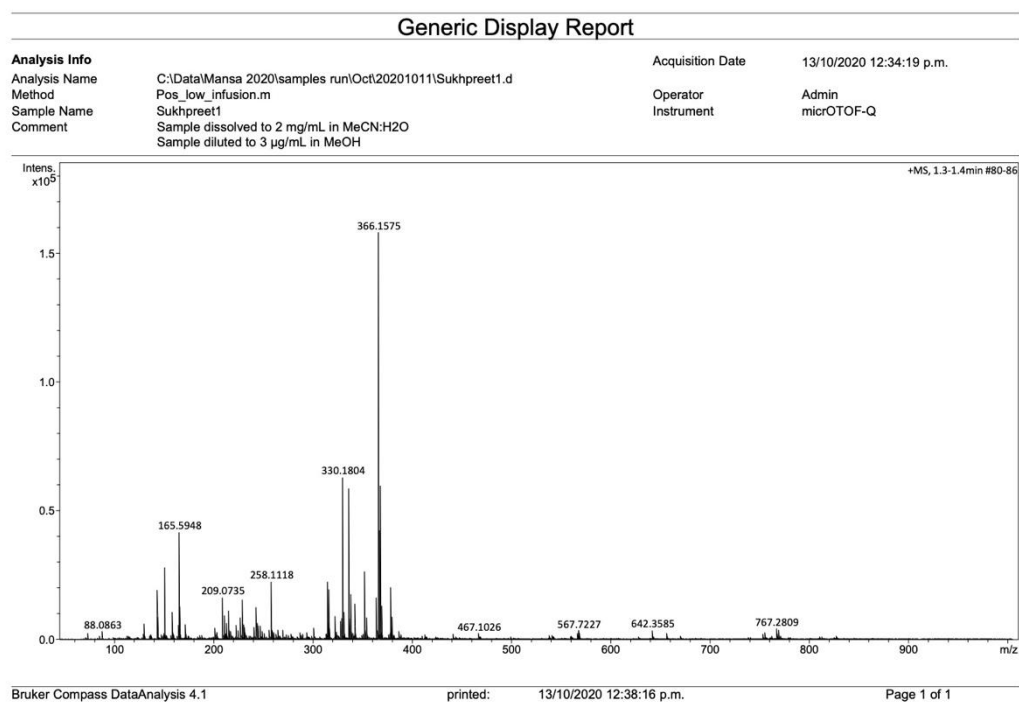


Figure 3.36a: Full high resolution mass spectrum of the product formed after the reaction of $[\text{Co}(\text{tren})(\text{en})]\text{Cl}_3$ with ammonia and formaldehyde.

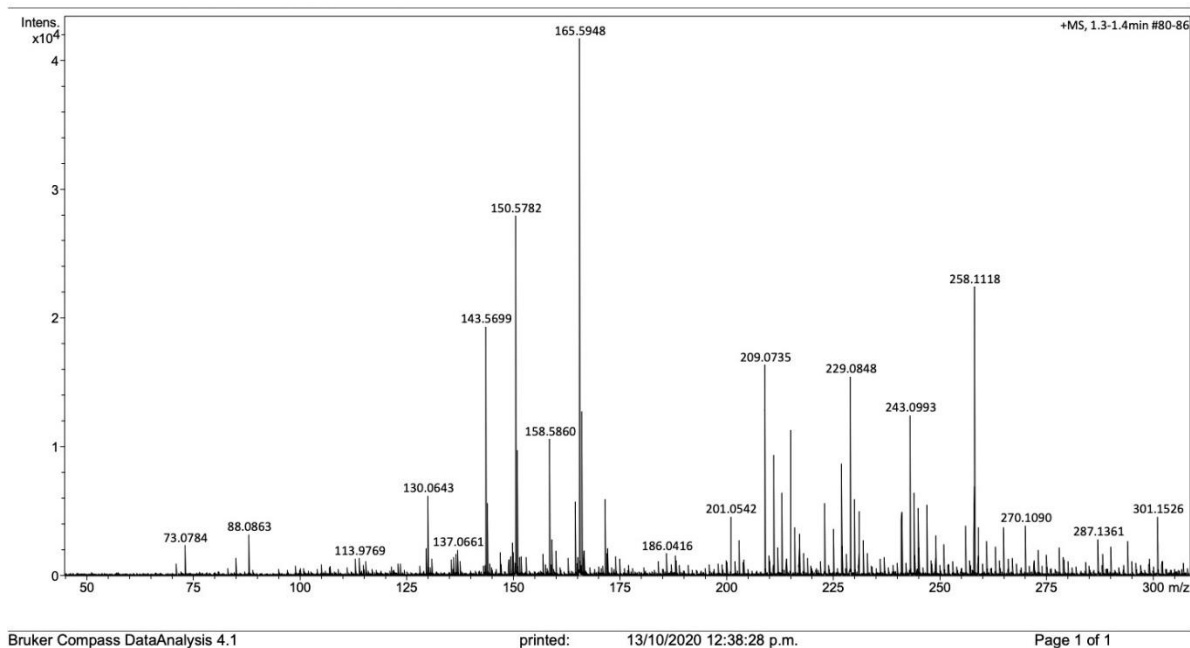


Figure 3.36b: High resolution mass spectrum of the product formed after the reaction of [Co(tren)(en)]Cl₃ with ammonia and formaldehyde, showing the region m/z 300-50.

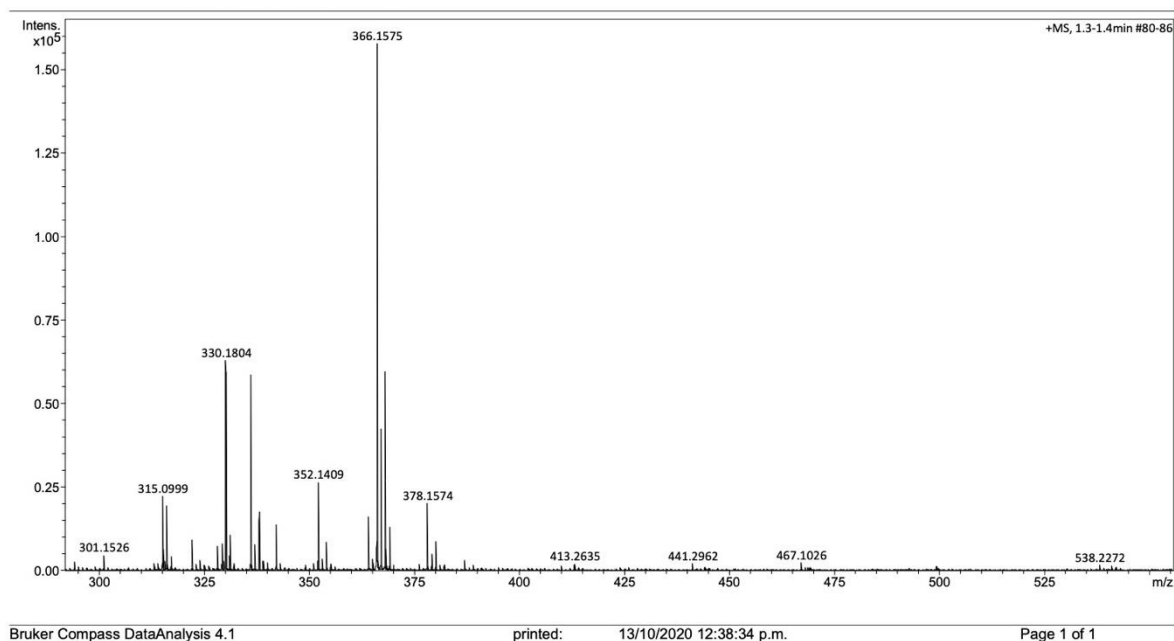


Figure 3.36c: High resolution mass spectrum of the product formed after the reaction of [Co(tren)(en)]Cl₃ with ammonia and formaldehyde, showing the base peak region m/z 376-362).

The product obtained from this reaction differs from those of the other Co(III) complexes studied, in that it is well resolved and not at all noisy. The base peak in the spectrum appears

at m/z 366.1575. This is consistent with a species having the molecular formula $C_{12}H_{30}N_7ClCo^+$ (calculated m/z 366.1580) in which Co(III) has been reduced to Co(II). The presence of a chloride ion is strongly suggested by another peak at m/z 368.1544 of approximately 1/3 the intensity of the base peak. The next highest intensity peak at m/z 330.1804 is consistent with loss of HCl from the base peak to give an ion having molecular formula $C_{12}H_{29}N_7Co^+$ (calculated m/z 330.1810), figure 3.39(a).

A chemically reasonable structure for the species giving rise to the base peak can be drawn, and is shown in Figure 3.37a. This results from capping of the tren and en ligands with a $N(CH_2)_3$ - moiety, and formation of a $Co(N-C-N)$ four-membered ring on the opposite side of the complex. Such a structure is consistent with the ^{13}C NMR data discussed above, with the ‘capping’ C atoms in the $\delta = 67$ -69 ppm region, the ‘en-type’ C atoms in the $\delta = 53$ -55 ppm region, and the carbon of the $Co(N-C-N)$ chelate ring around $\delta = 33$ ppm. However, the fact that multiple peaks are observed in this region strongly suggests the presence of isomers. Figure 3.37 shows four possible isomers of this complex.

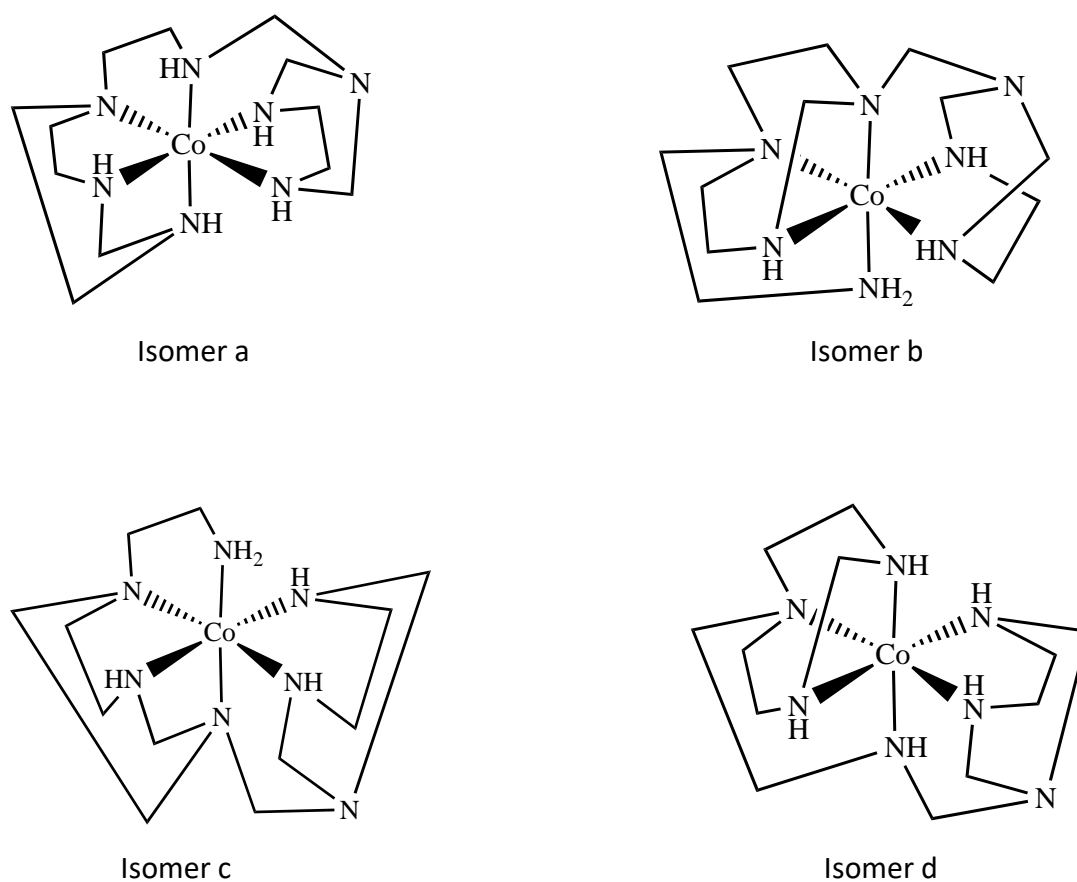
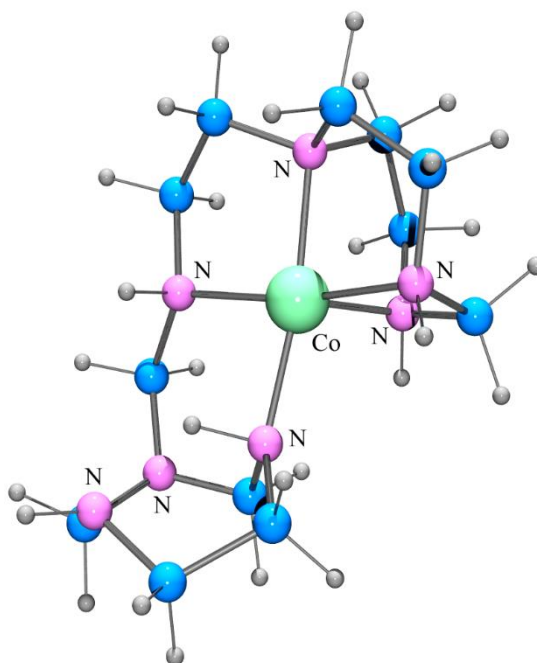


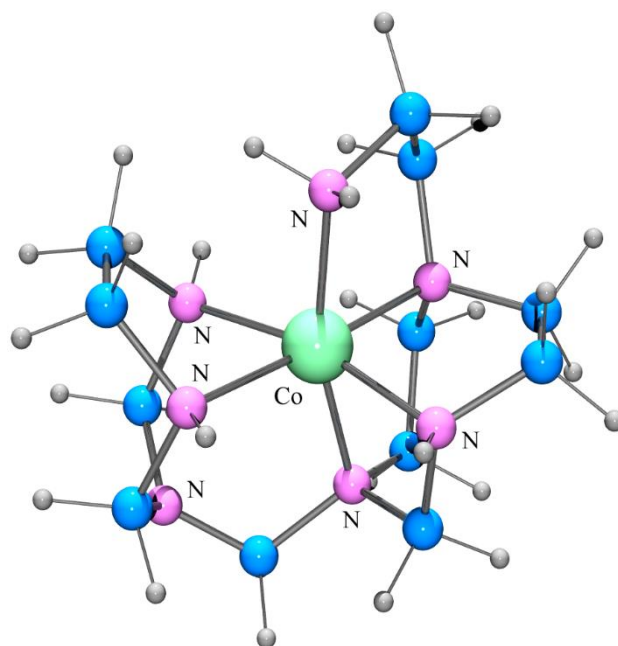
Figure 3.37: Structures of different isomers of the cage complex $[Co(tren)(en)]^{3+}$.

These isomers differ in the relative positionings of the capping N atom and the C atom of the Co(N-C-N) chelate ring. In the top two isomers, the capping N atom lies below what was the tertiary N atom of the tren ligand, and is either *cis* or *trans* to the C atom of the four-membered chelate ring, whereas in the bottom two isomers, the reverse is the case; the capping N atom lies above the tertiary N atom and is either *cis* or *trans* to the C atom of the four-membered chelate ring. Note that H atoms are not included in these structures, as it is very likely that these will lead to still further isomers as a result of differing possible orientations of protons on secondary N atoms.

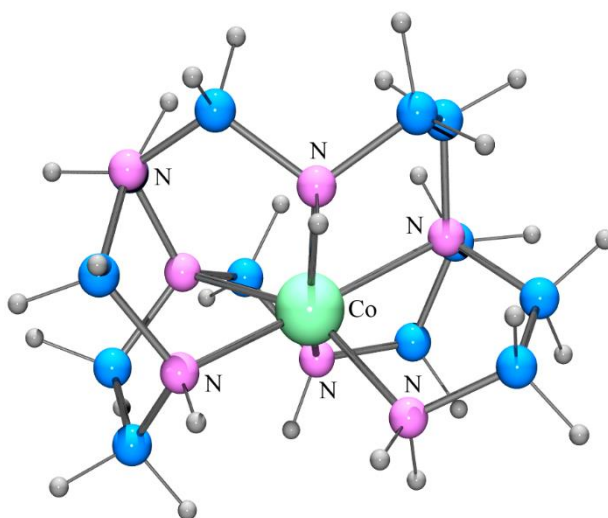
The structures of the four above isomers were optimised by DFT using conditions outlined in the experimental section. The results of these are as shown below in figure 3.38.



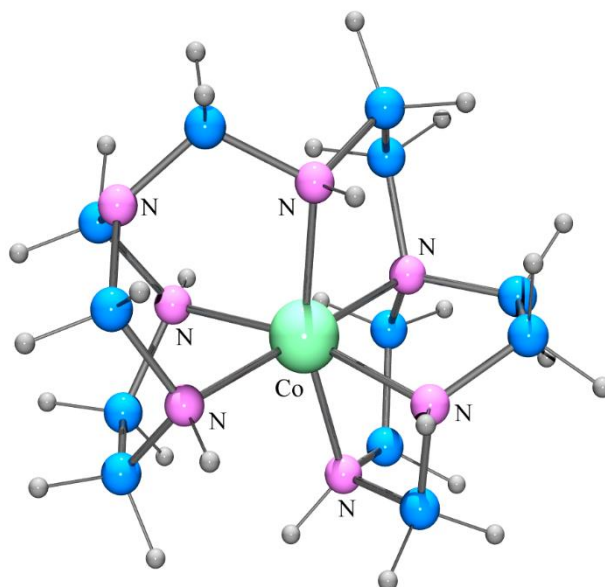
Isomer a fails to give a reasonable optimised structure, with the Co(III) ion becoming 5-coordinate.



Isomer b retains its overall structure, and gives an energy of $-628209.261571 \text{ kcal mol}^{-1}$.



Isomer c retains its overall structure, and gives an energy of $-628189.049490 \text{ kcal mol}^{-1}$.



Isomer d retains its overall structure, and gives an energy of $-628209.484337 \text{ kcal mol}^{-1}$.

Figure 3.38: Optimised structures of the four isomers and their energies.

From these results, it can be seen that isomer d is the most stable, but only by $0.222766 \text{ kcal mol}^{-1}$ over isomer b. Isomer c lies 20.434847 higher in energy than isomer d. It is therefore reasonable to expect that a near 50:50 mixture of isomers b and d will be present at room temperature, and this could well explain the complexity of the ^{13}C NMR spectrum of this compound. As mentioned previously, various N-H isomers could complicate matters still further.

Having assigned the base peak and one other intense peak in the mass spectrum of the product, it remains to assign other peaks. One prominent peak at m/z 165.59 can be assigned to the fragment $\text{C}_3\text{H}_8\text{N}_2\text{ClCo}^+$ (calculated m/z 165.97) which incorporates the formed $\text{Co}(\text{N}-\text{C}-\text{N})$ chelate ring, figure 3.39(b). The peak at m/z 258.11 can be assigned to the fragment having the molecular formula $\text{C}_9\text{H}_{21}\text{N}_5\text{Co}^+$ (calculated m/z 258.11), which is formed by the loss of the en ligand and capping of the tren ligand, along with reduction of cobalt(III) to cobalt(I), figure 3.39(c). The peak at m/z 209.07 can be assigned to the fragment having the molecular formula $\text{C}_4\text{H}_{18}\text{N}_6\text{Co}^+$ (calculated m/z 209.09), which contains the cap and the $\text{Co}(\text{N}-\text{C}-\text{N})$ chelate rings, and reducing the cobalt(III) ion to cobalt(I), figure 3.39(d).

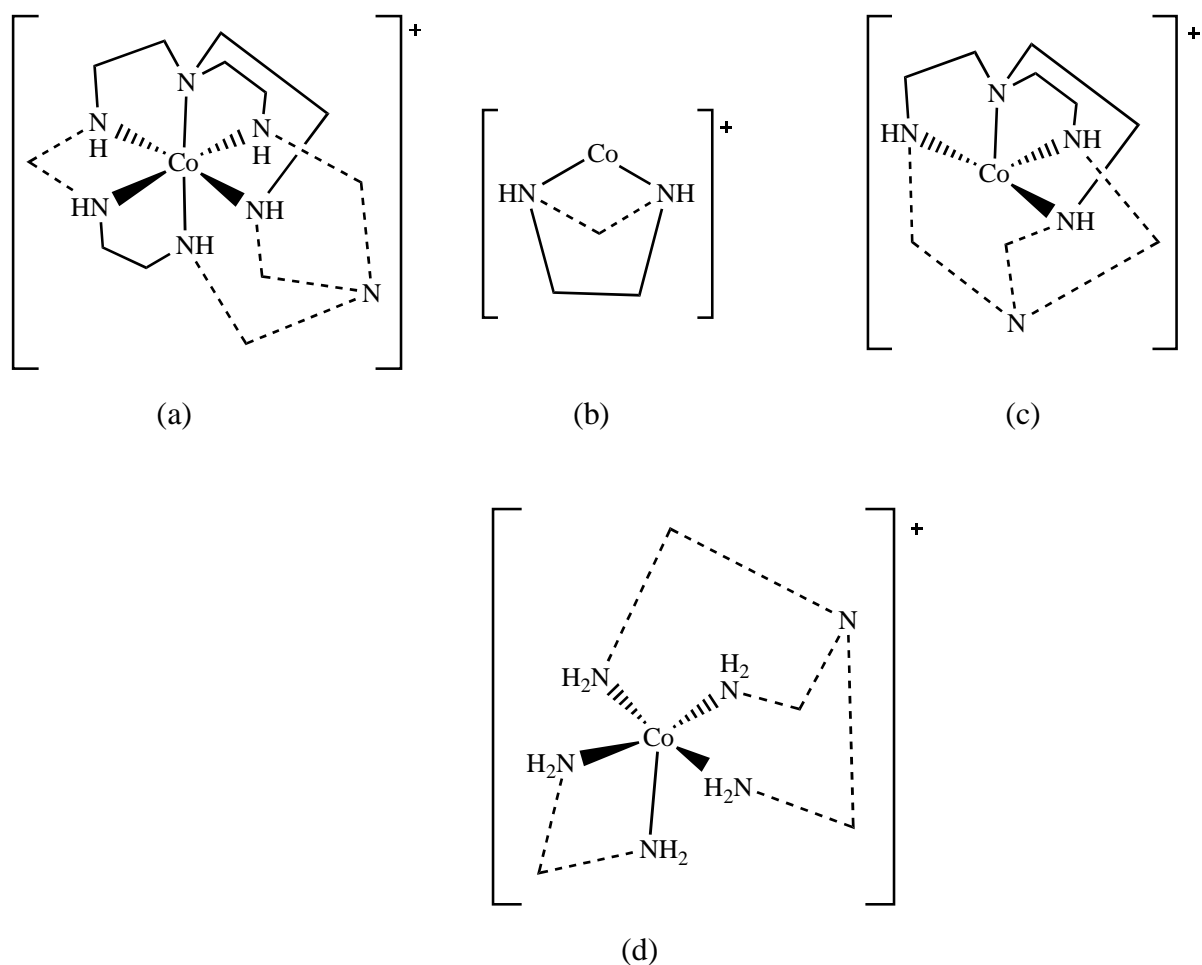


Figure 3.39: (a) Structure of the newly cage structure which is consistent with the peak observed in the mass spectrum at m/z 330.18; (b) Fragment consisting of en ligand along with the cage formed between its N atoms through carbon; (c) Fragment formed by the loss of en ligand and the cage around en ligand. This fragment consists of tren ligand and the cage structure around it; (d) Fragment consisting of N atoms that are involved in the formation of cage structure only and the cage itself.

CHAPTER 4

CONCLUSION

This thesis presents the attempts to prepare new multidentate cage-type amine ligands by linking di-, tri-, and tetra-dentate amine ligands coordinated to cobalt(III) through intramolecular condensation with formaldehyde and ammonia. The cobalt(III) complexes used in this study are $[\text{Co}(\text{tren})(\text{en})]^{3+}$, $[\text{Co}(\text{dien})_2]^{3+}$, $[\text{Co}(\text{bamp})_2]^{3+}$, and $[\text{Co}(\text{NH}_3)_6]^{3+}$. All the ligands and starting materials have been synthesised and characterised by NMR spectroscopy and ESI-MS spectrometry. Attempts to synthesise the pure uns-penp ligand was not successful. The reaction of the cobalt(III) complexes with formaldehyde and ammonia gave products in which the coordinated nitrogen atoms of the ligands were linked via either an N-(CH₂)₃-cap, or a single C atom. The NMR data were difficult to interpret for these complexes because of the formation of number of possible isomers but the ESI-MS data gave evidence for these types of linked complexes. Unfortunately, none of the linked complexes could be crystallised and therefore X-ray crystal structures could not be obtained.

The best characterised of the complexes is the one derived from $[\text{Co}(\text{tren})(\text{en})]^{3+}$. Consideration of both NMR and ESI-MS data suggest that four possible isomers can be formed. Structural optimisation using DFT showed that three of these were viable, and of these, the two most favoured had very similar energies, suggesting that both would be present in similar amounts under ambient conditions.

Similar linked structures are thought to have been formed in the other complexes studied as well, and similarly there are a number of isomers possible in all cases. Again, it was difficult to completely characterise these in the absence of X-ray data. Therefore obvious future work would involve developing methods for crystallising these complexes. It would also be optimal to choose starting materials which would result in the smallest number of possible isomers, as this should make crystallisation easier. These studies would help in understanding the different mechanisms of forming links between coordinated primary-primary, primary-secondary, and secondary-secondary amines. The isomers formed during the reaction could be isolated and their reactivities and properties could be studied to understand the mechanism

of the formation of the linked complexes. It was hoped to carry out such studies, but unfortunately, COVID intervened.

REFERENCES

- (1) Lawrance, G. A. *Introduction to Coordination Chemistry*; A Wiley Series of Advanced Textbooks; University of Newcastle, Callaghan, NSW, Australia, 2010.
- (2) Vladsinger. *Isomerism*; 2011.
- (3) Curtis, N. F.; House, D. A. *Chemistry and Industry - London*. **1961**, 1708–1709.
- (4) Curtis, N. F. The Advent of Macrocyclic Chemistry. *Supramol. Chem.* **2012**, *24* (7), 439–447. <https://doi.org/10.1080/10610278.2012.688123>.
- (5) Fabbrizzi, L. *Cryptands and Cryptates*; WORLD SCIENTIFIC (EUROPE), 2017. <https://doi.org/10.1142/q0107>.
- (6) Kang, S. O.; Llinares, J. M.; Day, V. W.; Bowman-James, K. Cryptand-like Anion Receptors. *Chem. Soc. Rev.* **2010**, *39* (10), 3980–4003. <https://doi.org/10.1039/C0CS00083C>.
- (7) Park, C. H.; Simmons, H. E. Macrobicyclic Amines. III. Encapsulation of Halide Ions by in,in-1,(k + 2)-Diazabicyclo[k.l.m.]Alkane Ammonium Ions. *J. Am. Chem. Soc.* **1968**, *90* (9), 2431–2432. <https://doi.org/10.1021/ja01011a047>.
- (8) Simmons, H. E.; Park, C. H. Macrobicyclic Amines. I. Out-in Isomerism of 1,(K+2)-Diazabicyclo[k.l.m.]Alkanes. *J. Am. Chem. Soc.* **1968**, *90* (9), 2428–2429. <https://doi.org/10.1021/ja01011a045>.
- (9) Yan Z. Voloshin; Kostromina, N. A.; Kramer, R. *Clathrochelates: Synthesis, Structure and Properties*, First Edition 2002.; Elsevier, 2002.
- (10) Creaser, I. I.; Harrowfield, J. M.; Herlt, A. J.; Sargeson, A. M.; Springborg, J.; Geue, R. J.; Snow, M. R. Sepulchrate: A Macrobicyclic Nitrogen Cage for Metal Ions. *J. Am. Chem. Soc.* **1977**, *99* (9), 3181–3182. <https://doi.org/10.1021/ja00451a062>.
- (11) Creaser, I. I.; Geue, R. J.; Harrowfield, J. M.; Herlt, A. J.; Sargeson, A. M.; Snow, M. R.; Springborg, J. Synthesis and Reactivity of Aza-Capped Encapsulated Cobalt(III) Ions. *J. Am. Chem. Soc.* **1982**, *104* (22), 6016–6025. <https://doi.org/10.1021/ja00386a030>.
- (12) Geue, R. J.; McCarthy, M. G.; Sargeson, A. M.; Skelton, B. W.; White, A. H. Stereospecific Template Synthesis of a Macrotetracyclic Hexaazacryptate: X-Ray Crystal Structure of (9,17-Dimethyl-13-Nitro-1,3,5,7,11,15-Hexaazatetracyclo[11.5.1.13,9.15,1]Heneicosane)Cobalt(III) Chloride. *Inorg. Chem.* **1985**, *24* (11), 1607–1609. <https://doi.org/10.1021/ic00205a001>.
- (13) Hammershoi, A.; Sargeson, A. M. Macrotricyclic Hexaamine Cage Complexes of Cobalt(III): Synthesis, Characterization and Properties. *Inorg. Chem.* **1983**, *22* (24), 3554–3561. <https://doi.org/10.1021/ic00166a014>.
- (14) Behm, C.; Boreham, P.; Creaser, I.; Korybutdaszkiewicz, B.; Maddalena, D.; Sargeson, A.; Snowdon, G. Novel Cationic Surfactants Derived From Metal Ion Cage Complexes: Potential Antiparasitic Agents. *Aust. J. Chem.* **1995**, *48* (5), 1009–1030.
- (15) Angus, P. M.; Elliott, A. J.; Sargeson, A. M.; Willis, A. C. Template Synthesis of Amidine- and Amide-Functionalised Cobalt(III) Hexaaza Cage Complexes. *J. Chem. Soc. Dalton Trans.* **2000**, No. 17, 2933–2938. <https://doi.org/10.1039/B002531N>.
- (16) Morgenstern, B.; Neis, C.; Zaszka, A.; Romba, J.; Weyhermüller, T.; Hegetschweiler, K. Formation and Base Hydrolysis of Oxidimethaneamine Bridges in CoIII–Amine Complexes. *Inorg. Chem.* **2013**, *52* (20), 12080–12097. <https://doi.org/10.1021/ic4019053>.

- (17) Frisch, M. J.; Trucks, G. W.; Schlegel, H. B.; Scuseria, G. E.; Robb, M. A.; Cheeseman, J. R.; Scalmani, G.; Barone, V.; Peterson, G. A.; Nakatsuji, H.; Li, X.; Caricato, M.; Marenich, A. V.; Bloino, J.; Janesko, B. G.; Gomperts, R.; Mennucci, B.; Hratchian, H. P.; Ortiz, J. V.; Izmaylov, A. F.; Sonnenberg, J. L.; Williams-Young, D.; Ding, F.; Lipparini, F.; Egidi, F.; Goings, J.; Peng, B.; Petrone, A.; Henderson, T.; Ranasinghe, D.; Zakrzewski, V. G.; Gao, J.; Rega, N.; Zheng, G.; Liang, W.; Hada, M.; Ehara, M.; Toyota, K.; Fukuda, R.; Hasegawa, J.; Ishida, M.; Nakajima, T.; Honda, Y.; Kitao, O.; Nakai, H.; Vreven, T.; Throssell, K.; Montgomery, J. A., Jr.; Peralta, J. E.; Ogliaro, F.; Bearpark, M. J.; Heyd, J. J.; Brothers, E. N.; Kudin, K. N.; Staroverov, V. N.; Keith, T. A.; Kobayashi, R.; Normand, J.; Raghavachari, K.; Rendell, A. P.; Burant, J. C.; Iyengar, S. S.; Tomasi, J.; Cossi, M.; Millam, J. M.; Klene, M.; Adamo, C.; Cammi, R.; Ochterski, J. W.; Martin, R. L.; Morokuma, K.; Farkas, O.; Foresman, J. B.; Fox, D. J. *Gaussian 16, Revision C.01*; Gaussian, Inc.: Wallingford CT, 2016.
- (18) Zhao, Y.; Truhlar, D. G. The M06 Suite of Density Functionals for Main Group Thermochemistry, Thermochemical Kinetics, Noncovalent Interactions, Excited States, and Transition Elements: Two New Functionals and Systematic Testing of Four M06-Class Functionals and 12 Other Functionals. *Theor. Chem. Acc.* **2008**, *120* (1), 215–241. <https://doi.org/10.1007/s00214-007-0310-x>.
- (19) Schatz, M.; Leibold, M.; Foxon, S. P.; Weitzer, M.; Heinemann, F. W.; Hampel, F.; Walter, O.; Schindler, S. Syntheses and Characterization of Copper Complexes of the Ligand (2-Aminoethyl)Bis(2-Pyridylmethyl)Amine (Uns-Penp) and Derivatives. *Dalton Trans.* **2003**, No. 8, 1480–1487. <https://doi.org/10.1039/B208740E>.
- (20) Organic Syntheses. **1927**, *Coll. Vol. 1*, 119. <https://doi.org/10.15227/orgsyn.007.0008>.
- (21) Liu, C.; Lei, H.; Zhang, Z.; Chen, F.; Cao, R. Oxygen Reduction Catalyzed by a Water-Soluble Binuclear Copper(II) Complex from a Neutral Aqueous Solution. *Chem. Commun.* **2017**, *53* (22), 3189–3192. <https://doi.org/10.1039/C6CC09206C>.
- (22) McClure, M. Synthesis and Symmetry of Two Cobalt(III) Complexes with Tetradentate Ligands. *J. Chem. Educ.* **2008**, *85* (3), 420. <https://doi.org/10.1021/ed085p420>.
- (23) Otter, C. A.; Hartshorn, R. M. Preparation and Photochemistry of Cobalt(III) Amino and Amino Acidato Complexes Containing Tripodal Polypyridine Ligands. *Dalton Trans.* **2004**, No. 1, 150–156. <https://doi.org/10.1039/B311809F>.
- (24) Schlessinger, G. G.; Britton, D.; Rhodes, T.; Ng, E. Chloropentaamminecobalt(III) Chloride. In *Inorganic Syntheses*; John Wiley & Sons, Ltd, 1967; pp 160–163. <https://doi.org/10.1002/9780470132401.ch43>.
- (25) Searle, G.; Lincoln, S.; Keene, F.; Teague, S.; Rowe, D. Bis(Tridentate)Cobalt(III) Complexes with Diethylenetriamine and 4-Methyldiethylenetriamine [2,2'-Methyliminodi(Ethylamine)]: Assignment of Geometric Configurations by ¹H and ¹³C N.M.R. Spectroscopy. *Aust. J. Chem.* **1977**, *30* (6), 1221–1228.
- (26) Bjerrum, J.; McReynolds, J. P.; Oppegard, A. L.; Parry, R. W. Hexamminecobalt(III) Salts. In *Inorganic Syntheses*; John Wiley & Sons, Ltd, 1946; pp 216–221. <https://doi.org/10.1002/9780470132333.ch69>.
- (27) Gainsford, G. J.; Geue, R. J.; Sargeson, A. M. Synthesis of Macrotricyclic Polyazacryptates on Metal Ions: X-Ray Crystal Structures of [(3,11-Dimethyl-7-Nitro-1,5,9,13,16,19-Hexa-Azatricyclo[9.3.3.3.3,7]icosane)Cobalt(III)](3+) and [(3,11-Dimethyl-7,15-Dinitro-1,5,9,13,18,21-Hexa-Azatricyclo[9.5.3.3.3,7]-Docosane)Cobalt(III)](3+) Ions. *J. Chem. Soc. Chem. Commun.* **1982**, No. 4, 233–235. <https://doi.org/10.1039/C39820000233>.
- (28) Hamilton, D. E. The Synthesis of Cobalt(III) Sepulcrate from Tris(Ethylenediamine)Cobalt(III) and Its Purification by Ion-Exchange

Chromatography: An Experiment for the Advanced Undergraduate Inorganic Laboratory. *J. Chem. Educ.* **1991**, *68* (6), A144. <https://doi.org/10.1021/ed068pA144>.